PhD Program in Translational and Molecular Medicine

DIMET

UNIVERSITY OF MILANO-BICOCCA

SCHOOL OF MEDICINE AND SCHOOL OF SCIENCE

Molecular Mechanisms of Cancer Drug Resistance

Coordinator: Prof. Andrea Biondi

Tutor: Dr. Roberto Giovannoni

Dr. Gabriele Romano

Matr.No.709074

XXVIII Cycle

Academic Year

2014-2015

...un terzo di istinto,

un terzo di memoria,

un terzo di volontà...

Table of Contents

CHAPTER 1 6

INTRODUCTION 6

CHEMORESISTANCE: INTRINSIC MOLECULAR MECHANISMS 7
DRUG TRANSPORTERS 7
DRUG METABOLISM 8
DRUG TARGETS 9
DNA DAMAGE REPAIR SYSTEMS 10
TUMOR SUPPRESSOR GENES 11
INDUCTION OF APOPTOSIS 13
PRO-SURVIVAL SIGNALS 14
ACQUIRED DRUG RESISTANCE: THE ROLE OF MICROENVIRONMENT 16
ECM STRUCTURE AND CELL ADHESION SIGNALING 16
VASCULARIZATION, NEO-ANGIOGENESIS AND ANGIOGENETIC SIGNALS 18
CANCER ASSOCIATED FIBROBLASTS 20
IMMUNE SYSTEM 21
EPITHELIAL TO MESENCHYMAL TRANSITION AND TUMOR STEM CELLS 22
SHOOTING TO THE TARGET: THE PERSONALIZED MEDICINE 26
DRUG RESISTANCE EXPERIMENTAL MODELS 29
CANCER CELL LINES 30
CELL LINE XENOGRAFTS 32
PATIENT DERIVED XENOGRAFTS 33
IMMUNOCOMPETENT ALLOGRAFTS 35
GEMMS 36
THE RIGHT MODEL 36
SCOPE OF THE THESIS 38
CHAPTER 2: RESVERATROL INHIBITS PROLIFERATION AND STRONGLY DECREASES MOTILITY IN GLIOMA STEM CELLS, MODULATING THE WNT SIGNALING PATHWAY 38
CHAPTER 3: A FUNCTIONAL BIOLOGICAL NETWORK CENTERED ON XRCC3: A NEW POSSIBLE MARKER OF CHEMORADIOTHERAPY RESISTANCE IN RECTAL CANCER PATIENTS 38
CHAPTER 4: INHIBITION OF GSK3B BYPASS DRUG RESISTANCE OF P53-NULL 39
COLON CARCINOMAS BY ENABLING NECROPTOSIS IN RESPONSE TO 39
CHEMOTHERAPY 39

CHAPTER 5: THE TGF-B PATHWAY IS ACTIVATED BY 5-FLUOROURACIL TREATMENT IN DRUG RESISTANT COLORECTAL CARCINOMA CELLS 39
REFERENCES **40**

CHAPTER 2 **58**

RESVERATROL INHIBITS PROLIFERATION AND STRONGLY DECREASES MOTILITY IN GLIOMA STEM CELLS, MODULATING THE WNT SIGNALING PATHWAY **58**

CHAPTER 3 **84**

A FUNCTIONAL BIOLOGICAL NETWORK CENTERED ON XRCC3: A NEW POSSIBLE MARKER OF CHEMORADIOTHERAPY RESISTANCE IN RECTAL CANCER PATIENTS **84**

CHAPTER 4 **120**

INHIBITION OF GSK3B BYPASS DRUG RESISTANCE OF P53-NULL COLON CARCINOMAS BY ENABLING NECROPTOSIS IN RESPONSE TO CHEMOTHERAPY **120**

CHAPTER 5 **159**

THE TGF-B PATHWAY IS ACTIVATED BY **159**
5-FLUOROURACIL TREATMENT IN DRUG RESISTANT COLORECTAL CARCINOMA CELLS **159**

CHAPTER 6 **189**

CONCLUSIONS, TRANSLATIONAL RELEVANCE AND FUTURE PERSPECTIVES **189**
CHAPTER 2 - RESVERATROL AND GBM: A POSSIBLE STRATEGY TO CIRCUMVENT CHEMOTHERAPY FAILURE 190
CHAPTER 3 - COMPUTATIONAL BIOLOGY AND CLINICAL STUDIES: THE INTERESTING EXAMPLE OF XRCC3 191
CHAPTER 4 – GSK3B IS A MASTER REGULATOR OF CRC CHEMORESISTANCE 192
CHAPTER 5 – TGFB IS AN ACTIVE PLAYER IN CRC CHEMORESISTANCE 194

Chapter 1

Introduction

Chemoresistance: intrinsic molecular mechanisms

Drug resistance is the most influent factor affecting the effectiveness of cancer therapy. More than 90% of patients with metastatic disease do not respond to cancer chemotherapy [1]. Drug resistance is a complex phenomenon that could be intrinsic or acquired by the tumor [2].

Administration of chemotherapeutics to chemoresistant tumors, for example, can eventually lead to the selection of the most aggressive cell clones within the tumor and to the development of cross-resistance with other drugs.

Here we provide an overview of the principal mechanisms involved in cancer chemoresistance (**Fig.1**) with the help of examples with translational relevance.

Drug transporters

One of the most known mechanisms of chemoresistance is the active drug expulsion by tumor cells operated by ABC transporter proteins such as P-glycoprotein or Multi-drug Resistance Protein (MRP) [3,4]. ABC transporters can actively pump drugs out of the cells, thus impairing the ability of chemotherapeutics to reach the cellular compartment in which they are active [5]. ABC transporters overexpression was detected in several leukemic and solid tumors cancer cell lines, and such over-expression was linked to cancer drug resistance [6,7]. ABCB5 transporter, for example, is overexpressed in tumor cells of colon cancer patients. The ABCB5-expressing tumor cell population was also reported to be treatment's refractory and to exhibit resistance to 5FU–induced apoptosis in a colorectal cancer xenograft model of 5FU monotherapy [8]. ABC transporter inhibitors have been

developed in order to overcome drug resistance. P-glycoprotein inhibitors with high specificity and sensitivity have been widely tested *in vitro*, but their clinical efficacy is still limited as a consequence of toxicity, adverse drug interaction, and numerous pharmacokinetic issues [9].

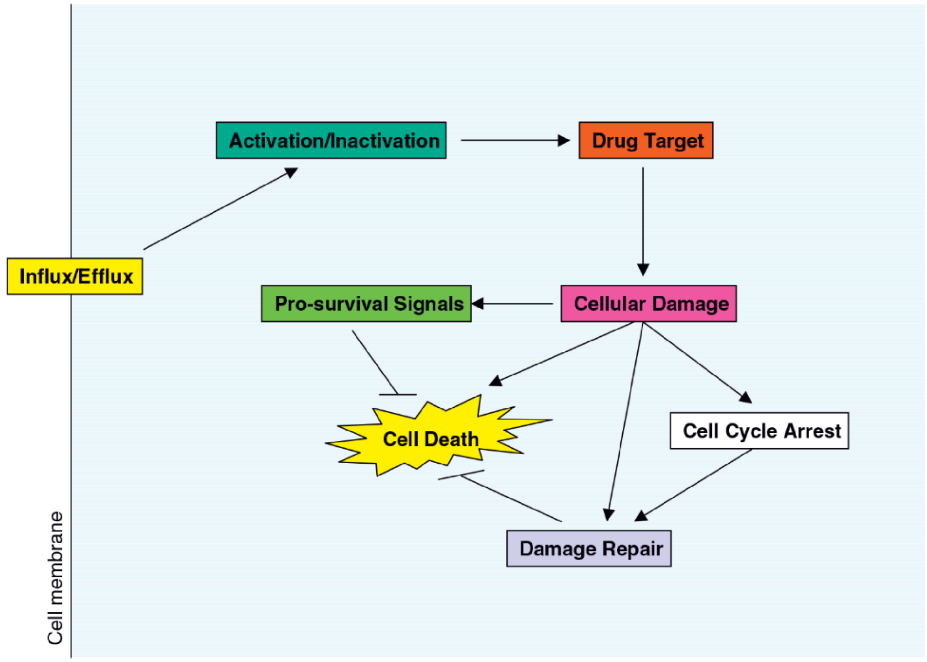

Figure 1 Cancer specific molecular mechanisms of drug resistance [1].

Drug metabolism

Several mechanisms of drug inactivation have been shown to influence the ability of the chemotherapeutics to reach their molecular targets. 5-Fluorouracil (5FU), for example, is the gold standard chemotherapeutic for the treatment of colon cancer. 5FU is normally catabolized by dihydropyrimidine dehydrogenase (DPD) [10]. High levels of expression of DPD have been correlated to 5FU resistance [11], as a consequence of the

increased degradation operated by DPD. A more interesting result was obtained in a metastatic pre-clinical model of xenotransplanted human colon carcinoma cells: DPD mRNA levels were found upregulated in liver metastasis and inversely correlated with 5FU sensitivity. In this model, liver metastasis are found much more resistant than in the primary tumors, indicating a role of DPD in acquisition of drug resistance [12]. Moreover, drugs such as Irinotecan (a topoisomerase I inhibitor) need to be activated prior to be effective. Irinotecan is activated by carboxylesterase 2 (CES2), and transformed into its active form SN-38. High CES2 expression in tumor tissues is associated with longer overall survival Pancreatic Ductal Adenocarcinoma patients who underwent neoadjuvant FOLFIRINOX (leucovorin, 5FU, Irinotecan, Oxalipatin) treatment [13].

Drug targets

Chemotherapeutics efficacy could be affected by the alteration of their cellular targets. The 5FU metabolite fluorodeoxyuridine monophosphate (FdUMP) selectively inhibits thymidylate synthase (TS). Low tumor TS expression has been associated to better response to therapy in colorectal cancer patients [14,15]. Moreover, 5FU administration is able to increase TS expression as a consequence of the disruption of a negative feedback mechanism: ligand-free TS binds to its own mRNA and inhibits its own translation[16]. When stably bound by FdUMP, TS can no longer bind its own mRNA and suppress translation, resulting in increased protein expression and, eventually, to a decreased efficacy of 5FU chemotherapeutic action.

Taxanes (such as paclitaxel or docetaxel) are chemotherapeutics acting against microtubules, a fundamental cytoskeletal structure. Microtubules are involved in mitotic spindle formation, vesicles transport and cell shape maintenance. Tubulin (α and β) is the basic unit of microtubules, and alteration in its expression or protein sequence have been associated to paclitaxel resistance [17–19]. In a recent work on non-small cell lung cancer (NSCLC) tumor specimens, TUBB3 (β-tubulin III) expression was related with chemoresistance. More precisely, TUBB3 expression was related to poor prognosis and K-RAS mutation in NSCLC patients who received neoadjuvant chemotherapy (paclitaxel or gemcitabine based) [20].

DNA damage repair systems

The ability of a tumor cell to repair DNA damage could make the difference between cell survival and cell death. Several chemotherapeutics (5FU, Irinotecan, oxaliplatin) cause DNA damage as a final result of their therapeutic efficacy. Inherited defects in mismatch repair (MMR) genes, for example, can lead to hereditary non-polyposis colon cancer (HNPCC) and are also detected in sporadic tumors, including colorectal, breast, and ovarian cancer [21–23]. Microsatellite instability (MSI) phenotype is caused by MLH1 or MSH2 defects that eventually lead to the amplification of DNA repeated sequences. Gastric cancer patients showing an un-methylated form of MLH1 and a mutated MSH6 have a poor prognosis, due to chemoresistance to 5FU treatment [24]. Mutation or silencing of MMR genes was also associated to cisplatin resistance in ovarian cancer [25]. On the other side, colorectal cancers that show a MSI phenotype are generally associated to a better

prognosis and response to chemotherapeutics. This apparent contradiction is mainly due to the fact that the majority of MSI positive tumors are generally p53 wild-type, which is a key player in cell sensitivity to 5FU [26], (see next paragraph). As it can be deduced, chemoresistance is a multi-factor mechanism and the relationship between molecular players deeply influences the efficacy of the therapeutic regimen.

Tumor suppressor genes

The ideal chemotherapeutic drug should induce arrest of cancer cell proliferation and cancer cell death. However, drug administration often causes only one of the two desired effects. *TP53* gene (coding for the p53 protein) is one of the master regulator of cell proliferation and death, but it is found mutated in more than 50% of tumors [27]. In physiological state, p53 is activated by damage sensor proteins (ATM, ATR) which in turn inactivate MDM2, a negative regulator of p53 protein [28]. In consequence of activation, p53 can also induce the expression of GADD45B and p21, which are responsible for cell cycle arrest [29,30]. The induction of cell cycle arrest or cell death by p53 is dependent on the nature of the DNA damage, on the physiological contest and on the availability of co-transcription factors [31–33]. *TP53* mutation is reported to be strictly related to chemotherapeutic efficacy. In particular, 5FU-induced cell death is strongly impaired when *TP53* is mutated: loss of function or gain of function mutations are reported to impair tumor sensitivity to 5FU therapeutic action [34,35]. An interesting example comes from lymphoma experimental models, in which Eμ-myc mice are crossed with $INK4^{+/-}ARF^{+/-}$ or $p53^{-/+}$ mice. Eμ-myc tumors in $INK4^{+/-}ARF^{+/-}$

mice are more aggressive and resistant to chemotherapy as compared to the relative controls and they generally lose the *TP53* wild-type allele [36]. This indicates a strong selective pressure to disengage the p53 pathway during lymphoma development. The *TP53* mutation has been also reported to be responsible for resistance to doxorubicin, cisplatin and irinotecan in various types of cancer [37–39]. Tumor suppressor *BRCA1* and *BRCA2* are frequently mutated in familial breast and ovarian cancer. Cancers that arise in mutation carriers have often lost the wild type allele through somatic alterations during tumor progression [40]. BRCA1/2 play important roles in homologous recombination (HR) repair of DNA double-strand breaks [41]. Because of this, BRCA1/2-deficient cancers often have a better response to DNA crosslinking agents such as platinum analogues and to poly(ADP-ribose) polymerase (PARP) inhibitors [42,43]. However, over time, the majority of these BRCA1/2-deficient cancers become resistant and patients die because of refractory diseases. It was demonstrated that the restoration of BRCA1/2 activity is due to a process of intragenic secondary mutation that corrected the inactivating mutations in the open reading frame [44]. In the BRCA2-negative CAPAN-1 pancreatic adenocarcinoma cell line, BRCA2 was found active and functional: some of the analyzed clones derived for the tumor cell line revealed the loss of the primary inactivating mutation [45]. It is interesting to notice that all the clones that were found to have lost the primary mutation were chemoresistant to cisplatin and PARP inhibitors, but not to docetaxel (microtubule stabilizing agent) [44].

Induction of apoptosis

An effective chemotherapeutic strategy should cause induction of cell death. Apoptosis is a programmed cell death mechanism that can be activated by intracellular signaling (Bcl-2 pathway) or extracellular apoptotic stimuli (Tumor Necrosis Factor family and their Receptors superfamily) [46]. Apoptosis eventually leads to caspase activation (caspase 3 or 7 eventually) which causes chromatin condensation, membrane blebbing and nuclear fragmentation [46]. Bcl-2 family proteins can have pro-apoptotic (Bax, Bak, Bad, Bid) or anti-apoptotic (Bcl-XL, Mcl-1) functions. The apoptosis mechanism is finely regulated and the alteration of only one of the players involved can cause an impairment of the efficacy of the programmed cell death mechanism. Bcl-2 family members are deeply studied, and frequently found to be associated with chemoresistance phenomena. In B-cell lymphomas, Bcl-2 overexpression was related to STAT3 activation [47], one of the surrogate network activated in oncogene addicted cancer cells as a means to evade drug-induced execution [48]. However, Bcl-2 proteins function is often influenced by other modifying factors such as estrogen or progesterone positivity in breast cancer [49]. Once more, chemoresistance is not a “one-factor” process and it is strongly dependent on cellular context. TNF receptor superfamily members regulate the extrinsic pathway of apoptosis. The best studied of these receptors is Fas. Fas, when bound to its ligand FasL, recruits caspase 8 and constitutes the DISC (death inducing signaling complex). Caspase in the DISC can in turn activate the caspase cascade leading to apoptosis activation [50]. Fas-negative/FasL-positive breast tumors, for example, have a poorer prognosis in consequence of

adjuvant chemotherapy [51]. Fas promoter tri-methylation in H3K9 causes a repression of Fas expression and loss of sensitivity to 5FU in colorectal cancer models [52]. Moreover, Fas downregulation results in T-lymphocytes-mediated cell death, and a consequent immune evasion [52].

Pro-survival signals

Protein Tyrosine Kinases (PTKs) are major players in cellular processes of cell survival and cell death. PTKs are frequently activated by chemoresistant cancer cells to "compensate" impaired mechanisms fundamental for cell survival [1,2]. The most studied family of PTKs is probably the EFGR family, among which there are EGFR, Her1, Her2, Her3 and Her4. Binding of grow factors (such as EGF) leads to receptor dimerization and activation of prosurvival downstream pathways, such as PI3K/Akt signaling [53]. EGFR overexpression and mutation has been correlated with poor prognosis and lack of response after chemotherapeutic treatment [54]. Many EGFR inhibitors have been developed and currently used in therapy. Cetuximab, for example, is a monoclonal antibody directed against EGFR and it is currently used in the treatment of colon cancer. KRAS mutated tumors, however, are completely resistant to cetuximab action, as KRAS is downstream EGFR [55]. In addition, co-expression of EGFR or HER3 with HER2 renders cells more resistant to anticancer drugs [56]. However, by acquiring an increased dependence on a specific growth factor for survival, chemoresistant cells may become more sensitive to inhibition of this signaling. In glioma and ovarian cancer chemoresistant cells, gefitinib (an EGFR inhibitor) inhibits both an enhanced EGF-triggered pathway and a

constitutive HER3-mediated Akt activation. Gefitinib administration is able to cause growth inhibition more efficaciously than chemotherapeutic treatment, indicating that combined HER3 and EGFR inhibition could be relevant in chemorefractory tumors [57]. Other types of kinases are involved in chemoresistance phenomena. An interesting example of chemoresistance-related kinase is Glycogen Synthase Kinase 3 β (GSK3β). GSK3β is a serine/threonine protein kinase that regulates multiple signaling pathways, and it is generally described as a tumor suppressor [58]. GSK3β, in fact, is known to participate into the "destruction complex" which leads to β-catenin degradation, a strong promoter of epithelial transformation [59]. Paradoxically, it was shown that deregulated expression, activity and phosphorylation of GSK3β are distinct features of gastrointestinal cancers and glioblastoma and that GSK3β sustains the survival and proliferation of these tumor cells [60–63]. A role for aberrant GSK3β in these tumor types is supported by the observation that pharmacological inhibition of its activity reduces the survival and proliferation of cancer cells and predisposes them to apoptosis *in vitro* and in tumor xenografts. More recently, an isoform GSK3 (GSK3β) was shown to have a potential role also in pancreatic ductal adenocarcinoma (PDA): pancreatic cancer cells showed higher expression and activity of GSK3β than non-neoplastic cells, which were associated with changes in its differential phosphorylation [64]. Inhibition of GSK3β significantly reduced the proliferation and survival of cancer cells, sensitized them to gemcitabine and ionizing radiation, and attenuated their migration and invasion.

Acquired drug resistance: the role of microenvironment

De novo drug resistance is generally due to a transient protection of cancer cells operated by the tumor microenvironment. This kind of resistance can be divided in two different subtypes: soluble factor-mediated drug resistance (SFM-DR), which is induced by cytokines, chemokines and growth factors secreted by fibroblast-like tumor stroma; and cell adhesion-mediated drug resistance (CAM-DR), which is mediated by the adhesion of tumor cell integrins to stromal fibroblasts or to components of the extracellular matrix (ECM), such as fibronectin, laminin and collagen [65]. SFM-DR is strongly regulated by transcriptional mechanisms, whereas CAM-DR is generally associated to post-transcriptional regulations [65]. Environment mediated drug resistance (EMDR) main outcome is the protection of a small subset of cells (Minimal Residual Disease) from therapy, until they acquire a resistant-phenotype.

The tumor stroma is composed of endothelial cells, carcinoma-associated fibroblasts (CAFs), adipocytes, mesenchymal cells, mesenchymal stem cells (MSCs; bone marrow derived, BM-MSCs, or carcinoma associated, CA-MSCs), and cells from the immune and inflammatory systems (Fig. 2) [66].

ECM structure and cell adhesion signaling

The structural organization of the tumor stroma can influence the amount of drug effectively reaching the tumor, the interstitial pressure and intracellular signaling pathways activation [67]. Over the last decade, many studies showed the fundamental role of adhesion molecules in relationship to chemotherapeutics sensitivity. A recent study on chemoresistant ovarian

cancer cells, for example, showed that taxol administration causes deep changes in microtubule dynamics. Taxol-treated chemoresistant cells showed faster attachment rates and decreased adhesion strength, which correlated with increased surface β1-integrin expression and decreased focal adhesion formation [68]. Fibronectin, another cell-matrix adhesion molecule, is shown to mediate Akt phosphorylation, via PI3K, and docetaxel resistance in ovarian and breast cancer models [69]. PI3K inhibitors administration was able to restore sensitivity to chemotherapeutic action, indicating a fundamental role of fibronectin adhesion in determining the cell fate after docetaxel treatment.

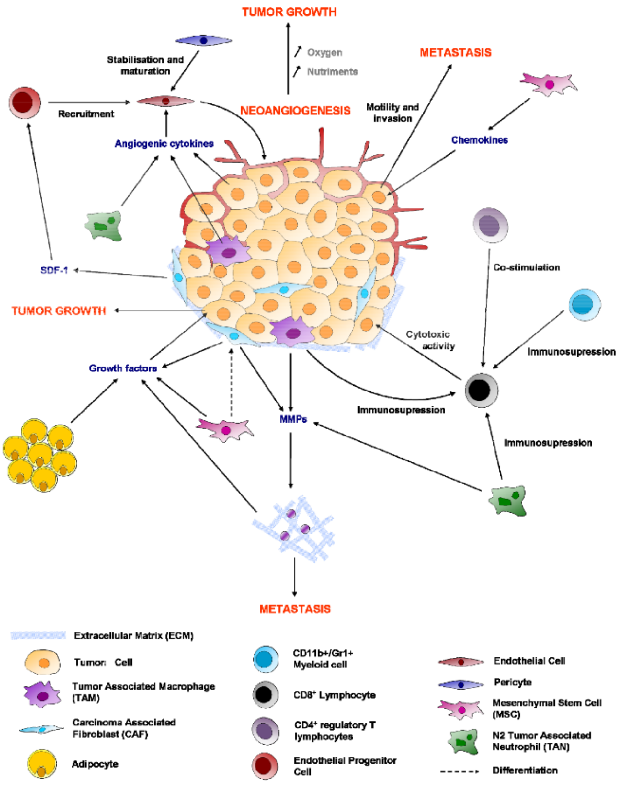

Figure 2 Tumor-stroma interactions involved in drug resistance [66].

Vascularization, neo-angiogenesis and angiogenetic signals

Chemoresistance and blood vasculature are strongly related. Neo-angiogenesis often causes resistance to apoptosis and pro-survival signals [70]. Various aspects of neo-angiogenesis can influence the response to therapeutic strategies.

Firstly, angiogenetic growth factors can act as pro-survival signals for both endothelial and tumor cells. VEGF, for example, is a strong inducer of neo-angiogenesis and it can be secreted by tumor as well as by endothelial cells [71]. VEGF can influence endothelial cell survival, through PI3K/Akt pathway and BCL-2 up-regulation [72,73]. FGF-2 is also known to protect endothelial cells to chemotherapeutic action, though mechanisms that are similar to VEGF [74]. Another important aspect to consider, is the direct effect of angiogenetic stimuli on and from tumor cells. An isoform of VEGF (VEGF-C), for example, was detected to induce resistance to cisplatin in gastric cancer cells, through the interaction with Rho GDP dissociation inhibitor 2 (RhoGDI2). The inhibition of VEGF-C/RhoGDI2 is able to re-sensitize chemoresistant cells to cisplatin action [75].

The interaction between endothelial and tumor cells is very strict and bi-directional, and can significantly influence the efficacy of the therapeutic strategy. Tumor associated endothelial cells show differences in terms of gene expression as compared to normal endothelial cells. In *in vivo* glioma models, it was shown that glioma associated endothelial cells over-expressed survivin, which is not normally expressed at high levels in normal brain endothelial cells. Such up-regulation conferred tumor associated

endothelial cells a strong multi-drug resistance (paclitaxel and temozolomide among the others) [76].

An additional phenomenon to consider is hypoxia, which often occurs inside tumor masses. Hypoxia can induce cells modifying their phenotype in order to overcome the oxygen deprivation and to survive. One of the key molecule acting during hypoxia is hypoxia-inducible transcription factor 1 (HIF-1) which transactivates hundreds of genes including angiogenic and autocrine growth factors and receptors, glycolytic enzymes and extracellular proteases [77]. In *in vivo* and *in vitro* models of colon cancer, oxygen deprivation resulted in proteasome-independent decreased expression of Bax and Bid, strongly impairing tumor cells sensitivity to agents with different mechanisms of action [78].

Despite a strong effort to develop anti-angiogenetic therapies, they have produced modest objective responses in clinical trials [79,80], but overall they have not yielded long-term survival benefits [81]. It is reasonable to expect that destroying the vasculature would severely compromise the delivery of oxygen and therapeutics to the solid tumor, producing hypoxia that would render many chemotherapeutics less effective. Indeed, some studies showed that antiangiogenic therapy can compromise the delivery of drugs to tumors [82], as well as antagonize the outcome of therapy [83,84]. New approaches consider the concept of “normalizing” tumor vasculature, in order to grant an optimal drug delivery to the tumor and a correct oxygenation. The correct dosage, the window of administration and the combination with chemotherapeutic drugs are some of the determinant

factors to be considered for the development of an efficacious cancer therapy [85].

Cancer Associated Fibroblasts

Cancer Associated Fibroblasts (CAFs) are one of the most abundant cell types in tumor stroma. A precise characterization of CAFs and the identification of their origin is lacking, but it is known that CAFs can express specific markers such as alpha smooth muscle actin (αSMA), fibroblast activation protein (FAP), tenascin-C or desmin [86]. CAFs can secrete soluble factors and/or regulate the ECM composition. In experimental models of colorectal cancer, interaction of tumor cells with CAFs results in hyperactivated TGF-β1 signaling and subsequent transdifferentiation of the fibroblasts into α-SMA-positive CAFs. In turn this leads to cumulative production of TGF-β1 and proteinases within the tumor microenvironment, creating a cancer-promoting feedback loop [87]. Moreover, it was recently shown that CAF-Derived Hepatocyte Growth Factor is able to inhibit Paclitaxel-induced apoptosis of lung cancer cells by up-regulating the PI3K/Akt signaling [88]. Interestingly, a similar mechanism has also been described in breast cancer models. Conditioned medium (CM) from breast CAFs not only induced Triple Negative Breast Cancer (TNBC) cells migration but it was also able to protect TNBC cells from Doxorubicin treatment. TNBC cells protection was specifically associated with high mobility group box 1 (HMGB1) production induced by CAFs [89]. HMGB1 neutralization, in fact, was able to re-sensitize TNBC cells to chemotherapeutic action, highlighting the relevance of CAF/TNBC cells interaction in drug resistance phenomenon.

Immune system

Immune system is responsible for the elimination of pathogens, damaging agents and developing tumors. Even if the immune system is a powerful weapon against tumors, cancer cells are often able to direct immune response in order to evade or preclude the intervention of immune cells. Both innate immunity and adaptive immunity can be impaired or evaded by tumors. As an example, co-culture with macrophages led to TGF-β mediated upregulation of Slug and L1CAM in colon cancer cells thereby elevating cell motility and apoptosis resistance [90]. Moreover, cathepsin-expressing macrophages protect breast cancer cells from cell death induced by taxol, etoposide and doxorubicin. Indeed, the combination of anti-cathepsin with taxol treatment enhances the anti-tumor efficacy, the late-stage survival and decreases the metastatic burden as compared to taxol alone in a breast cancer mouse model [91]. Tumor Associate Macrophages (TAMs) can also influence $CD8^+$ cytotoxic lymphocyte (CTL) action, for example reducing the efficacy of paclitaxel therapy in breast cancer [92]. In a mouse model of breast adenocarcinoma, it was shown that a doxorubicin treatment enhances the proliferation of IFN-γ and IL-17 producing $CD8^+$ T cells. Moreover, it was demonstrated a positive correlation between the CD8α, CD8β and IFN-γ expression and the efficacy of doxorubicin treatment in patients with breast cancer [93]. Another fundamental player in immune mediated drug resistance is the pool of regulatory T cells (Tregs). This kind of lymphocyte population acts on a plethora of different processes, and their role in cancer development and drug resistance is controversial. These cells seem to act in a context dependent manner, and tumors can take advantage

of their predominance in tumor microenvironment. The equilibrium between CTLs and Tregs in tumors seems fundamental to predict their response to chemotherapies. In fact, in an advanced non-small cell lung cancer context, a high Treg/CTL ratio is associated with a poor response to platinum-based chemotherapy [94] whereas their presence is associated with a better survival exclusively in chemotherapy treated patients with an early breast cancer [94].

Epithelial to Mesenchymal Transition and Tumor Stem Cells

The epithelial–mesenchymal transition (EMT) represents a cellular program that confers on neoplastic epithelial cells the biological traits needed to accomplish most of the steps of the invasion–metastasis cascade [95–97]. EMT Transcription Factors (EMT-TFs) are usually expressed by a cell in response to certain contextual signals received by the same cell; alternatively EMT-TFs expression may be forced experimentally. Most EMT-TFs are transcriptional repressors and many, such as Snail [98], Slug [99], Zeb1 [100] and Twist [101], directly repress mediators of epithelial adhesion, the most important of which is E-Cadherin. The expression of these EMT-TFs causes a profound re-arrangement of cell behavior and tissue organization with widespread functional ramification. In the context of carcinoma development, the EMT-inducing signals appear to originate in the adjacent stroma. For example, the TGF-β growth factor has emerged as a major regulator of EMT in development [102] and disease [103]. While certain carcinoma cells can be induced to readily undergo an EMT in response to treatment with TGF-β, the great majority of epithelial cell lines fail to do so

[104]. This indicates that in many biological contexts, exposure to TGF-β, while necessary, may not be sufficient to induce an EMT and may therefore require the collaborative actions of yet other signaling agents.

The activation of EMT programs has been associated with the acquisition of stem cell (SC) traits by normal and neoplastic cells [105,106]. Among other implications, this finding suggests that neoplastic cell populations do not need to invent novel SC programs in order to acquire a SC phenotype; instead, EMT programs would seem to provide a ready source of CSCs (cancer stem cells) by enabling the dedifferentiation of the more epithelial cells within carcinomas. This connection between EMT and epithelial SCs indicates that the EMT process is doubly dangerous for the cancer patient: by imparting mesenchymal traits to carcinoma cells, an EMT can generate cellular traits associated with high-grade malignancy, including motility, invasiveness and a resistance to apoptosis; these can lead in turn to metastatic dissemination [95]. In addition, by imparting the trait of self-renewal to carcinoma cells, the EMT creates cancer cells that are qualified to seed the large colonies of cancer cells that form metastases. CSCs exhibit a number of features that would not seem to be directly connected to the trait of self-renewal, but might nonetheless be positively regulated by EMT-TFs. For example, Twist has been shown to directly suppress apoptosis through various mechanisms: by suppressing the pro-apoptotic effects of the Myc oncogene [107] through activation of NF-kappaB signaling [108], and by repression of p53-induced pro-apoptotic genes [109]. The EMT- TF Slug has also been shown to antagonize p53-induced apoptosis, by repressing the Bcl-2 antagonist PUMA in normal hematopoietic progenitor

cells [110], and in the neoplastic cells of chronic myeloid leukemia cells [111]. The resulting elevated resistance to apoptosis might well contribute to a crucial property of metastasizing CSCs by promoting carcinoma cell survival during early steps of metastasis and, following dissemination, during their attempts at gaining a foothold in distant, potentially inhospitable tissue microenvironments.

Different consideration must be done when analyzing non-epithelial tumors, such as Glioblastoma multiforme (GBM). The origin of CSCs in GBM are not clear, but there are two major accredited theories. The first one states that GBM CSCs arise from mutated neural stem cells [112] . The second theory is that a more mature cell type acquires self-renewal capacity and gives rise to CSCs [112]. Whichever is the origin of GBM CSCs, it is widely accepted that tumor relapses are driven by CSCs having escaped multimodal therapy [113]. Possible explanations for treatment failure include insufficient drug delivery or the fact that the treatment targets only more differentiated tumor cells (the tumor bulk), while sparing the small subpopulation of CSC (e.g. via CSC specific mechanisms to escape chemotherapy-induced cell death) [114,115]. TMZ (8-Carbamoyl-3-methylimidazo (5, 1-d)-1, 2, 3, 5-tetrazin-4(3H)-one) is an alkylating agent commonly used for the chemotherapy of GBM. The expression of O6-methylguanine-DNA- methyltransferase (MGMT) in GBM CSCs, for example, results in a 10-fold increase of TMZ-resistance [116]. The chemoresistance of MGMT-positive CSCs fits well to the clinical observations that patients without methylation of the MGMT promoter rarely survive longer than 2 years [117]. However, MGMT is only one of the factors involved in GBM drug resistance, TMZ concentrations in the brain

parenchyma, TMZ dosing schemes, hypoxic microenvironments, niche factors, and the re-acquisition of stem cell properties by non-stem cells must be considered in order to approach a possible efficacious therapy against GBM [113]. In *in vivo* models of GBM, for example, it was shown that brain tumors could not have a precise hierarchy. It was observed, in fact, that $CD133^-$ cells derived from GBM patients not only were tumorigenic when implanted into the rat brains but also that they can give rise to tumors containing $CD133^+$ cells [118]. As CD133 is widely known to be a stemness marker [113], there are two main hypothesis: either CD133 is not an appropriate marker for brain CSCs or not-stem cells can “de-differentiate” to stem cells. A lot of work is needed to be conducted to clarify this point, in order to develop the most appropriate therapeutic strategy for GBM.

Shooting to the target: the personalized medicine

During the last decade, many mechanisms underlying the drug resistance phenomenon were uncovered and used to develop molecular target therapies. Despite very important achievements in the comprehension of molecular events characterizing tumor response to therapy, drug resistance remains a major health problem. The response rate to specific target therapy is around 10-20%, response are short-lived and definitely results in relapse and disease progression [119,120].

One of the reasons of targeted therapy frequent inefficacy is due to tumor heterogeneity. Tumors develop from successive clonal expansions of cells, which are not genetically stable and develop divergent genotypes. Heterogeneity is detectable among the same kind of tumor in different patients or even inside the tumor itself [121]. Inter-tumor heterogeneity is well exemplified by NSCLC (Non-Small Cell Lung Cancer) subtypes, among which there are KRAS, epidermal growth factor receptor (EGFR), phosphatidylinositol-4,5-bisphosphate 3-kinase catalytic subunit alpha (PI3KCA), PTEN mutations, anaplastic lymphoma kinase (ALK), ROS1 translocations, and fibroblast growth factor receptor 1 (FGFR1), platelet-derived growth factor receptor alpha (PDGFRA) amplifications [122]. These genetic subtypes set the stage for different therapeutic options for NSCLC. Among the others, EGFR activating mutations, mainly in-frame deletions in exon 19 and a missense mutation at codon 858 (L858R), are found in 13% of NSCLC cases and render patients responsive to EGFR inhibitors [123]. Currently, genotype screening for EGFR activating mutations is used to select patients to receive EGFR inhibitors as first-line treatment. About 5% of

NSCLC cancer patients harbor an EML4 and ALK fusion gene, encoding a fusion protein with constitutive activation of ALK, and these patients do not benefit from EGFR inhibitors [123]. However, they exhibit a 57% response rate and 9-month progression-free survival after treatment with an ALK inhibitor. KRAS mutations, which occur in 24% of NSCLC cases and appear mutually exclusive with EGFR mutations or with ALK translocations, are a strong predictor of non-responsiveness to EGFR inhibitors [124], and chemotherapy is the unique option for these patients. Genetic testing for somatic mutations in lung cancer biopsies is becoming the routine procedure prior to drug treatment and it is expected that this procedure will be modified to cover more subtypes, such as patients with FGFR1 amplifications or ROS1 translocations.

Intra-tumor genetic diversity is another factor strongly influencing the outcome of targeted therapies. It is widely known, in fact, that acquired resistance may sometimes result from the outgrowth of resistant clones that were originally present in the primary cancer at low frequency and are enriched over time under the selective pressure imposed by targeted therapies [125]. For example, the activating mutation T790M in the EGFR gene, which accounts for 50% of acquired resistance to the selective small molecule EGFR inhibitor gefitinib in NSCLC, was found to exist in a small fraction of tumor cells even before drug treatment [126]. Similarly, subpopulations of cells with MET amplification, which confers resistance in 20% of resistance cases to EGFR inhibitors [127], were identified in tumors prior to drug exposure.

The recognition of heterogeneous properties of tumors has profoundly influenced cancer treatment approach. It is now clear that the administration of a single drug for all the tumors of the same anatomical origin is an utopist view. The optimal therapeutic strategy should take in consideration the intra- and inter-tumor heterogeneity through the identification of the so-called “biomarkers”.

Biomarkers are measurable characteristics that can be used to guide clinical decision making, such as determining which patients should receive a particular treatment and/or early assessment of treatment response. Biomarker-guided personalized medicine is now a reality, as many drugs developed with this approach are now in clinical use or in clinical trials [123]. The detection of teranostic markers and of the best target medical therapy implies deep molecular characterization of tumor biology, which can be achieved only using appropriate cancer modelling systems.

Drug resistance experimental models

As described in the previous paragraph, oncology drug development switched from a generic "reduce proliferation and increase cell death" approach to a more targeted strategy, taking into account the heterogeneity of tumors and all the possible variables. However, the approval for anti-cancer drugs is lower than in any other disease area [128]. This lack of clinical efficacy has been pointed to the poor predicting value of pre-clinical models. The fact is that mouse pre-clinical models in oncology have had and continue to have a crucial role in drug development. Advances in oncology rely heavily on mouse models to confirm the biological relevance of candidate targets on tumor maintenance or growth, to establish a therapeutic window between efficacy and toxicity, to determine efficacious drug exposure targets for the clinic, to validate diagnostic hypotheses, and to identify biomarkers of tumor response [129]. Mouse models are easy to handle and manipulate, effective in reproducing and housing but there are some limitations, as it is intrinsic to every kind of model: life span is short, telomere length is altered and prevalence/onset of some tumors are different from human tumors. However, in the last ten years, the number of available models has exponentially increased, thanks to the genome editing techniques (Cas/CRISPR system), RNA interference (RNAi) technology as well as the great diffusion of Patient Derived Xenografts (PDX). In the following paragraphs is outlined a short overview of the principal models for anti-cancer drug studies (**Fig. 3**).

Cancer Cell Lines

One choice for cancer modelling could be using *in vitro* primary cell cultures. These are cells obtained directly from human cancers and thus are considered as a precious resource. However, it is difficult to control the quality of the tissue obtained from the operating room and it is important to identify the cells required for culture and ensure that these are present. Primary cell cultures are difficult to use, hard to obtain, and show relevant heterogeneity. For some tumour types, where it is very difficult to obtain primary cell cultures, cell lines may be the only option for study. Cell lines are widely used to explore new aspects of cancer biology, from the role of individual molecules, to the role of cellular processes. They are easy to use, grow rapidly, produce reproducible results and can be genetically manipulated [130]. Nevertheless, there are some disadvantages: cell lines are adapted to grow in cell culture medium, which provides a very different environment to that which they experienced in their originating tumor [131]. Within tumors, cancer cells are normally capable of independent growth and show reduced attachment to substrate (usually basement membrane proteins) and to other cells. In contrast, cell lines may become dependent on growth factors supplied as serum or other supplements and adherence to plastic. Conventional two dimensional (2D) platforms are well established but the absence of the third dimension (3D) can obscure the experimental observations, generating misleading and contradictory results [132]. Whereas cells on 2D are exposed to a uniform environment with sufficient oxygen and nutrients, cells in solid tumors are exposed to gradients of critical chemical and biological signals, which can exert both stimulatory and

inhibitory effects on tumor progression [133]. Finally, the lack of the complex 3D ECM network structures in monolayer cultures can affect drug-testing results: while anti-cancer agents applied to a monolayer cell culture typically reach cells without physical barriers, the same therapeutics delivered *in vivo* encounter an entirely different environment that significantly restricts the partition of the drugs throughout the entire tumor [134]. For these reasons, researchers have developed various 3D models that recapitulate certain features of solid tumor tissues, such as tumor morphology [135], gradient distribution of chemical and biological factors [136] and dynamic and reciprocal interactions between tumor and its stroma [135]. The intricate molecular network of tumor-associated stromal ECM is an important component of the tumor microenvironment, and plays crucial roles in cancer progression and invasion [137]. Advanced engineering technologies have enabled cancer researchers to create matrix-derived 3D tumor models that more closely recapitulate pathophysiological features of native tumor tissues [138]. The product, known as Matrigel™ or Cultrex® [139] consisting of collagen type IV, perlecan/HSPG2 and laminin, has been considered the material of choice for 3D cancer cell culture because provide a realistic and controllable environment. 3D models are more reliable platforms for generating predictive results but remain relatively simplistic and do not exhaustively represent the native tumor microenvironment [140]. It is for this reason that *in vitro* proof-of -concepts necessarily need to be confirmed by *in vivo* studies.

Cell line xenografts

The *in vivo* study of tumor cell lines was made possible by the development of athymic nude mice [141,142]. Nude mice are immunodeficient, a fundamental pre-requisite in order to avoid human cells rejection. Human cell lines xenografts are easy to handle, to treat and to monitor. However, all the concerns about cell lines still remains, among which the lack of heterogeneity in consequence of *in vitro* clonal selection. Moreover, it is obvious that it is not possible to test the efficacy of drugs targeting the immune system in immunodeficient models. However, distinct disease subtypes (estrogen receptor-positive breast cancer, triple-negative breast cancer, etc.) can be identified within cell line collections [143,144] suggesting that profiling drugs across a sufficiently wide range of cell line xenograft models could enable representation of the full diversity of the disease. In addition, xenografts can be divided in two classes, depending on the position of the growing tumor: heterotopic and orthotopic. In a heterotopic model, cells are injected in a different tissue from the primary tissue of origin (usually subcutaneously); in an orthotopic model, cells are injected in order to develop a tumor growing in the primary tissue of origin. In case of heterotopic xenografts, tumor cells may be inoculated on one flank of the animal or both flanks. Subcutaneous xenograft models have been popular because they are easy to establish, easy to manage, and allow ready quantitation of the tumor burden, but there is not a proper representation of context tissue and development of metastasis. Orthotopic xenograft models, in which the tumor cells are implanted in the tumor site of origin, are advantageous for their ability to mimic local tumor growth and

recapitulate the pathways of metastasis seen in human cancers. In addition, recent innovations in cell labelling techniques and small-animal imaging have enabled investigators to monitor the metastatic process and quantitate the growth and spread of orthotopically implanted tumors [145]. Recently,

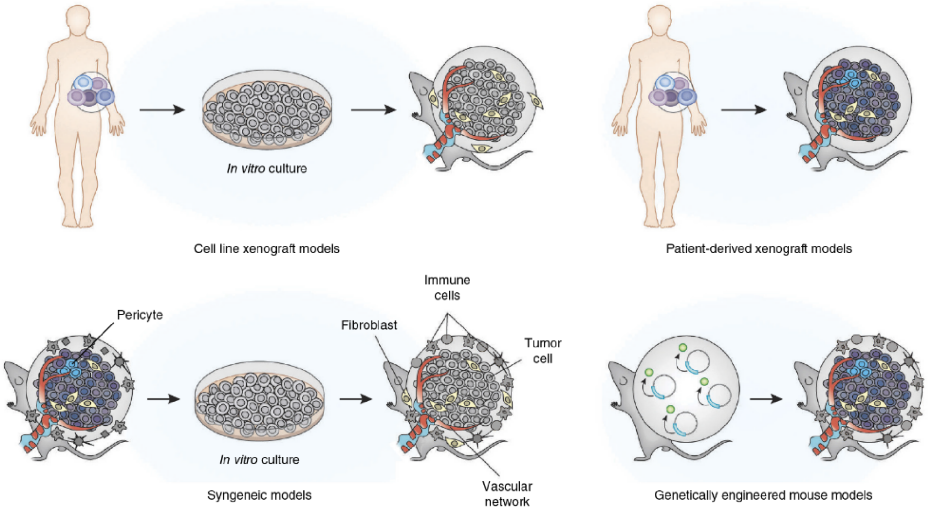

Figure 3 Pre-clinical *in vivo* models for anti-cancer drug discovery [129].

minimally invasive techniques have been developed. One example is represented by the TARCI technique, that is trans-anal rectal cell injection, in which cancer cells are injected into the rectal submucosal, instead of intervening surgically [146].

Patient derived Xenografts

Currently, there is a widespread effort in academia, the pharmaceutical industry and contract research organizations to directly implant human tumors into mice to generate a large number of so-called patient-derived xenografts (PDXs) [129]. In these models, tumors from patients are grafted into immunodeficient mice, avoiding the *in vitro* culture and the consequent

clonal selection. PDXs retain the histological features and genetic heterogeneity more reliably than cell line xenografts [147–149], and they are currently used for the so called “co-clinical” studies. The co-clinical approach synchronizes preclinical with clinical trials by running human patients and mouse models in parallel and allows real- time integration of information. Mouse models offer a mirror image to human clinical trials to discover/validate biomarkers and to facilitate clinical decision making and accelerate progress of clinical trials [123,150]. However, multiple passages in recipient animals, could eventually lead to the selection of some tumor clones [149], which not necessarily represent the initial tumor heterogeneity. However, such divergence could be useful to study the evolution of tumors, maybe also in consequence of anti-cancer drug administration [151].

PDXs are receiving substantial attention and investment, but it has not been established that PDX models are more reliable in predicting patient response to therapy than standard cell line xenografts. In addition, and as noted above, the immunocompromised systems needed to enable xenotransplantation do not allow for cancer immunotherapy evaluation, and subcutaneous engraftment poses additional limitations. Moreover, limitations of cell line xenografts remain, such as the lack of human microenvironment, the variable therapeutic response caused by species difference, a more rapid tumor growth rate than that seen in most cancer patients [123].

Immunocompetent Allografts

Immunocompetent models of mouse tumors have been established in order to take into account the relevance of the immune system in cancer therapy. In the allograft model, mouse tumor cells are transplanted into syngeneic mouse, in a heterotopic or orthotopic site. Mouse tumor cell lines are generally obtained from chemical mutagenesis or from GEMMs (Genetically Engineered Mouse Models) [129]. However, the panel of available mouse tumor cell lines is much more limited than human cell lines. Moreover, chemical mutated or GEMM derived cell lines usually carry a limited set of mutations and many studies showed that anti-tumor immune response is directly linked with mutational load [152–154]. In addition, it must be considered that the resulting allografted tumor is a mouse tumor, in a mouse microenvironment with a mouse immune system. It is possible to detect a lot of differences between mouse and human immune system, and a direct translational application of the experimental results is not always possible [155–157]. In order to overcome the problem of a mouse immune system, the so-called 'humanized mouse models' have been established by genetically replacing mouse genes with human genes or by reconstituting a human immune system in severe immunocompromised mice [158,159]. Although these approaches are still limited by incomplete repopulation of all hematopoietic lineages, incomplete differentiation and abnormal lymphoid structures, these models are useful for addressing specific questions.

GEMMs

Genetic manipulation of the mouse genome in order to introduce germline or conditional modifications has widely contributed to the discovery of the mechanisms involved in oncogenesis, tumor progression and tumor biology. GEMMs of cancer have been designed to harbor mutations that mimic the somatic alterations observed in human tumors [160]. These models are different from transplantable tumor models in that they recapitulate important features of cancer aetiology, such as protracted evolution in an immune competent system, which involves complex native tissue remodelling and stromal incorporation. However, all the withdrawals about treating a mouse cancer and not the human one have to be taken into consideration.

By interbreeding multiple strains of genetically modified alleles each with their own tissue specific and temporal control of gene expression, sophisticated models can be generated to explore tumorigenesis and therapeutic intervention [161,162]. One of the interesting uses of GEMMs is based on the concept of benchmarking against a desired phenotype [163]. As an example, in an inducible NRAS mouse model of melanoma, the genetic extinction of oncogenic NRAS results in complete tumor regression, hence defining a desired "ideal" state [164]. Benchmarking against such a molecular state allowed for identification of a drug combination that more closely simulates the efficacy of genetic NRAS extinction.

The right model

Given the previous considerations, it is clear that there is not a model better than an other one for the study of anti-cancer drugs. It is fundamental to

choose the right model on the basis of the biology of the target that is under analysis (pharmacokinetics, pharmacodynamics, efficacy, toxicity, immune system, tumor stroma etc.) and the goal of the study. Complex phenomena are rarely describable through a single simple model, but often require to be studied from a multi-faceted point of view.

A well-known example is that of the MET proto-oncogene, the receptor tyrosine kinase and its cognate ligand, hepatocyte growth factor (HGF). Mouse HGF does not functionally activate human MET, and therefore xenotransplantation experiments are not suitable for testing eventual paracrine effects of HGF-Met signalling [165]. Mouse models are useful only if they reproduce the biology of the studied phenomenon, as in the case of anti-programmed death-ligand 1 (PDL1) therapy. Clinical responses were observed in phase 1 clinical trials in non-small cell NSCLC, melanoma and renal cell carcinoma although preclinical efficacy was observed in a very limited number of models [166].

Preclinical activity in one or two well-chosen models may be sufficient to advance novel therapies into a clinical trial depending on the biology of the target and the mechanism of action of the drug.

Scope of the Thesis

Chapter 2: Resveratrol inhibits proliferation and strongly decreases motility in glioma stem cells, modulating the Wnt signaling pathway

Glioblastoma multiforme (GBM) is a grade IV astrocytoma with a highly infiltrative nature and wide intra-tumoral heterogeneity. Glioma Stem Cells (GSCs) are believed to be the real driving force of tumor initiation, progression and relapse. Our aim was to investigate Resveratrol (RSV, a polyphenolic phytoalexin) effects on cell viability, proliferation, morphology and motility in seven GSC lines isolated from GBM, with particular attention to the modulation of Wnt pathway.

Chapter 3: A functional biological network centered on XRCC3: a new possible marker of chemoradiotherapy resistance in rectal cancer patients

The prediction of response to Preoperative chemoradiotherapy (pCRT) can potentially classify disease subphenotypes of rectal cancer that could be used to approach an individualized therapeutic strategy. The aim of this work was to integrate gene expression analysis with a commonly used clinical predictive classifier in colorectal cancer, in order to identify important players in the prediction of the response to treatment.

Chapter 4: Inhibition of GSK3β Bypass Drug Resistance of p53-Null Colon Carcinomas by Enabling Necroptosis in Response to Chemotherapy

Impairment of apoptotic cascade is one of the main mechanisms known to be involved in drug resistance. In this work, our aim was to characterize the role of GSK3β in the processes of colorectal cancer drug resistance, using p53-null colon cancer cell lines with different sets of mutations ad *in vivo* xenograft studies. Obtained results were further validated in tumor samples from colorectal cancer patients in order to verify if GSK3β could be a potential teranostic marker in clinical practice.

Chapter 5: The TGF-β pathway is activated by 5-fluorouracil treatment in drug resistant colorectal carcinoma cells

TGF-β pathway is known to be a master regulator of the processes of tumor development and dissemination. However, TGF-β specific role in cancer chemoresistance has not been studied in depth. Our aim was to use gene and protein expression analysis and phenotypic assays in order to assess the involvement of TGF-β pathway in colon cancer chemoresistance. To achieve this aim 3D *in vitro* and *in vivo* xenograft models were used.

References

1. Longley D, Johnston P. Molecular mechanisms of drug resistance. J Pathol. 2005;205:275–92.

2. Wilson TR, Longley DB, Johnston PG. Chemoresistance in solid tumours. Ann Oncol. 2006;17:x315–24.

3. Gottesman MM, Fojo T, Bates SE. Multidrug resistance in cancer: role of ATP-dependent transporters. Nat Rev Cancer. 2002;2:48–58.

4. Ambudkar S V, Dey S, Hrycyna CA, Ramachandra M, Pastan I, Gottesman MM. Biochemical, cellular, and pharmacological aspects of the multidrug transporter. Annu Rev Pharmacol Toxicol. 1999;39:361–98.

5. Thomas H, Coley HM. Overcoming multidrug resistance in cancer: an update on the clinical strategy of inhibiting p-glycoprotein. Cancer Control. 10:159–65.

6. Goldman B. Multidrug resistance: can new drugs help chemotherapy score against cancer? J Natl Cancer Inst. 2003;95:255–7.

7. Krishna R, Mayer LD. Multidrug resistance (MDR) in cancer. Mechanisms, reversal using modulators of MDR and the role of MDR modulators in influencing the pharmacokinetics of anticancer drugs. Eur J Pharm Sci. 2000;11:265–83.

8. Wilson BJ, Schatton T, Zhan Q, Gasser M, Ma J, Saab KR, Schanche R, Waaga-Gasser A-M, Gold JS, Huang Q, Murphy GF, Frank MH, Frank NY. ABCB5 Identifies a Therapy-Refractory Tumor Cell Population in Colorectal Cancer Patients. Cancer Res. 2011;71:5307–16.

9. Callaghan R, Luk F, Bebawy M. Inhibition of the multidrug resistance P-glycoprotein: time for a change of strategy? Drug Metab Dispos. 2014;42:623–31.

10. Longley DB, Harkin DP, Johnston PG. 5-Fluorouracil: Mechanisms of Action and Clinical Strategies. Nat Rev Cancer. 2003;3:330–8.

11. Salonga D, Danenberg KD, Johnson M, Metzger R, Groshen S, Tsao-Wei DD, Lenz HJ, Leichman CG, Leichman L, Diasio RB, Danenberg P V. Colorectal tumors responding to 5-fluorouracil have low gene expression levels of dihydropyrimidine dehydrogenase, thymidylate synthase, and thymidine phosphorylase. Clin Cancer Res. 2000;6:1322–7.

12. Okumura K, Shiomi H, Mekata E, Kaizuka M, Endo Y, Kurumi Y, Tani T. Correlation between chemosensitivity and mRNA expression level of 5-fluorouracil-related metabolic enzymes during liver metastasis of colorectal cancer. Oncol Rep. 2006;15:875–82.

13. Capello M, Lee M, Wang H, Babel I, Katz MH, Fleming JB, Maitra a., Wang H, Tian W, Taguchi a., Hanash SM. Carboxylesterase 2 as a Determinant of Response to Irinotecan and Neoadjuvant FOLFIRINOX Therapy in Pancreatic Ductal Adenocarcinoma. JNCI J Natl Cancer Inst. 2015;107:djv132–djv132.

14. Johnston PG, Lenz HJ, Leichman CG, Danenberg KD, Allegra CJ, Danenberg P V, Leichman L. Thymidylate synthase gene and protein expression correlate and are associated with response to 5-fluorouracil in human colorectal and gastric tumors. Cancer Res. 1995;55:1407–12.

15. Lenz HJ, Hayashi K, Salonga D, Danenberg KD, Danenberg P V, Metzger R, Banerjee D, Bertino JR, Groshen S, Leichman LP, Leichman CG. p53 point mutations and thymidylate synthase messenger RNA levels in disseminated colorectal cancer: an analysis of response and survival. Clin Cancer Res. 1998;4:1243–50.

16. Chu E, Koeller DM, Johnston PG, Zinn S, Allegra CJ. Regulation of thymidylate synthase in human colon cancer cells treated with 5-fluorouracil and interferon-gamma. Mol Pharmacol. 1993;43:527–33.

17. Giannakakou P, Sackett DL, Kang YK, Zhan Z, Buters JT, Fojo T, Poruchynsky MS. Paclitaxel-resistant human ovarian cancer cells have mutant beta-tubulins that exhibit impaired paclitaxel-driven polymerization. J Biol Chem. 1997;272:17118–25.

18. Kavallaris M, Tait AS, Walsh BJ, He L, Horwitz SB, Norris MD, Haber M. Multiple microtubule alterations are associated with Vinca alkaloid resistance in human leukemia cells. Cancer Res. 2001;61:5803–9.

19. Jordan MA, Wendell K, Gardiner S, Derry WB, Copp H, Wilson L. Mitotic block induced in HeLa cells by low concentrations of paclitaxel (Taxol) results in abnormal mitotic exit and apoptotic cell death. Cancer Res. 1996;56:816–25.

20. Levallet G, Bergot E, Antoine M, Creveuil C, Santos AO, Beau-Faller M, de Fraipont F, Brambilla E, Levallet J, Morin F, Westeel V, Wislez M, Quoix E, et al. High TUBB3 expression, an independent prognostic marker in patients with early non-small cell lung cancer treated by preoperative chemotherapy, is regulated by K-Ras signaling pathway. Mol Cancer Ther. 2012;11:1203–13.

21. Issa JP. The epigenetics of colorectal cancer. Ann N Y Acad Sci. 2000;910:140–53; discussion 153–5.

22. King BL, Carcangiu ML, Carter D, Kiechle M, Pfisterer J, Pfleiderer A, Kacinski BM. Microsatellite instability in ovarian neoplasms. Br J Cancer. 1995;72:376–82.

23. Paulson TG, Wright FA, Parker BA, Russack V, Wahl GM. Microsatellite instability correlates with reduced survival and poor disease prognosis in breast cancer. Cancer Res. 1996;56:4021–6.

24. Yamashita K, Arimura Y, Saito M, Suzuki H, Furuhata T, Hirata K, Shinomura Y. Gastric cancers with microsatellite instability sharing clinical features, chemoresistance and germline MSH6 variants. Clin J Gastroenterol. 2013;6:122–6.

25. Brown R, Hirst GL, Gallagher WM, McIlwrath AJ, Margison GP, van der Zee AG, Anthoney DA. hMLH1 expression and cellular responses of ovarian tumour cells to treatment with cytotoxic anticancer agents. Oncogene. 1997;15:45–52.

26. Mori S, Ogata Y, Shirouzu K. Biological features of sporadic colorectal carcinoma with high-frequency microsatellite instability: special reference to tumor proliferation and apoptosis. Int J Clin Oncol. 2004;9:322–9.

27. Levine AJ. p53, the cellular gatekeeper for growth and division. Cell. 1997;88:323–31.

28. Ljungman M. Dial 9-1-1 for p53: mechanisms of p53 activation by cellular stress. Neoplasia. 2:208–25.

29. Dotto GP. p21WAF1/Cip1: more than a break to the cell cycle? Biochim Biophys Acta - Rev Cancer. 2000;1471:M43–56.

30. Zhan Q, Chen IT, Antinore MJ, Fornace AJ. Tumor suppressor p53 can participate in transcriptional induction of the GADD45 promoter in the absence of direct DNA binding. Mol Cell Biol. 1998;18:2768–78.

31. Vousden KH. p53: death star. Cell. 2000;103:691–4.

32. Schmitt C a, Rosenthal CT, Lowe SW. Genetic analysis of chemoresistance in primary murine lymphomas. Nat Med. 2000;6:1029–35.

33. Oda K, Arakawa H, Tanaka T, Matsuda K, Tanikawa C, Mori T, Nishimori H, Tamai K, Tokino T, Nakamura Y, Taya Y. p53AIP1, a potential mediator of p53-dependent apoptosis, and its regulation by Ser-46-phosphorylated p53. Cell. 2000;102:849–62.

34. Bunz F, Hwang PM, Torrance C, Waldman T, Zhang Y, Dillehay L, Williams J, Lengauer C, Kinzler KW, Vogelstein B. Disruption of p53 in human cancer cells alters the responses to therapeutic agents. J Clin Invest. 1999;104:263–9.

35. Van Oijen MG, Slootweg PJ. Gain-of-function mutations in the tumor suppressor gene p53. Clin Cancer Res. 2000;6:2138–45.

36. Johnstone RW, Ruefli AA, Lowe SW. Apoptosis: a link between cancer genetics and chemotherapy. Cell. 2002;108:153–64.

37. Lavarino C, Pilotti S, Oggionni M, Gatti L, Perego P, Bresciani G, Pierotti M a, Scambia G, Ferrandina G, Fagotti A, Mangioni C, Lucchini V, Vecchione F, et al. P53 Gene Status and Response To Platinum/Paclitaxel-Based Chemotherapy in Advanced Ovarian Carcinoma. J Clin Oncol. 2000;18:3936–45.

38. Gadducci A, Cianci C, Cosio S, Carnino F, Buttitta F, Fanucchi A, Conte PF, Genazzani AR. p53 status is neither a predictive nor a prognostic variable in

patients with advanced ovarian cancer treated with a paclitaxel-based regimen. Anticancer Res. 2000;20:4793–9.

39. Johnson KR, Fan W. Reduced expression of p53 and p21WAF1/CIP1 sensitizes human breast cancer cells to paclitaxel and its combination with 5-fluorouracil. Anticancer Res. 2002;22:3197–204.

40. Narod S a, Foulkes WD. BRCA1 and BRCA2: 1994 and beyond. Nat Rev Cancer. 2004;4:665–76.

41. Venkitaraman AR. Cancer susceptibility and the functions of BRCA1 and BRCA2. Cell. 2002;108:171–82.

42. Farmer H, McCabe N, Lord CJ, Tutt ANJ, Johnson D a, Richardson TB, Santarosa M, Dillon KJ, Hickson I, Knights C, Martin NMB, Jackson SP, Smith GCM, et al. Targeting the DNA repair defect in BRCA mutant cells as a therapeutic strategy. Nature. 2005;434:917–21.

43. Ratnam K, Low JA. Current development of clinical inhibitors of poly(ADP-ribose) polymerase in oncology. Clin Cancer Res. 2007;13:1383–8.

44. Wang W, Figg WD. Secondary BRCA1 and BRCA2 alterations and acquired chemoresistance. Cancer Biol Ther. 2008;7:1004–5.

45. Edwards SL, Brough R, Lord CJ, Natrajan R, Vatcheva R, Levine D a, Boyd J, Reis-Filho JS, Ashworth A. Resistance to therapy caused by intragenic deletion in BRCA2. Nature. 2008;451:1111–5.

46. Hengartner MO. The biochemistry of apoptosis. Nature. 2000;407:770–6.

47. Kang J, Jun S, Chong F, Zi V, Ooi Q, Vali S, Kumar A. Overexpression of Bcl-2 induces STAT-3 activation via an increase in mitochondrial superoxide. 2015;

48. Lee H-J, Zhuang G, Cao Y, Du P, Kim H-J, Settleman J. Drug resistance via feedback activation of Stat3 in oncogene-addicted cancer cells. Cancer Cell. 2014;26:207–21.

49. Teixeira C, Reed JC, Pratt MA. Estrogen promotes chemotherapeutic drug resistance by a mechanism involving Bcl-2 proto-oncogene expression in human breast cancer cells. Cancer Res. 1995;55:3902–7.

50. Nagata S. Fas ligand-induced apoptosis. Annu Rev Genet. 1999;33:29–55.

51. Botti C, Buglioni S, Benevolo M, Giannarelli D, Papaldo P, Cognetti F, Vici P, Di Filippo F, Del Nonno F, Venanzi FM, Natali PG, Mottolese M. Altered expression of FAS system is related to adverse clinical outcome in stage I-II breast cancer patients treated with adjuvant anthracycline-based chemotherapy. Clin Cancer Res. 2004;10:1360–5.

52. Paschall A V, Yang D, Lu C, Choi J-H, Li X, Liu F, Figueroa M, Oberlies NH, Pearce C, Bollag WB, Nayak-Kapoor A, Liu K. H3K9 Trimethylation Silences Fas Expression To Confer Colon Carcinoma Immune Escape and 5-Fluorouracil Chemoresistance. J Immunol. 2015;1402243.

53. Blume-Jensen P, Hunter T. Oncogenic kinase signalling. Nature. 2001;411:355–65.

54. Nagane M, Levitzki A, Gazit A, Cavenee WK, Huang HJ. Drug resistance of human glioblastoma cells conferred by a tumor-specific mutant epidermal growth factor receptor through modulation of Bcl-XL and caspase-3-like proteases. Proc Natl Acad Sci U S A. 1998;95:5724–9.

55. Messersmith WA, Ahnen DJ. Targeting EGFR in colorectal cancer. N Engl J Med. 2008;359:1834–6.

56. Chen X, Yeung TK, Wang Z. Enhanced Drug Resistance in Cells Coexpressing ErbB2 with EGF Receptor or ErbB3. Biochem Biophys Res Commun. 2000;277:757–63.

57. Servidei T, Riccardi A, Mozzetti S, Ferlini C, Riccardi R. Chemoresistant tumor cell lines display altered epidermal growth factor receptor and HER3 signaling and enhanced sensitivity to gefitinib. Int J Cancer. 2008;123:2939–49.

58. Forde JE, Dale TC. Glycogen synthase kinase 3: a key regulator of cellular fate. Cell Mol Life Sci. 2007;64:1930–44.

59. Vogelstein B, Kinzler KW. Cancer genes and the pathways they control. Nat Med. 2004;10:789–99.

60. Shakoori A, Mai W, Miyashita K, Yasumoto K, Takahashi Y, Ooi A, Kawakami K, Minamoto T. Inhibition of GSK-3 beta activity attenuates proliferation of human colon cancer cells in rodents. Cancer Sci. 2007;98:1388–93.

61. Shakoori A, Ougolkov A, Yu ZW, Zhang B, Modarressi MH, Billadeau DD, Mai M, Takahashi Y, Minamoto T. Deregulated GSK3β activity in colorectal cancer: Its association with tumor cell survival and proliferation. Biochem Biophys Res Commun. 2005;334:1365–73.

62. Miyashita K, Kawakami K, Nakada M, Mai W, Shakoori A, Fujisawa H, Hayashi Y, Hamada J -i., Minamoto T. Potential Therapeutic Effect of Glycogen Synthase Kinase 3 Inhibition against Human Glioblastoma. Clin Cancer Res. 2009;15:887–97.

63. Mai W, Kawakami K, Shakoori A, Kyo S, Miyashita K, Yokoi K, Jin M, Shimasaki T, Motoo Y, Minamoto T. Deregulated GSK3{beta} sustains gastrointestinal cancer cells survival by modulating human telomerase reverse transcriptase and telomerase. Clin Cancer Res. 2009;15:6810–9.

64. Kitano A, Shimasaki T, Chikano Y, Nakada M, Hirose M, Higashi T, Ishigaki Y, Endo Y, Takino T, Sato H, Sai Y, Miyamoto K-I, Motoo Y, et al. Aberrant glycogen synthase kinase 3β is involved in pancreatic cancer cell invasion and resistance to therapy. PLoS One. 2013;8:e55289.

65. Meads MB, Gatenby R a, Dalton WS. Environment-mediated drug resistance: a major contributor to minimal residual disease. Nat Rev Cancer. 2009;9:665–74.

66. Castells M, Thibault B, Delord J-P, Couderc B. Implication of Tumor Microenvironment in Chemoresistance: Tumor-Associated Stromal Cells Protect Tumor Cells from Cell Death. Int J Mol Sci. 2012;13:9545–71.

67. Correia AL, Bissell MJ. The tumor microenvironment is a dominant force in multidrug resistance. Drug Resist Updat. 2012;15:39–49.

68. McGrail DJ, Khambhati NN, Qi MX, Patel KS, Ravikumar N, Brandenburg CP, Dawson MR. Alterations in Ovarian Cancer Cell Adhesion Drive Taxol

Resistance by Increasing Microtubule Dynamics in a FAK-dependent Manner. Sci Rep. 2015;5:9529.

69. Xing H, Weng D, Chen G, Tao W, Zhu T, Yang X, Meng L, Wang S, Lu Y, Ma D. Activation of fibronectin/PI-3K/Akt2 leads to chemoresistance to docetaxel by regulating survivin protein expression in ovarian and breast cancer cells. Cancer Lett. 2008;261:108–19.

70. Holmgren L, O'Reilly MS, Folkman J. Dormancy of micrometastases: balanced proliferation and apoptosis in the presence of angiogenesis suppression. Nat Med. 1995;1:149–53.

71. Ferrara N, Gerber H-P, LeCouter J. The biology of VEGF and its receptors. Nat Med. 2003;9:669–76.

72. Samuel S, Fan F, Dang LH, Xia L, Gaur P, Ellis LM. Intracrine vascular endothelial growth factor signaling in survival and chemoresistance of human colorectal cancer cells. Oncogene. 2011;30:1205–12.

73. Dias S, Shmelkov S V, Lam G, Rafii S. VEGF(165) promotes survival of leukemic cells by Hsp90-mediated induction of Bcl-2 expression and apoptosis inhibition. Blood. 2002;99:2532–40.

74. Tran J, Master Z, Yu JL, Rak J, Dumont DJ, Kerbel RS. A role for survivin in chemoresistance of endothelial cells mediated by VEGF. Proc Natl Acad Sci U S A. 2002;99:4349–54.

75. Cho HJ, Kim I-K, Park S-M, Baek KE, Nam I-K, Park S-H, Ryu K-J, Choi J, Ryu J, Hong S-C, Jeong S-H, Lee Y-J, Ko G-H, et al. VEGF-C mediates RhoGDI2-induced gastric cancer cell metastasis and cisplatin resistance. Int J Cancer. 2014;135:1553–63.

76. Virrey JJ, Guan S, Li W, Schönthal AH, Chen TC, Hofman FM. Increased survivin expression confers chemoresistance to tumor-associated endothelial cells. Am J Pathol. 2008;173:575–85.

77. Semenza GL. Targeting HIF-1 for cancer therapy. Nat Rev Cancer. 2003;3:721–32.

78. Erler JT, Cawthorne CJ, Williams KJ, Koritzinsky M, Wouters BG, Wilson C, Miller C, Demonacos C, Stratford IJ, Dive C. Hypoxia-mediated down-regulation of Bid and Bax in tumors occurs via hypoxia-inducible factor 1-dependent and -independent mechanisms and contributes to drug resistance. Mol Cell Biol. 2004;24:2875–89.

79. Yang JC, Haworth L, Sherry RM, Hwu P, Schwartzentruber DJ, Topalian SL, Steinberg SM, Chen HX, Rosenberg SA. A randomized trial of bevacizumab, an anti-vascular endothelial growth factor antibody, for metastatic renal cancer. N Engl J Med. 2003;349:427–34.

80. Cobleigh MA, Langmuir VK, Sledge GW, Miller KD, Haney L, Novotny WF, Reimann JD, Vassel A. A phase I/II dose-escalation trial of bevacizumab in previously treated metastatic breast cancer. Semin Oncol. 2003;30:117–24.

81. Mayer RJ. Two steps forward in the treatment of colorectal cancer. N Engl J Med. 2004;350:2406–8.

82. Ma J, Pulfer S, Li S, Chu J, Reed K, Gallo JM. Pharmacodynamic-mediated reduction of temozolomide tumor concentrations by the angiogenesis inhibitor TNP-470. Cancer Res. 2001;61:5491–8.

83. Murata R, Nishimura Y, Hiraoka M. An antiangiogenic agent (TNP-470) inhibited reoxygenation during fractionated radiotherapy of murine mammary carcinoma. Int J Radiat Oncol Biol Phys. 1997;37:1107–13.

84. Fenton BM, Paoni SF, Ding I. Effect of VEGF receptor-2 antibody on vascular function and oxygenation in spontaneous and transplanted tumors. Radiother Oncol. 2004;72:221–30.

85. Jain RK. Normalization of tumor vasculature: an emerging concept in antiangiogenic therapy. Science. 2005;307:58–62.

86. Xing F, Saidou J, Watabe K. Cancer associated fibroblasts (CAFs) in tumor microenvironment. Front Biosci. 2010;15:166–79.

87. Hawinkels LJ a C, Paauwe M, Verspaget HW, Wiercinska E, van der Zon JM, van der Ploeg K, Koelink PJ, Lindeman JHN, Mesker W, ten Dijke P, Sier

CFM. Interaction with colon cancer cells hyperactivates TGF-β signaling in cancer-associated fibroblasts. Oncogene. 2014;33:97–107.

88. Ying L, Zhu Z, Xu Z, He T, Li E, Guo Z, Liu F, Jiang C, Wang Q. Cancer Associated Fibroblast-Derived Hepatocyte Growth Factor Inhibits the Paclitaxel-Induced Apoptosis of Lung Cancer A549 Cells by Up-Regulating the PI3K/Akt and GRP78 Signaling on a Microfluidic Platform. PLoS One. 2015;10:e0129593.

89. Amornsupak K, Insawang T, Thuwajit P, O-Charoenrat P, Eccles S a, Thuwajit C. Cancer-associated fibroblasts induce high mobility group box 1 and contribute to resistance to doxorubicin in breast cancer cells. BMC Cancer. 2014;14:955.

90. Schäfer H, Struck B, Feldmann E-M, Bergmann F, Grage-Griebenow E, Geismann C, Ehlers S, Altevogt P, Sebens S. TGF-β1-dependent L1CAM expression has an essential role in macrophage-induced apoptosis resistance and cell migration of human intestinal epithelial cells. Oncogene. 2013;32:180–9.

91. Shree T, Olson OC, Elie BT, Kester JC, Garfall AL, Simpson K, Bell-Mcguinn KM, Zabor EC, Brogi E, Joyce J a. Macrophages and cathepsin proteases blunt chemotherapeutic response in breast cancer. Genes Dev. 2011;25:2465–79.

92. DeNardo DG, Brennan DJ, Rexhepaj E, Ruffell B, Shiao SL, Madden SF, Gallagher WM, Wadhwani N, Keil SD, Junaid S a., Rugo HS, Shelley Hwang E, Jirström K, et al. Leukocyte complexity predicts breast cancer survival and functionally regulates response to chemotherapy. Cancer Discov. 2011;1:54–67.

93. Mattarollo SR, Loi S, Duret H, Ma Y, Zitvogel L, Smyth MJ. Pivotal role of innate and adaptive immunity in anthracycline chemotherapy of established tumors. Cancer Research. 2011. 4809-4820 p.

94. Liu H, Zhang T, Ye J, Li H, Huang J, Li X, Wu B, Huang X, Hou J. Tumor-infiltrating lymphocytes predict response to chemotherapy in patients with advance non-small cell lung cancer. Cancer Immunol Immunother. 2012;61:1849–56.

95. Singh a, Settleman J. EMT, cancer stem cells and drug resistance: an emerging axis of evil in the war on cancer. Oncogene. 2010;29:4741–51.

96. Thiery JP, Acloque H, Huang RYJ, Nieto MA. Epithelial-mesenchymal transitions in development and disease. Cell. 2009;139:871–90.

97. Acloque H, Adams MS, Fishwick K, Bronner-Fraser M, Nieto MA. Epithelial-mesenchymal transitions: The importance of changing cell state in development and disease. J Clin Invest. 2009;119:1438–49.

98. Cano a, Pérez-Moreno M a, Rodrigo I, Locascio A, Blanco MJ, del Barrio MG, Portillo F, Nieto M a. The transcription factor snail controls epithelial-mesenchymal transitions by repressing E-cadherin expression. Nat Cell Biol. 2000;2:76–83.

99. Bolós V, Peinado H, Pérez-Moreno M a, Fraga MF, Esteller M, Cano A. The transcription factor Slug represses E-cadherin expression and induces epithelial to mesenchymal transitions: a comparison with Snail and E47 repressors. J Cell Sci. 2003;116:499–511.

100. Eger A, Aigner K, Sonderegger S, Dampier B, Oehler S, Schreiber M, Berx G, Cano A, Beug H, Foisner R. DeltaEF1 is a transcriptional repressor of E-cadherin and regulates epithelial plasticity in breast cancer cells. Oncogene. 2005;24:2375–85.

101. Yang M-H, Hsu DS-S, Wang H-W, Wang H-J, Lan H-Y, Yang W-H, Huang C-H, Kao S-Y, Tzeng C-H, Tai S-K, Chang S-Y, Lee OK-S, Wu K-J. Bmi1 is essential in Twist1-induced epithelial-mesenchymal transition. Nat Cell Biol. 2010;12:982–92.

102. Oft M, Peli J, Rudaz C, Schwarz H, Beug H, Reichmann E. TGF-Beta1 and Ha-Ras collaborate in modulating the phenotypic plasticity and invasiveness of epithelial tumor cells. Genes Dev. 1996;10:2462–77.

103. Yang M-H, Wu M-Z, Chiou S-H, Chen P-M, Chang S-Y, Liu C-J, Teng S-C, Wu K-J. Direct regulation of TWIST by HIF-1alpha promotes metastasis. Nat Cell Biol. 2008;10:295–305.

104. Brown K a, Aakre ME, Gorska AE, Price JO, Eltom SE, Pietenpol J a, Moses HL. Induction by transforming growth factor-beta1 of epithelial to

mesenchymal transition is a rare event in vitro. Breast Cancer Res. 2004;6:R215–31.

105. Mani S a, Guo W, Liao M-J, Eaton EN, Ayyanan A, Zhou AY, Brooks M, Reinhard F, Zhang CC, Shipitsin M, Campbell LL, Polyak K, Brisken C, et al. The epithelial-mesenchymal transition generates cells with properties of stem cells. Cell. 2008;133:704–15.

106. Morel A-P, Lièvre M, Thomas C, Hinkal G, Ansieau S, Puisieux A. Generation of breast cancer stem cells through epithelial-mesenchymal transition. PLoS One. 2008;3:e2888.

107. Valsesia-Wittmann S, Magdeleine M, Dupasquier S, Garin E, Jallas AC, Combaret V, Krause A, Leissner P, Puisieux A. Oncogenic cooperation between H-Twist and N-Myc overrides failsafe programs in cancer cells. Cancer Cell. 2004;6:625–30.

108. Pham CG, Bubici C, Zazzeroni F, Knabb JR, Papa S, Kuntzen C, Franzoso G. Upregulation of Twist-1 by NF-kappaB blocks cytotoxicity induced by chemotherapeutic drugs. Mol Cell Biol. 2007;27:3920–35.

109. Maestro R, Dei Tos AP, Hamamori Y, Krasnokutsky S, Sartorelli V, Kedes L, Doglioni C, Beach DH, Hannon GJ. Twist is a potential oncogene that inhibits apoptosis. Genes Dev. 1999;13:2207–17.

110. Wu WS, Heinrichs S, Xu D, Garrison SP, Zambetti GP, Adams JM, Look a. T. Slug antagonizes p53-mediated apoptosis of hematopoietic progenitors by repressing puma. Cell. 2005;123:641–53.

111. Mancini M, Petta S, Iacobucci I, Salvestrini V, Barbieri E, Santucci MA. Zinc-finger transcription factor slug contributes to the survival advantage of chronic myeloid leukemia cells. Cell Signal. 2010;22:1247–53.

112. Gilbertson RJ, Rich JN. Making a tumour's bed: glioblastoma stem cells and the vascular niche. Nat Rev Cancer. 2007;7:733–6.

113. Beier D, Schulz JB, Beier CP. Chemoresistance of glioblastoma cancer stem cells - much more complex than expected. Mol Cancer. 2011;10:128.

114. Bao S, Wu Q, McLendon RE, Hao Y, Shi Q, Hjelmeland AB, Dewhirst MW, Bigner DD, Rich JN. Glioma stem cells promote radioresistance by preferential activation of the DNA damage response. Nature. 2006;444:756–60.

115. Hirschmann-Jax C, Foster AE, Wulf GG, Nuchtern JG, Jax TW, Gobel U, Goodell MA, Brenner MK. A distinct “side population” of cells with high drug efflux capacity in human tumor cells. Proc Natl Acad Sci U S A. 2004;101:14228–33.

116. Hermisson M, Klumpp A, Wick W, Wischhusen J, Nagel G, Roos W, Kaina B, Weller M. O6-methylguanine DNA methyltransferase and p53 status predict temozolomide sensitivity in human malignant glioma cells. J Neurochem. 2006;96:766–76.

117. Hegi ME, Diserens A-C, Gorlia T, Hamou M-F, de Tribolet N, Weller M, Kros JM, Hainfellner J a, Mason W, Mariani L, Bromberg JEC, Hau P, Mirimanoff RO, et al. MGMT gene silencing and benefit from temozolomide in glioblastoma. N Engl J Med. 2005;352:997–1003.

118. Wang J, Sakariassen P, Tsinkalovsky O, Immervoll H, Bøe SO, Svendsen A, Prestegarden L, Røsland G, Thorsen F, Stuhr L, Molven A, Bjerkvig R, Enger P. CD133 negative glioma cells form tumors in nude rats and give rise to CD133 positive cells. Int J Cancer. 2008;122:761–8.

119. Engelman JA, Settleman J. Acquired resistance to tyrosine kinase inhibitors during cancer therapy. Curr Opin Genet Dev. 2008;18:73–9.

120. O’Hare T, Zabriskie MS, Eiring AM, Deininger MW. Pushing the limits of targeted therapy in chronic myeloid leukaemia. Nat Rev Cancer. 2012;12:513–26.

121. Marusyk A, Polyak K. Tumor heterogeneity: Causes and consequences. Biochim Biophys Acta - Rev Cancer. 2010;1805:105–17.

122. Heist RS, Engelman JA. SnapShot: Non-Small Cell Lung Cancer. Cancer Cell. 2012;21:448–448.e2.

123. Huang M, Shen A, Ding J, Geng M. Molecularly targeted cancer therapy: some lessons from the past decade. Trends Pharmacol Sci. 2014;35:41–50.

124. Linardou H, Dahabreh IJ, Kanaloupiti D, Siannis F, Bafaloukos D, Kosmidis P, Papadimitriou CA, Murray S. Assessment of somatic k-RAS mutations as a mechanism associated with resistance to EGFR-targeted agents: a systematic review and meta-analysis of studies in advanced non-small-cell lung cancer and metastatic colorectal cancer. Lancet Oncol. 2008;9:962–72.

125. Turner NC, Reis-Filho JS. Genetic heterogeneity and cancer drug resistance. Lancet Oncol. 2012;13:e178–85.

126. Kobayashi S, Boggon TJ, Dayaram T, Jänne PA, Kocher O, Meyerson M, Johnson BE, Eck MJ, Tenen DG, Halmos B. EGFR Mutation and Resistance of Non–Small-Cell Lung Cancer to Gefitinib. N Engl J Med. 2005;352:786–92.

127. Engelman JA, Zejnullahu K, Mitsudomi T, Song Y, Hyland C, Park JO, Lindeman N, Gale C-M, Zhao X, Christensen J, Kosaka T, Holmes AJ, Rogers AM, et al. MET Amplification Leads to Gefitinib Resistance in Lung Cancer by Activating ERBB3 Signaling. Science (80-). 2007;316:1039–43.

128. Hay M, Thomas DW, Craighead JL, Economides C, Rosenthal J. Clinical development success rates for investigational drugs. Nat Biotechnol. 2014;32:40–51.

129. Gould SE, Junttila MR, de Sauvage FJ. Translational value of mouse models in oncology drug development. Nat Med. 2015;21:431–9.

130. Cree IA, Glaysher S, Harvey AL. Efficacy of anti-cancer agents in cell lines versus human primary tumour tissue. Curr Opin Pharmacol. 2010;10:375–9.

131. Fernando A, Glaysher S, Conroy M, Pekalski M, Smith J, Knight LA, Di Nicolantonio F, Cree IA. Effect of culture conditions on the chemosensitivity of ovarian cancer cell lines. Anticancer Drugs. 2006;17:913–9.

132. Hutmacher DW. Biomaterials offer cancer research the third dimension. Nat Mater. 2010;9:90–3.

133. Mehta G, Hsiao AY, Ingram M, Luker GD, Takayama S. Opportunities and challenges for use of tumor spheroids as models to test drug delivery and efficacy. J Control Release. 2012;164:192–204.

134. Goodman TT, Ng CP, Pun SH. 3-D tissue culture systems for the evaluation and optimization of nanoparticle-based drug carriers. Bioconjug Chem. 2008;19:1951–9.

135. Gurski L a, Xu X, Labrada LN, Nguyen NT, Xiao L, van Golen KL, Jia X, Farach-Carson MC. Hyaluronan (HA) interacting proteins RHAMM and hyaluronidase impact prostate cancer cell behavior and invadopodia formation in 3D HA-based hydrogels. PLoS One. 2012;7:e50075.

136. Fracasso G, Colombatti M. Effect of therapeutic macromolecules in spheroids. 2000;36:159–78.

137. Dutta RC, Dutta AK. Cell-interactive 3D-scaffold; advances and applications. Biotechnol Adv. 2009;27:334–9.

138. Hutmacher DW, Loessner D, Rizzi S, Kaplan DL, Mooney DJ, Clements J a. Can tissue engineering concepts advance tumor biology research? Trends Biotechnol. 2010;28:125–33.

139. Fridman R, Benton G, Aranoutova I, Kleinman HK, Bonfil RD. Increased initiation and growth of tumor cell lines, cancer stem cells and biopsy material in mice using basement membrane matrix protein (Cultrex or Matrigel) co-injection. Nat Protoc. 2012;7:1138–44.

140. Xu X, Farach-Carson MC, Jia X. Three-dimensional in vitro tumor models for cancer research and drug evaluation. Biotechnol Adv. 2014;32:1256–68.

141. Pantelouris E. Absence of Thymus in a Mouse Mutant. Nature. 1968;217:370–1.

142. Rygaard J, Povlsen CO. Heterotransplantation of a human malignant tumour to “Nude” mice. Acta Pathol Microbiol Scand. 1969;77:758–60.

143. Neve RM, Chin K, Fridlyand J, Yeh J, Baehner FL, Fevr T, Clark L, Bayani N, Coppe J-P, Tong F, Speed T, Spellman PT, DeVries S, et al. A collection of

breast cancer cell lines for the study of functionally distinct cancer subtypes. Cancer Cell. 2006;10:515–27.

144. Domcke S, Sinha R, Levine D a, Sander C, Schultz N. Evaluating cell lines as tumour models by comparison of genomic profiles. Nat Commun. 2013;4:2126.

145. Sano D, Myers JN. Xenograft models of head and neck cancers. Head Neck Oncol. 2009;1:32.

146. Donigan M, Norcross LS, Aversa J, Colon J, Smith J, Madero-Visbal R, Li S, McCollum N, Ferrara A, Gallagher JT, Baker CH. Novel murine model for colon cancer: non-operative trans-anal rectal injection. J Surg Res. 2009;154:299–303.

147. Hidalgo M, Amant F, Biankin A V, Budinská E, Byrne AT, Caldas C, Clarke RB, de Jong S, Jonkers J, Mælandsmo GM, Roman-Roman S, Seoane J, Trusolino L, et al. Patient-derived xenograft models: an emerging platform for translational cancer research. Cancer Discov. 2014;4:998–1013.

148. DeRose YS, Wang G, Lin Y-C, Bernard PS, Buys SS, Ebbert MTW, Factor R, Matsen C, Milash BA, Nelson E, Neumayer L, Randall RL, Stijleman IJ, et al. Tumor grafts derived from women with breast cancer authentically reflect tumor pathology, growth, metastasis and disease outcomes. Nat Med. 2011;17:1514–20.

149. Li S, Shen D, Shao J, Crowder R, Liu W, Prat A, He X, Liu S, Hoog J, Lu C, Ding L, Griffith OL, Miller C, et al. Endocrine-therapy-resistant ESR1 variants revealed by genomic characterization of breast-cancer-derived xenografts. Cell Rep. 2013;4:1116–30.

150. Clohessy JG, Pandolfi PP. Mouse hospital and co-clinical trial project-from bench to bedside. Nat Rev Clin Oncol. 2015;12:491–8.

151. Das Thakur M, Stuart DD. Molecular pathways: Response and resistance to BRAF and MEK inhibitors in BRAFV600E tumors. Clin Cancer Res. 2014;20:1074–80.

152. Yadav M, Jhunjhunwala S, Phung QT, Lupardus P, Tanguay J, Bumbaca S, Franci C, Cheung TK, Fritsche J, Weinschenk T, Modrusan Z, Mellman I, Lill

JR, et al. Predicting immunogenic tumour mutations by combining mass spectrometry and exome sequencing. Nature. 2014;515:572–6.

153. Gubin MM, Zhang X, Schuster H, Caron E, Ward JP, Noguchi T, Ivanova Y, Hundal J, Arthur CD, Krebber W-J, Mulder GE, Toebes M, Vesely MD, et al. Checkpoint blockade cancer immunotherapy targets tumour-specific mutant antigens. Nature. 2014;515:577–81.

154. Snyder A, Makarov V, Merghoub T, Yuan J, Zaretsky JM, Desrichard A, Walsh L a, Postow M a, Wong P, Ho TS, Hollmann TJ, Bruggeman C, Kannan K, et al. Genetic Basis for Clinical Response to CTLA-4 Blockade in Melanoma. N Engl J Med. 2014;2189–99.

155. Mestas J, Hughes CCW. Of mice and not men: differences between mouse and human immunology. J Immunol. 2004;172:2731–8.

156. Platzer B, Stout M, Fiebiger E. Antigen cross-presentation of immune complexes. Front Immunol. 2014;5:140.

157. Hsieh CS, Macatonia SE, O'Garra A, Murphy KM. T cell genetic background determines default T helper phenotype development in vitro. J Exp Med. 1995;181:713–21.

158. Ito R, Takahashi T, Katano I, Ito M. Current advances in humanized mouse models. Cell Mol Immunol. 2012;9:208–14.

159. Shultz LD, Brehm M a, Garcia-Martinez JV, Greiner DL. Humanized mice for immune system investigation: progress, promise and challenges. Nat Rev Immunol. 2012;12:786–98.

160. Singh M, Murriel CL, Johnson L. Genetically engineered mouse models: closing the gap between preclinical data and trial outcomes. Cancer Res. 2012;72:2695–700.

161. Cook N, Jodrell DI, Tuveson DA. Predictive in vivo animal models and translation to clinical trials. Drug Discov Today. 2012;17:253–60.

162. Rottenberg S, Borst P. Drug resistance in the mouse cancer clinic. Drug Resist Updat. 2012;15:81–9.

163. Kwong LN, Heffernan TP, Chin L. A Systems Biology Approach to Personalizing Therapeutic Combinations. Cancer Discov. 2013;3:1339–44.

164. Kwong LN, Costello JC, Liu H, Jiang S, Helms TL, Langsdorf AE, Jakubosky D, Genovese G, Muller FL, Jeong JH, Bender RP, Chu GC, Flaherty KT, et al. Oncogenic NRAS signaling differentially regulates survival and proliferation in melanoma. Nat Med. 2012;18:1503–10.

165. Wilson TR, Fridlyand J, Yan Y, Penuel E, Burton L, Chan E, Peng J, Lin E, Wang Y, Sosman J, Ribas A, Li J, Moffat J, et al. Widespread potential for growth-factor-driven resistance to anticancer kinase inhibitors. Nature. 2012;487:505–9.

166. Herbst RS, Soria J-C, Kowanetz M, Fine GD, Hamid O, Gordon MS, Sosman J a., McDermott DF, Powderly JD, Gettinger SN, Kohrt HEK, Horn L, Lawrence DP, et al. Predictive correlates of response to the anti-PD-L1 antibody MPDL3280A in cancer patients. Nature. 2014;515:563–7.

Chapter 2

Resveratrol inhibits proliferation and strongly decreases motility in glioma stem cells, modulating the Wnt signaling pathway

Chiara Cilibrasi[1,2,3], Gabriele Riva[1,2,3], **Gabriele Romano**[1,4], Valentina Butta[1,2], Laura Paoletta[1], Leda Dalprà[1,5], Marialuisa Lavitrano[1], Roberto Giovannoni[1], Angela Bentivegna[1,3 §]

1. Department of Surgery and Translational Medicine, University of Milano-Bicocca, via Cadore 48, 20900 Monza, Italy. **2.** PhD Program in Neuroscience, University of Milano-Bicocca. **3.** NeuroMI, Milan center of Neuroscience. **4.** PhD Program in Translational and Molecular Medicine (DIMET), University of Milano-Bicocca **5.**Medical Genetics Laboratory, S. Gerardo Hospital, via Pergolesi 33, 20900 Monza, Italy

(*Submitted to:* **BMC Cancer**)

Abstract

Background Glioblastoma multiforme (GBM) is a grade IV astrocytoma and the most common form of malignant brain tumor in adults. GBM remains one of the most fatal and least successfully treated solid tumors: current therapies provide a median survival of 12-15 months after diagnosis, due to the high recurrence rate. Glioma Stem Cells (GSCs) are believed to be the real driving force of tumor initiation, progression and relapse. Therefore, better therapeutic strategies GSC-targeted are needed. Resveratrol (RSV) is a polyphenolic phytoalexin found in fruits and vegetables displaying pleiotropic health benefits. Many studies have already highlighted its chemopreventive and chemotherapeutic activities in a wide range of solid tumors.

Methods In this work, we analyzed the effects of RSV exposure on cell viability (MTT, Trypan blue dye exclusion assays), proliferation (mitotic index analysis), morphology and motility (wound healing assay) in seven GSC lines isolated from GBM patients. For the first time in our knowledge we also investigated RSV impact on Wnt signaling pathway in GSCs, evaluating the expression of seven WNT signaling pathway-related genes and c-Myc protein levels.

Results Results showed that response to RSV exposure was highly heterogeneous among GSC lines, but generally it was able to inhibit cell proliferation, increasing cell mortality, and strongly decrease cell motility, modulating the Wnt signaling pathway.

Conclusions Treatment with RSV may represent a new interesting therapeutic approach, in order to affect GSC proliferation and motility, even if further investigations are certainly needed in order to deeply understand the GSC heterogeneous response.

Keywords

Glioblastoma Multiforme, Glioma Stem Cells, Resveratrol, cancer cell proliferation, cancer cell migration, Wnt signaling pathway, gene expression

Introduction

Glioblastoma multiforme (GBM) is a grade IV astrocytoma and the most common form of malignant brain tumor in adults [1]. GBM remains one of the most fatal and least successfully treated solid tumors: current therapies provide a median survival of 12-15 months after diagnosis, due to the high recurrence rate [2, 3].

One of the factors underlying tumor recurrence and poor long-term survival is the marked intratumoral heterogeneity, mirrored by the presence of distinct sub-populations of cells showing different tumorigenic capabilities [4]. In particular Glioma stem cells (GSCs), a small subpopulation of cells with stem-like properties, such as an enhanced self-renewal capacity and a multilineage differentiation potential, are believed to be the real driving force for tumor initiation, progression and relapse [5, 6]. The highly invasive nature of GSCs is another crucial factor that makes this tumor extremely difficult to eradicate, thus resulting in a disseminated disease that is impossible to completely resect [1].

Resveratrol (*trans*-3,4',5 tryhidrostilbene) (RSV) is a natural polyphenolic phytoalexin found in fruits and vegetables, acting as a phytoestrogen and displaying pleiotropic health benefits. This compound has received considerable attention over the last decades, first for its use in treating cardiovascular diseases and then for its neuroprotective effect associated with its ability to cross the blood brain barrier [7]. RSV beneficial effects are underlined by its anti-oxidant and anti-inflammatory action, including the activation of enzymes such as sirtuin1 (SIRT1), a NAD-dependent deacetylase [8].

Interest in RSV took a further upsurge when, in a pioneering study by Jang and Pezzuto, were reported its chemopreventive and antineoplastic activities, demonstrating the efficacy of this phytoalexin in all the three major stages of carcinogenesis (initiation, promotion and progression) [9]. Afterwards many studies have highlighted that RSV has anti-proliferative, pro-apoptotic [10-12] and anti-migratory effects [13-16] in a wide range of human cancer cells. Chemopreventive properties of phytoestrogens such as RSV, has emerged also from epidemiological observations indicating that the incidence of some cancers is much lower in people, who consume high amounts of phytoestrogens [17].

Moreover it has been observed that RSV can directly or indirectly affect self-renewal pathways, frequently impaired or aberrantly activated through either genetic or epigenetic alterations in cancer stem cells [18]. In particular, RSV was shown to be able to significantly inhibit Wnt signaling pathway, a highly evolutionarily conserved pathway that plays a crucial role in stem cell homeostasis, in different tumors [11, 19, 20].

In this study we investigated the effect of RSV on seven established GSC lines, isolated from GBM patients, evaluating its effect on cell viability, proliferation, morphology and motility. For the first time in our knowledge we investigated RSV impact on Wnt signaling pathway in GSCs. We evidenced that RSV differently affects the GSC lines, but, interestingly, in most of the cases it was able to inhibit cell proliferation, increase cell mortality, and strongly decrease cell motility. Moreover, it modulated the expression of Wnt-related genes and induced an evident c-myc protein level reduction.

Methods

Cell Lines and Cell Culture Conditions

All the Glioma stem cell (GSC) lines used in this work (GBM2, GBM7, G144, G179, G166, GliNS2, GBM04) were isolated from patients affected by glioblastoma [21, 22] and extensively characterized for their stem cell properties. In 2013, our research group characterized their cytogenomic and epigenomic profiles [23]. The stemness properties of the GSC lines were periodically monitored, as already described by Baronchelli et al. in 2013. Cell expansion was carried out in a proliferation permissive medium composed by DMEM F-12 (Euroclone) and Neurobasal 1:1 (Invitrogen), B-27 supplement without vitamin A (Invitrogen), 2 mM L-glutamine (Euroclone), 10 ng/ml recombinant human bFGF and 20 ng/ml recombinant human EGF (Miltenyi Biotec), 20 UI/ml penicillin and 20 µg/ml streptomycin (Euroclone) (complete medium). GSCs were cultured in adherent culture condition in T-25 cm^3 flasks coated with 10 µg/ml laminin (Invitrogen), in 5% CO_2/95% O_2 atmosphere.

Drug and treatments

RSV (P.M.=228,24 g/mol) was dissolved in dimethylsulfoxide (DMSO) to make a 100 mM stock solution and then diluted to the final selected concentration (10-50-100-200 µM) with complete cell culture medium. The stock preparation was stored at -20°C. DMSO had no effect on the cell survival. All procedures were carried out in the dark because RSV is photosensitive.

MTT assay

Cell metabolic activity was assessed by the MTT (3-[4,5dimethylthiazol-2-yl]-2,5-diphenyl tetrazolium bromide) assay in order to evaluate the efficacy of RSV. Cells were seeded in 96 well-plates at a density of $4x10^4$ cells/well in 100 µl of culture medium and incubated at 37°C. After 24h, RSV at various concentrations (10-50-

100-200 µM) was added to cell culture medium. After the drug incubation time (24, 48 or 72 hs) MTT solution (1 mg/ml, Sigma) was added to each well and cells were incubated for 3 hs at 37°C. Therefore, formazan was solubilized in absolute ethanol and the absorbance of the dye was measured spectrophotometrically with FLUOstar Omega microplate reader (BMG Labtech) at 595 nm. The percentage of inhibition was determined by comparing the absorbance values of drug-treated cells with that of untreated controls: [(treated-cell absorbance/untreated cell absorbance) × 100]. The results reported are the mean values of two different experiments performed at least in triplicate.

Trypan blue dye exclusion assay

Cells were plated in 60 mm Petri dishes at a density of $1,2x10^6$ cells/ dish and cultured overnight. Then, the cells were treated with different concentrations of RSV (10-100 µM) for 48 or 72 hs. Thereafter, the cells were stained using trypan blue dye (Sigma) to count cell numbers and determine the drug cytotoxic/antiproliferative effects. The treated samples were compared with the untreated controls. The results reported are the mean values of two different experiments.

Mitotic index analysis

The mitotic index (MI) was assessed in order to evaluate RSV effect on cell proliferation. $2x10^6$ cells were seeded in T-25 cm^3 in 5 ml of medium. Subsequently, cells in exponential growth phase were treated with 100 µM RSV for 48 hs. Then metaphase chromosome spreads were obtained using standard procedures as previously described [23].The chromosomes were QFQ-banded using quinacrine mustard (Roche) and slides were mounted in McIlvaine buffer. Slides were analyzed using Nikon Eclipse 80i fluorescence microscope (Nikon) equipped with a COHU High Performance CCD camera. MI was evaluated counting the percentage of mitosis scoring at last 1000 nuclei. Data were obtained as mean values derived from

two independent experiments.

Morphological analysis

To evaluate cell morphology cells were seeded in 6-well plates without laminin coating in proliferative permissive medium at $3x10^3$-10^4 cells/ml, depending on cell growth rate, specific for each GSC line. After 24 hs, cells were treated with RSV (10-50-100-200 μM) for different times of exposure (24-48-72 hs). The cell morphology was evaluated through the observation at phase contrast microscopy, comparing RSV treated and untreated cells. Representative images were taken for each cell line and for each treatment.

Wound healing assay

To evaluate cell motility, cells were plated in 6-well plates without laminin coating in proliferative permissive medium and grown to confluency. Cells were growth-arrested for 24 hs in a medium without growth factors. Then a sterile tip was used to create a scratch in the cell layer and images were captured (0 hs time point). Therefore cells were treated with various concentrations of RSV (10-50-100-200 μM) and pictures were taken after 48, 72 and 96 hs to evaluate wound closure. Matching untreated control cultures were also assessed. Wounds were evaluated using TScratch freeware software (http://www.cse-lab.ethz.ch/), which calculated the fraction of open image area at a later time point compared to the initial time point. The migration distances were expressed as percentages over control values and were calculated as wound area at a given time compared to the initial wound surface.

RNA extraction

RNA extraction from untreated and 100 μM RSV 96 hs treated cells was performed using the miRNeasy Mini Kit (Qiagen), according to the manufacturer's protocol.

Real time – PCR array

RT^2Profiler PCR Arrays (Qiagen) was assessed on untreated and 100 µM RSV 96 hs treated cells in order to evaluate RSV effect on the expression of genes involved in WNT pathway. RNA samples from treated and untreated cells were converted into first-strand cDNA using the RT^2 First Strand Kit (Qiagen). Then, RT^2 Profiler PCR Arrays were assessed according to the manufacturer's protocol using a 12 wells array PCR custom, containing primers for 7 WNT pathway-focused genes (*WNT1, FZD4, CTNNB1, EP300, CREBBP, TCF7, MYC*), and for 2 housekeeping genes (*HPRT1, TBP*). Briefly the cDNA was mixed with an appropriate RT SYBR Green Mastermix. This mixture was aliquoted into the wells of the PCR Array and PCR was performed by means of a real time cycler (Applied Biosystems) properly programmed (1 cycle: 10 min 95°C, 40 cycles: 15 s 95°C, 1 min 60°C). Relative gene expression was determined using data from the real-time cycler and the $\Delta\Delta C_t$ method. The cut-off values for gene expression fold changes was established at +/- 1,5: values $\geq$ +1,5 indicate gene upregulation, while values $\leq$ -1,5 indicate gene downregulation. The gene expression fold changes data were obtained as mean values derived from two independent experiments.

Protein extracts and Western Blotting

Cells were treated for 72 hs with RSV 100 µM. At the end of the treatments cells were trypsinized, collected and lysed using the following buffer: TrisHCl 50 mM, NaCl 500 mM, EDTA 1 mM, EGTA 1 mM, NP-40 0,5% (vol/vol), Protease inhibitor cocktail (Sigma Aldrich) 2% (vol/vol), Phosphatase Inhibitor Cocktail #2 (Sigma Aldrich) 1% (vol/vol), Phosphatase Inhibitor Cocktail #3 (Sigma Aldrich) 1% (vol/vol). Lysates were quantified with Micro-BCA assay (Thermo Scientific), following manufacturer's instructions; 15 µg of protein lysates were loaded on NuPAGE Bis-Tris pre-cast mini gels (Life Technologies). At the end of the run, gels were then

blotted on Nitrocellulose membranes using iBlot 2 (Life Technologies).

After blocking, membranes were incubated with the following primary antibodies: anti c-Myc (Rabbit Monoclonal, Cell Signaling Technology [D84C12]), anti-GAPDH (Mouse Monoclonal, Sigma-Aldrich [GAPDH-71.1]. Secondary HRP-conjugated antibodies used were: ECL™Anti Rabbit and ECL™Anti Mouse (GE Healthcare). Western Blots images were digitally acquired with G-BOX (Syngene). Quantitative densitometry of Western Blot was performed with ImageJ 1.49q (Rasband, W.S, U. S. National Institutes of Health, Bethesda, Maryland, USA, http://imagej.nih.gov/ij/, 1997-2014). The results are expressed as means of four independent experiments. Two-tailed paired t-test was used to detect significant differences in protein expression between Control and Treated groups (GraphPad Prism 6, GraphPad Software, Inc.); p-value<0.05 was considered as significant.

Statistical analysis

Statistical analysis was carried out performing Yates' chi-square test (mitotic index) or t-test (MTT assay, Trypan blue assay, wound healing assay, western blot) on raw data, by means of Excel spreadsheet (Microsoft Office 2007, Microsoft Corporation). The critical level of significance was set at $p<0,05$.

Results

Sensibility and resistance to RSV measured by metabolic activity

The effect of RSV on the metabolic activity was determined by means of MTT assay (Fig. 1, Additional file 1). Metabolic activity values were almost unchanged in all GSC lines after 24 hs of treatment; on the contrary after 48 hs, GBM2, G179 and GBM04 cell lines showed a significant decrease in metabolic activity ($p<0,05$), at the highest doses of RSV in a dose-dependent manner, compared to the matching

untreated cells. Otherwise G166 and G144 showed very faint decrease, and GBM7 and GliNS2 showed even an increase. Exposure to increasing doses of RSV for 72 hs resulted again in a progressive reduction in metabolic activity in GBM2 and G179 cell lines, while GBM04 seems not to be affected by the prolongation of the treatment. Metabolic activity values of GBM7 and GliNS2 remained stable after 48 hs and 72 hs of treatment. G144, GBM7, GliNS2 and G166 can, therefore, be considered resistant to the treatment.

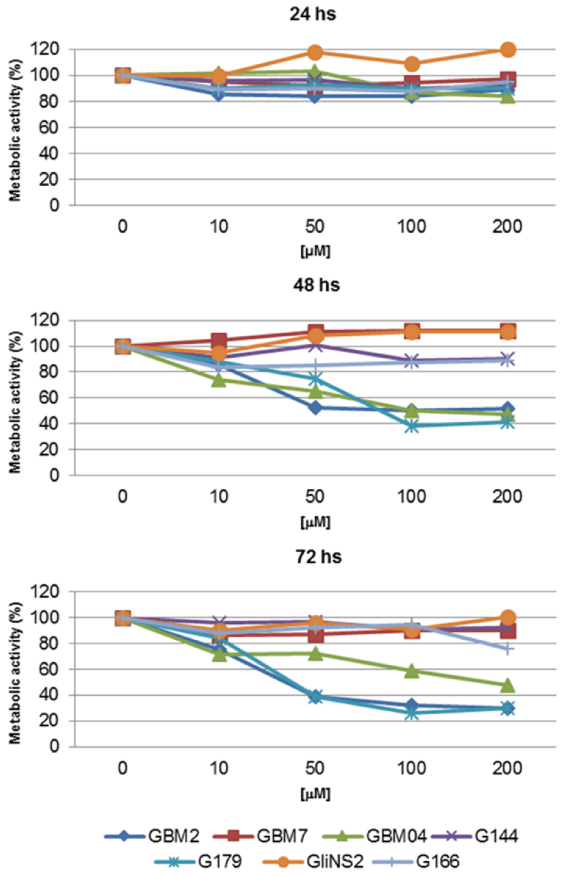

Figure 1. ***RSV effect on GSC metabolic activity. Metabolic activity was analyzed by MTT assay****. Results represent the means from two different experiments performed at least in triplicate and are reported as percentage of drug-treated cells relative to untreated cells.*

RSV effect on GSC viability

GSCs viability was evaluated by means of the Trypan blue dye exclusion assay. The administration of 10 µM RSV didn't induce any relevant changes in GSCs viability after both 48 and 72 hs. Again, GBM2, G179 and GBM04 were the most sensitive cell lines after 48 hs of treatment with 100 µM RSV, showing a significant increase in the percentage of cell mortality (Fig. 2). 72 hs of exposure resulted in a progressive increase in cell death in GBM2 cell line, while G179 and GBM04 cell line seemed not to be affected by the prolongation of the treatment. All the other cell lines showed

lower cell mortality after both 48 hs and 72 hs of 100 µM RSV treatment. These data suggest that in responsive GSCs, RSV had mainly a cytotoxic effect, which is definitely more evident at the highest drug concentration.

RSV effect on GSC proliferation

In order to study the effect of RSV exposure on cellular proliferation, we evaluated the mitotic index (MI). This parameter has very important clinical implications because the mitotic activity is a crucial property related to the tumor aggressiveness. 100 µM RSV for 48 hs revealed a significant decrease of MI in five out of seven cell lines (Fig. 3). In particular in GBM2 and G179 cell lines, which have already been shown to be very sensitive to the drug treatment, the MI was almost zero after RSV administration. GBM04 and GBM7 cell lines didn't show any statistically significant change in MI, probably because the proliferation rate is extremely low even in the untreated cells.

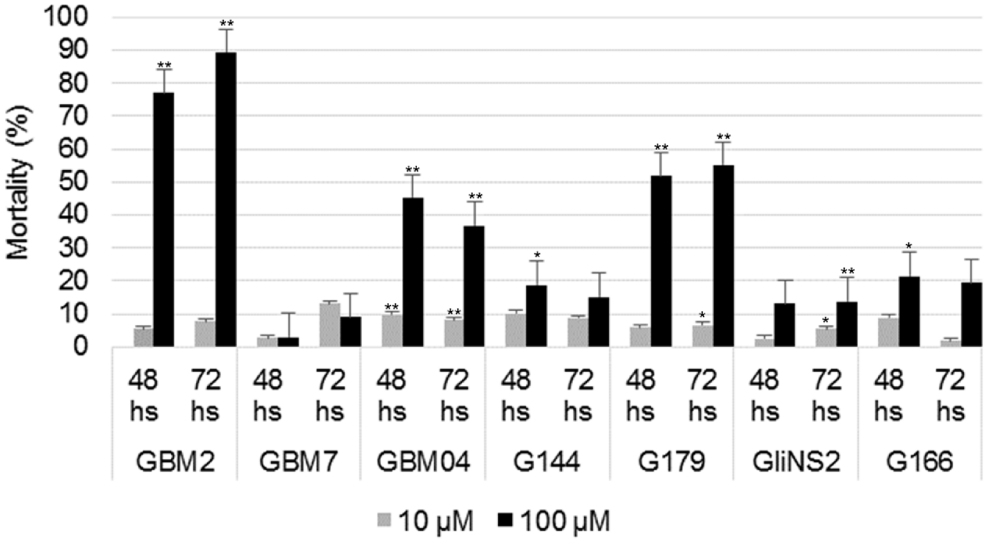

Figure 2. ***RSV effect on GSC viability.*** *Cell viability was analyzed by Trypan blue dye exclusion assay after exposure to two different concentrations of RSV (10-100 µM) for 48 and 72 hs. Results are reported as percentage of cell mortality in drug-treated cells relative to untreated cells and are the means of two different experiments ±SEM. T-test on raw data: * p<0,05; **p<0,001.*

RSV does not induce any morphological change in GSCs

GSC morphology analysis highlighted that generally both untreated and RSV treated GSCs grew in non-adherent growth pattern as neurospheres, forming colonies varying in size. Generally RSV administration did not induce any relevant modification in cellular shape (Fig. 4). An exception is GBM2 cell line, which showed mild changes in morphology after 48 and 72 hs of treatment with low or intermediate concentrations of RSV (10-50-100 μM), revealing the presence of cellular processes and spindle-like structures (Fig. 4). At the highest concentration (200 μM) the morphological changes were less evident probably because of the prevailing cytotoxic effect of the drug.

RSV inhibits GSC motility

The effect of RSV on cell motility was investigated using the wound healing assay. This test was not performed on G166 cell line because, despite the long time of cultivation, cells did not grow to confluence. As shown in the representative images of G179 cell line reported in figure 5A, the untreated cells highlighted a gradual increase of cells in the scratched zone after all the time points. On the contrary, GSCs treated with

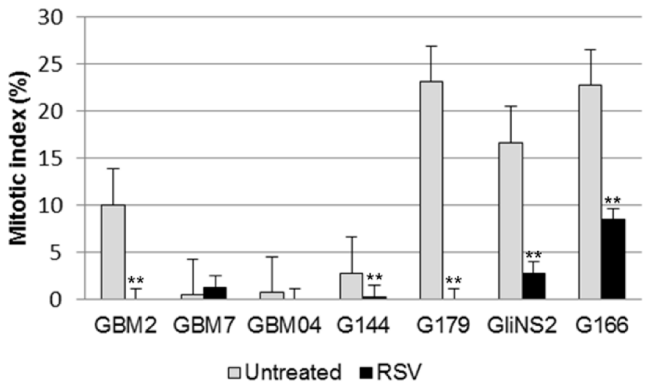

Figure 3. ***RSV effect on GSCs proliferation****. Cell proliferation was evaluated through the determination of the mitotic index. Results are reported as percentages resulting from means of two independent experiments ±SEM. Yates' Chi-square test on raw data: *p<0,01; **p<0,0001.*

different concentrations of RSV seemed to have a reduced ability to migrate and fill the wounded area as compared to the control cells (Fig. 5A).

The quantitative data reported in figure 5B confirm that RSV strongly reduced cellular motility in all GSC lines, in a dose- and time- dependent manner, compared to the untreated cells (Additional file 2). Already after 48 hs of treatment, all GSC lines, and in particular G144, GBM7 and GBM2, showed a significant reduction of their motility, especially at the highest doses of RSV (100-200 µM) (p<0,01). The inhibition of GSCs migration was even more evident after 72 and 96 hs. An interesting behavior was registered for GBM04. In this cell line, the migration slightly decreased only at the higher dosages after 48 and 72 hs, while after 96 hs of RSV exposure cells showed a significant reduction of motility (p<0,0001). However the treatment with the highest dose of RSV for 96 hs, in GBM04, GliNS2 and GBM7 cell lines did not allow us to obtain an adequate number of cells to

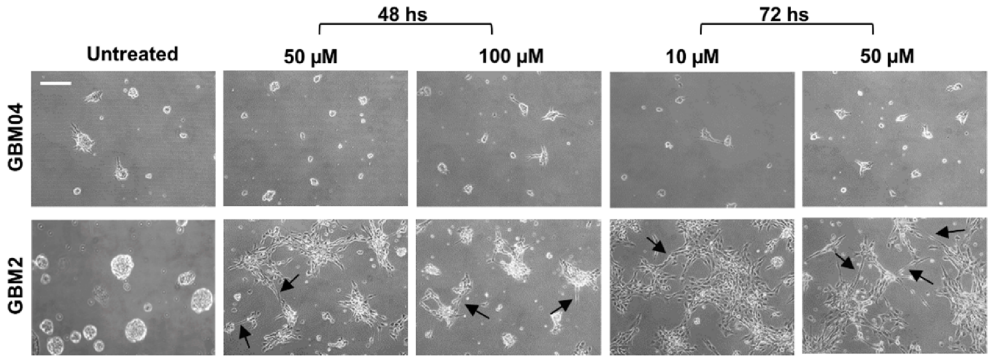

Figure 4. ***Representative images of GSC morphology after treatment with different concentrations of RSV for 24, 48 and 72 hs.*** *Generally RSV did not induce any relevant morphological change in GSCs, as shown in GBM04 cell line. On the contrary 48 and 72 hs exposure to low or intermediate concentrations of RSV induced mild changes in GBM2 cell morphology. Black arrows indicate cellular process and spindle-like structures. (bar = 100 µm).*

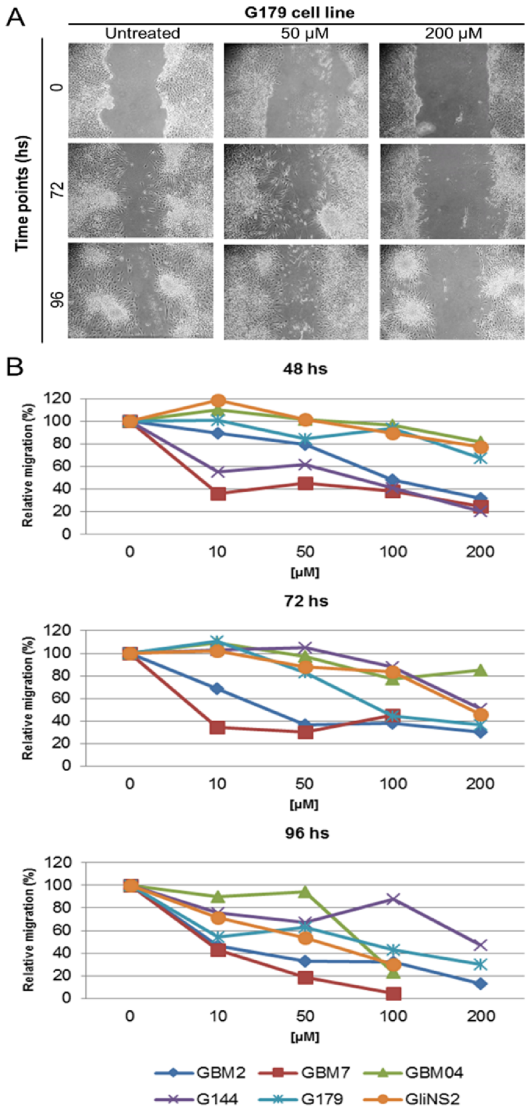

Figure 5. ***RSV reduced GSC motility.*** *The migration ability of GSCs was carried out by the Wound Healing Assay. Monolayers of growth-arrested GSCs were scraped and treated with different concentrations of RSV for 48, 72 and 96 hs. A. Representative images were taken at different time points to evaluate wound closure. B. The migration was quantified by means of the TScratch software and results are reported as percentages over control values and calculated as the wound area at a given time compared to the initial wound surface.*

conduct the experiment, probably because of the prevailing cytotoxic effect of the drug and the extremely low rate of proliferation of these cell lines. GBM7 showed this behavior even after 72 hs of exposure to the highest drug concentration.

RSV effect on Wnt-signaling pathway

The WNT signaling expression profile was performed using Wnt-specific PCR arrays on untreated and 100 µM RSV treated cells for 96 hs in order to explore the expression variations of 7 WNT-related genes. Results showed that RSV was able to modulate Wnt signaling pathway in all GSC lines (Tab. 1). In particular, expression of the ligand WNT1 and the downstream oncogene MYC changed in five out of seven cell lines and often in the same direction.

In fact in GBM2, GBM7, G166, G179 cell lines both WNT1 and MYC were upregulated, while in G144 cell line these two genes were downregulated. The expression levels of FZD4, TCF7 and CREBBP changed only in three or four out of seven GSC lines after RSV exposure. CTNNB1, the most important effector of Wnt signaling pathway, and EP300, generally showed unchanged expression levels.

To investigate if the observed transcriptional upregulation of MYC induced by RSV was associated to an increase in c-Myc protein expression, protein extracts of 3 GSC lines (G144, GliNS2 and GBM2), which highlighted different alterations in MYC expression levels, were analyzed by western blot. As shown in figure 6, RSV administration caused a significant reduction of c-Myc protein in GBM2 cell lines as compared to untreated cells (p=0,0197). Contrarily, no significant effect was observed in G144 or in GliNS2 cells.

	GBM2		GBM7		GMB04		G144		G166		G179		GliNS2	
	F.R.	*Trend*	*F.R.*	*Trend*	*F.R.*	*Trend*	*F.R.*	*Trend*	*F.R.*	*Trend*	*F.R.*	*Trend*	*F.R.*	*Trend*
WNT1	1.7	↑	1.9	↑	1.1	=	-2.1	↓	1.5	↑	1.6	↑	1.5	↑
FZD4	1.6	↑	1.1	=	2.7	↑	1.5	↑	1.2	=	1.4	=	-1.2	=
CTNNB1	1.3	=	1.1	=	-1.1	=	1.8	↑	-1.3	=	-1.8	↓	-1.3	=
EP300	-1.5	↓	1.3	=	-1.1	=	-1.0	=	-1.2	=	-1.0	=	-1.2	=
CREBBP	-1.4	=	1.1	=	-1.6	↓	1.2	=	1.5	↑	-1.3	=	-1.5	↓
TCF7	2.9	↑	6.5	↑	1.1	=	1.5	↑	-1.6	↓	-1.1	=	-1.3	=
c-MYC	23.2	↑	1.7	↑	7.0	↑	-2.4	↓	2.6	↑	4.6	↑	1.2	=

Table. 1 ***Fold regulation and trend of the expression variations of 7 Wnt signaling pathway-related genes induced by 96 hs of exposure to RSV 100 µM.***

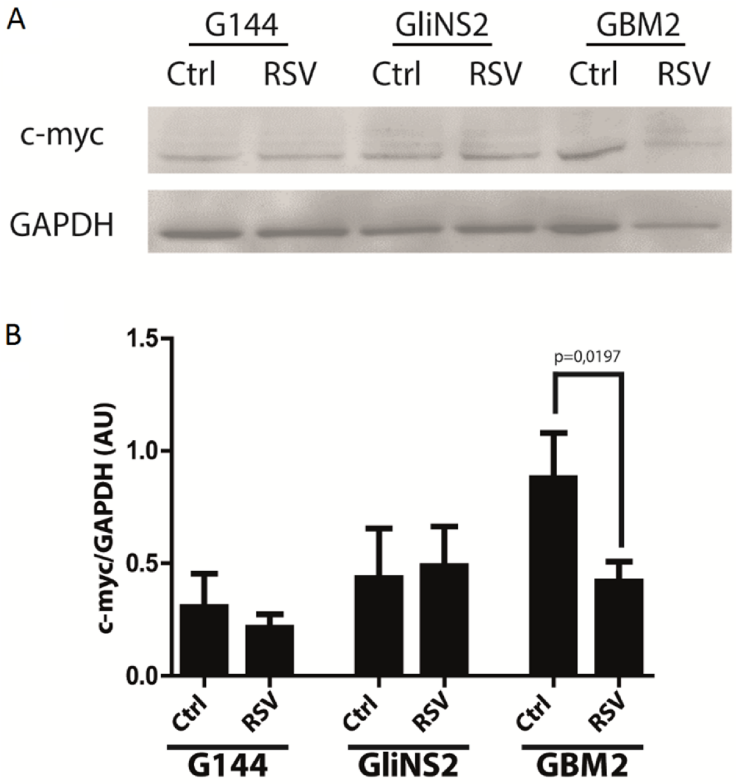

Figure 6. ***c-Myc protein levels are downregulated by RSV administration in GBM2 cells.*** A. *Representative images of western blot analysis of c-Myc on G144, GliNS2 and GBM2 cells total protein extracts. GAPDH was used as loading control.* B. *Quantitative densitometry analysis of 4 independent experiments. c-Myc protein levels were normalized on GAPDH and expressed in Arbitrary Units (AU). Bars represent SEM. Indicated p-values were obtained after two-tailed paired t-test.*

Discussion

Glioblastoma multiforme (GBM) is the most common and malignant type of brain tumor [2, 3]. It is characterized by a cellular hierarchy that culminates with a glioma stem cells (GSCs) population characterized by an enhanced self-renewal, an elevated invasive behavior and the ability to drive tumor formation, maintenance and progression [6]. Unsatisfactory results of standard multimodal GBM treatments have resulted in multiple efforts to search for new therapeutic strategies for the eradication of the stem cell subpopulation in order to achieve an effective treatment for this tumor. The isolation and identification of GSCs have widened the understanding on the biology of GBM and cultured GSC lines are a valuable model for testing drug susceptibility [23-25].

In this study we analyzed for the first time the efficacy of RSV on 7 established GSC lines from GBM, whose cytogenetic, genomic and epigenomic profiles were extensively characterized [23].

RSV is a naturally occurring polyphenol synthesized by a variety of plant species in response to injury, UV irradiation and fungal attack [26]. Accumulating evidences indicated that RSV is able to inhibit multiple cellular events associated with tumor initiation, promotion, and progression, and, therefore, might be a promising chemopreventive and chemotherapeutic agent [9, 27]. Accordingly, the U87 and U251 glioma cell lines have been reported to respond to this drug with cell cycle arrest, induction of autophagy and apoptosis [28, 29] and RSV has been shown to suppress the angiogenesis and tumor growth of gliomas even *in vivo* [30, 31]. Moreover this drug might be useful for the treatment of brain tumors because of its ability to cross the blood brain barrier [32].

In order to characterize the antineoplastic effects of RSV in our GSC lines we evaluated, first of all, cell metabolic activity, viability and proliferation after drug administration.

MTT assays revealed a significant reduction of cell metabolic activity in three cell lines out of seven (GBM2, G179 and GBM04) especially after the longer times of regimens (48 and 72 hs). These data were also confirmed by Trypan blue dye exclusion assays which suggested that in these three cell lines RSV had mainly a cytotoxic effect, which was generally dose-dependent and, only in GBM2, also time-dependent.

RSV effect on cell proliferation was evaluated through MI determination. This parameter showed a marked reduction in five cell lines out of seven. In particular, GBM2 and G179 cell lines, which already highlighted a significant inhibition of metabolic activity and viability, revealed also a drastic decrease of the MI. Contrariwise GBM7 and GBM04 cell lines did not show any significant change in MI,

probably because of the extremely low proliferation rate, even in the untreated cells.

To determine if RSV was able to induce any morphological change we evaluated GSCs morphology at different time of exposure to increasing concentrations of RSV through the observation at phase contrast microscopy. In contrast to what has been shown by Castino and colleagues, who demonstrated that RSV promoted the appearance of a long-lasting more differentiated phenotype in cultured U87MG cells [33], RSV treatment did not induce any relevant modification in the cellular shape of our GSC lines. The only exception is GBM2 cell line that showed mildly changes in cell morphology after 48 and 72 hs of treatment with intermediate concentrations of RSV (50-100 μM).

Since one of the hallmarks of GSCs is the elevated invasive behavior, we analyzed their motility by means of the wound healing assay. We demonstrated that the migration of all the examined GSC lines was greatly impaired by RSV. Interestingly this inhibition was evident already after 48 hs of drug exposure in G144, GBM7 and GBM2 cell lines.

Another feature of GSCs is the aberrant activation of several embryonic signaling pathways, such as Wnt signaling pathway, which has been reported to regulate self-renewal of GSCs, as well as migration and differentiation [34-36]. Therefore, for the first time in our knowledge, we evaluated RSV ability to modulate Wnt signaling pathway in GSCs, analyzing the expression of 7 genes (*WNT1, FZD4, CTNNB1, EP300, CREBBP, TCF7, MYC*), after RSV 100 μM exposure for 96 hs.

RSV modulated heterogeneously the expression of these 7 genes in all the GSC lines. Interestingly previous studies demonstrated that TCF-7 transcriptional factor, and p300 and CREBBP coactivators, play a key role in controlling the switch between self-renewal and differentiation [37, 38]. In particular it has been shown that in GBM cells the transcriptional co-activator p300 regulates cell differentiation,

activating GFAP and repressing Nestin genes [39]. RSV did not induce any significant change in *TCF7*, *EP300* and *CREBBP* expression levels in our GSCs. This might support the lack of a differentiation morphology in our GSCs. Surprisingly the Wnt signaling pathway target gene *MYC* showed an increased transcriptional activity in five out of seven cell lines and especially in GBM2; moreover four cell lines with this alteration showed also the same variation in the expression of the upstream gene *WNT1*. However, RSV drastically decreased c-Myc protein level in GBM2 cell line. These findings are consistent with the observed anti-proliferative effects induced by RSV in GBM2 cell line and suggest that the transcriptional up-regulation of *MYC* could be due to a feedback mechanism of cells lacking c-Myc protein. On the other hand, the relevant decrease in c-Myc protein level could be due to the activation of post-translational regulatory mechanisms. In particular it has been demonstrated that SIRT1, which is strongly activated by RSV, deacetylates and affects c-Myc stability, with a negative feedback loop [40] .

Conclusions

Collectively our results showed, first of all, a wide variability in biological response towards the treatment with RSV across our GSC lines. This could be due to the different genetic background of these cell lines and thus represents a reflection of one of the hallmarks of GBM that is the extreme inter-tumor heterogeneity.

Generally, RSV had a significant anti-proliferation and anti-migratory effect in GSCs, usually in a dose- and time-dependent manner, while it did not induce any relevant variation in cell morphology. It was able to modulate the expression of Wnt signaling pathway-related genes, inducing, generally, a transcriptional upregulation of *MYC*, but interestingly it was also able to induce a drastic decrease of c-Myc protein level. Treatment with RSV may represent a new interesting therapeutic

approach, even if further investigations are certainly needed in order to deeply understand the GSC heterogeneous response.

Abbreviations

GBM, Glioblastoma multiforme; GSCs, Glioma stem cells; RSV, Resveratrol; SIRT1, Sirtuin1**,** MTT, 3-(4,5-Dimethylthiazol-2-yl)-2,5-Diphenyltetrazolium Bromide; MI, Mitotic index

Competing interests

The authors declare that they have no competing interests.

Authors' contribution

CC, GR, GR, VB, LP performed the experiments. CC, AB drafted the manuscript. AB, LD, RG and ML designed and coordinated the study. RG revised the manuscript. All authors read and approved the final manuscript.

Acknowledgments

This work was supported by FAR 2011 n. 12-1-62 and n. 12-155 from University of Milano-Bicocca (to LD and AB, respectively) and by FIRB-RBAP06LAHL from Ministry of Education, University and Scientific Research (to ML).

The authors want to gratefully acknowledge Professor Austin Smith (Wellcome Trust – Medical Research Council Stem Cell Institute, University of Cambridge, Cambridge UK) and Dr. Antonio Daga (Laboratorio di Trasferimento Genico, IRCCS-AOU San Martino-IST, Genova, Italy) for kindly

providing us with the cell lines used in this study.

References

1. Louis DN, Ohgaki H, Wiestler OD, Cavenee WK, Burger PC, Jouvet A, Scheithauer BW, Kleihues P: **The 2007 WHO classification of tumours of the central nervous system**. *Acta Neuropathol* 2007, **114**(2):97-109.
2. Furnari FB, Fenton T, Bachoo RM, Mukasa A, Stommel JM, Stegh A, Hahn WC, Ligon KL, Louis DN, Brennan C *et al*: **Malignant astrocytic glioma: genetics, biology, and paths to treatment**. *Genes Dev* 2007, **21**(21):2683-2710.
3. Wen PY, Kesari S: **Malignant gliomas in adults**. *N Engl J Med* 2008, **359**(5):492-507.
4. Dirks PB: **Brain tumor stem cells: bringing order to the chaos of brain cancer**. *J Clin Oncol* 2008, **26**(17):2916-2924.
5. Reya T, Morrison SJ, Clarke MF, Weissman IL: **Stem cells, cancer, and cancer stem cells**. *Nature* 2001, **414**(6859):105-111.
6. Ignatova TN, Kukekov VG, Laywell ED, Suslov ON, Vrionis FD, Steindler DA: **Human cortical glial tumors contain neural stem-like cells expressing astroglial and neuronal markers in vitro**. *Glia* 2002, **39**(3):193-206.
7. Sun AY, Wang Q, Simonyi A, Sun GY: **Resveratrol as a therapeutic agent for neurodegenerative diseases**. *Mol Neurobiol* 2010, **41**(2-3):375-383.
8. Baur JA: **Resveratrol, sirtuins, and the promise of a DR mimetic**. *Mech Ageing Dev* 2010, **131**(4):261-269.
9. Jang M, Cai L, Udeani GO, Slowing KV, Thomas CF, Beecher CW, Fong HH, Farnsworth NR, Kinghorn AD, Mehta RG *et al*: **Cancer chemopreventive**

activity of resveratrol, a natural product derived from grapes. *Science* 1997, **275**(5297):218-220.

10. Clément MV, Hirpara JL, Chawdhury SH, Pervaiz S: **Chemopreventive agent resveratrol, a natural product derived from grapes, triggers CD95 signaling-dependent apoptosis in human tumor cells**. *Blood* 1998, **92**(3):996-1002.
11. Roccaro AM, Leleu X, Sacco A, Moreau AS, Hatjiharissi E, Jia X, Xu L, Ciccarelli B, Patterson CJ, Ngo HT *et al*: **Resveratrol exerts antiproliferative activity and induces apoptosis in Waldenström's macroglobulinemia**. *Clin Cancer Res* 2008, **14**(6):1849-1858.
12. Liang YC, Tsai SH, Chen L, Lin-Shiau SY, Lin JK: **Resveratrol-induced G2 arrest through the inhibition of CDK7 and p34CDC2 kinases in colon carcinoma HT29 cells**. *Biochem Pharmacol* 2003, **65**(7):1053-1060.
13. Sun CY, Hu Y, Guo T, Wang HF, Zhang XP, He WJ, Tan H: **Resveratrol as a novel agent for treatment of multiple myeloma with matrix metalloproteinase inhibitory activity**. *Acta Pharmacol Sin* 2006, **27**(11):1447-1452.
14. Tang FY, Su YC, Chen NC, Hsieh HS, Chen KS: **Resveratrol inhibits migration and invasion of human breast-cancer cells**. *Mol Nutr Food Res* 2008, **52**(6):683-691.
15. Yu H, Pan C, Zhao S, Wang Z, Zhang H, Wu W: **Resveratrol inhibits tumor necrosis factor-alpha-mediated matrix metalloproteinase-9 expression and invasion of human hepatocellular carcinoma cells**. *Biomed Pharmacother* 2008, **62**(6):366-372.
16. Gagliano N, Moscheni C, Torri C, Magnani I, Bertelli AA, Gioia M: **Effect of resveratrol on matrix metalloproteinase-2 (MMP-2) and Secreted Protein**

Acidic and Rich in Cysteine (SPARC) on human cultured glioblastoma cells. *Biomed Pharmacother* 2005, **59**(7):359-364.

17. Hwang KA, Choi KC: **Anticarcinogenic Effects of Dietary Phytoestrogens and Their Chemopreventive Mechanisms**. *Nutr Cancer* 2015, **67**(5):796-803.
18. Sarkar FH, Li Y, Wang Z, Kong D: **Cellular signaling perturbation by natural products**. *Cell Signal* 2009, **21**(11):1541-1547.
19. Hope C, Planutis K, Planutiene M, Moyer MP, Johal KS, Woo J, Santoso C, Hanson JA, Holcombe RF: **Low concentrations of resveratrol inhibit Wnt signal throughput in colon-derived cells: implications for colon cancer prevention**. *Mol Nutr Food Res* 2008, **52 Suppl 1**:S52-61.
20. Mishra L, Shetty K, Tang Y, Stuart A, Byers SW: **The role of TGF-beta and Wnt signaling in gastrointestinal stem cells and cancer**. *Oncogene* 2005, **24**(37):5775-5789.
21. Pollard SM, Yoshikawa K, Clarke ID, Danovi D, Stricker S, Russell R, Bayani J, Head R, Lee M, Bernstein M *et al*: **Glioma stem cell lines expanded in adherent culture have tumor-specific phenotypes and are suitable for chemical and genetic screens**. *Cell Stem Cell* 2009, **4**(6):568-580.
22. Griffero F, Daga A, Marubbi D, Capra MC, Melotti A, Pattarozzi A, Gatti M, Bajetto A, Porcile C, Barbieri F *et al*: **Different response of human glioma tumor-initiating cells to epidermal growth factor receptor kinase inhibitors**. *J Biol Chem* 2009, **284**(11):7138-7148.
23. Baronchelli S, Bentivegna A, Redaelli S, Riva G, Butta V, Paoletta L, Isimbaldi G, Miozzo M, Tabano S, Daga A *et al*: **Delineating the cytogenomic and epigenomic landscapes of glioma stem cell lines**. *PLoS One* 2013, **8**(2):e57462.

24. Lee J, Kotliarova S, Kotliarov Y, Li A, Su Q, Donin NM, Pastorino S, Purow BW, Christopher N, Zhang W *et al*: **Tumor stem cells derived from glioblastomas cultured in bFGF and EGF more closely mirror the phenotype and genotype of primary tumors than do serum-cultured cell lines**. *Cancer Cell* 2006, **9**(5):391-403.

25. Riva G, Baronchelli S, Paoletta L, Butta V, Biunno I, Lavitrano M, Dalprà L, Bentivegna A: **In vitro anticancer drug test: A new method emerges from the model of glioma stem cells**. *Toxicology Reports* 2014, **1**(0):188-199.

26. Gagliano N, Aldini G, Colombo G, Rossi R, Colombo R, Gioia M, Milzani A, Dalle-Donne I: **The potential of resveratrol against human gliomas**. *Anticancer Drugs* 2010, **21**(2):140-150.

27. Kundu JK, Surh YJ: **Molecular basis of chemoprevention by resveratrol: NF-kappaB and AP-1 as potential targets**. *Mutat Res* 2004, **555**(1-2):65-80.

28. Jiang H, Zhang L, Kuo J, Kuo K, Gautam SC, Groc L, Rodriguez AI, Koubi D, Hunter TJ, Corcoran GB *et al*: **Resveratrol-induced apoptotic death in human U251 glioma cells**. *Mol Cancer Ther* 2005, **4**(4):554-561.

29. Filippi-Chiela EC, Villodre ES, Zamin LL, Lenz G: **Autophagy interplay with apoptosis and cell cycle regulation in the growth inhibiting effect of resveratrol in glioma cells**. *PLoS One* 2011, **6**(6):e20849.

30. Tseng SH, Lin SM, Chen JC, Su YH, Huang HY, Chen CK, Lin PY, Chen Y: **Resveratrol suppresses the angiogenesis and tumor growth of gliomas in rats**. *Clin Cancer Res* 2004, **10**(6):2190-2202.

31. Kimura Y, Sumiyoshi M, Baba K: **Antitumor activities of synthetic and natural stilbenes through antiangiogenic action**. *Cancer Sci* 2008, **99**(10):2083-2096.

32. Wang Q, Xu J, Rottinghaus GE, Simonyi A, Lubahn D, Sun GY, Sun AY: **Resveratrol protects against global cerebral ischemic injury in gerbils**. *Brain Res* 2002, **958**(2):439-447.

33. Castino R, Pucer A, Veneroni R, Morani F, Peracchio C, Lah TT, Isidoro C: **Resveratrol reduces the invasive growth and promotes the acquisition of a long-lasting differentiated phenotype in human glioblastoma cells**. *J Agric Food Chem* 2011, **59**(8):4264-4272.

34. Paw I, Carpenter RC, Watabe K, Debinski W, Lo HW: **Mechanisms regulating glioma invasion**. *Cancer Lett* 2015, **362**(1):1-7.

35. Bowman A, Nusse R: **Location, location, location: FoxM1 mediates β-catenin nuclear translocation and promotes glioma tumorigenesis**. *Cancer Cell* 2011, **20**(4):415-416.

36. Kim YS, Farrar W, Colburn NH, Milner JA: **Cancer stem cells: potential target for bioactive food components**. *J Nutr Biochem* 2012, **23**(7):691-698.

37. Wu JQ, Seay M, Schulz VP, Hariharan M, Tuck D, Lian J, Du J, Shi M, Ye Z, Gerstein M *et al*: **Tcf7 is an important regulator of the switch of self-renewal and differentiation in a multipotential hematopoietic cell line**. *PLoS Genet* 2012, **8**(3):e1002565.

38. Teo JL, Kahn M: **The Wnt signaling pathway in cellular proliferation and differentiation: A tale of two coactivators**. *Adv Drug Deliv Rev* 2010, **62**(12):1149-1155.

39. Panicker SP, Raychaudhuri B, Sharma P, Tipps R, Mazumdar T, Mal AK, Palomo JM, Vogelbaum MA, Haque SJ: **p300- and Myc-mediated regulation of glioblastoma multiforme cell differentiation**. *Oncotarget* 2010, **1**(4):289-303.

40. Yuan J, Minter-Dykhouse K, Lou Z: **A c-Myc-SIRT1 feedback loop regulates cell growth and transformation**. *J Cell Biol* 2009, **185**(2):203-211.

Supplementary Data

Table S1. Statistical analysis (*p*-values, t-test) of the effects of RSV on cell viability (MTT assay). *p*-values are referred to the specific treatment compared to the respective untreated cells.

RSV treatment												
Dose	**10 μM**			**50 μM**			**100 μM**			**200 μM**		
Time (hs)	**24**	**48**	**72**	**24**	**48**	**72**	**24**	**48**	**72**	**24**	**48**	**72**
GBM2	n.s.	.001	.01	n.s.	.0001	.0001	n.s.	.0001	.0001	n.s.	.0001	.0001
GBM7	n.s.	n.s.	.0001	n.s.	.05	.0001	n.s.	.05	.01	n.s.	.05	.01
GBM04	n.s.	.001	.01	n.s.	.0001	.01	.05	.0001	.001	.0001	.0001	.0001
G144	n.s.	.05	n.s.	n.s.	n.s.	n.s.	.01	.01	.01	.001	.05	.001
G179	n.s.	.01	.05	n.s.	.0001	.0001	.05	.0001	.0001	n.s.	.0001	.0001
GliNS2	n.s.	n.s.	.001	.001	.05	n.s.	.05	.01	.001	.0001	.01	n.s.
G166	.01	.001	.01	.001	.01	.05	.05	.001	n.s.	.05	.001	.0001

n.s.= not statistically significant

Table S2. Statistical analysis (p-values, t-test) of the effects of RSV on cell motility (wound healing assay). p-values are referred to the specific treatment compared to the respective untreated cells.

RSV treatment												
Dose	**10 μM**			**50 μM**			**100 μM**			**200 μM**		
Time (hs)	**48**	**72**	**96**	**48**	**72**	**96**	**48**	**72**	**96**	**48**	**72**	**96**
GBM2	n.s.	n.s.	.01	n.s.	.05	.001	.0001	.01	.001	.0001	.01	.0001
GBM7	.01	.05	.001	.05	.05	.0001	.01	.05	.0001	.01	n.p.	n.p.
GBM04	n.s.	n.s.	n.s.	n.s.	n.s.	n.s.	n.s.	.05	.0001	n.s.	n.s.	n.p.
G144	.001	n.s.	n.s.	.01	n.s.	.05	.001	n.s.	n.s.	.0001	.01	.01
G179	n.s.	n.s.	.001	n.s.	n.s.	.01	n.s.	.001	.0001	.01	.0001	.0001
GliNS2	n.s.	n.s.	.05	n.s.	n.s.	.001	n.s.	n.s.	.0001	.05	.0001	n.p.

n.s.= not statistically significant

n.p.= not performed

Chapter 3

A functional biological network centered on XRCC3: a new possible marker of chemoradiotherapy resistance in rectal cancer patients

Marco Agostini[abc], Andrea Zangrando[ci], Chiara Pastrello[d], Edoardo D'Angelo[acl], **Gabriele Romano**[e], Roberto Giovannoni[e], Marco Giordan[f], Isacco Maretto[a], Chiara Bedin[ac], Carlo Zanon[ci], Maura Digito[a], Giovanni Esposito[g], Claudia Mescoli[h], Marialuisa Lavitrano[e], Flavio Rizzolio[jk], Igor Jurisica[d], Antonio Giordano[k], Salvatore Pucciarelli[a] & Donato Nitti[a] .

[a] Department of Surgical, Oncological and Gastroenterological Sciences; Section of Surgery; University of Padova; Padua, Italy; [b] The Methodist Hospital Research Institute; Houston, TX USA; [c] Istituto di Ricerca Pediatrica- Città della Speranza; Padova, Italy; [d] Princess Margaret Cancer Centre; University Health Network and TECHNA Institute for the Advancement of Technology for Health; Toronto, Canada [e] Department of Surgery and Interdisciplinary Medicine; University of Milano-Bicocca; Milan, Italy; [f] Biostatistics and Data Management; IASMA; Research and Innovation Centre; Trento, Italy; [g] Immunology and Molecular Oncology Unit; Istituto Oncologico Veneto - IRCCS; Padua, Italy; [h] Department of Medical Diagnostic Sciences and Special Therapies; University of Padua;Padua, Italy; [i]Department of Woman and Child Health; University of Padua; Padua, Italy; [j]Department of Translational Research; National Cancer Institute – CRO-IRCSS; Aviano, Italy; [k] Sbarro Institute for Cancer Research and Molecular Medicine; Center for Biotechnology;College of Science and Technology; Temple University, Philadelphia, PA USA; [l] Euroclone S.p.a. Pero, (MI)

Published in: **Cancer Biology & Therapy** 16:7, 1--12; August 2015.

Keywords

biological network, integrated approach, microarray, preoperative chemoradiotherapy, rectal cancer, treatment response, XRCC3

Abbreviations

RC=Rectal cancer; pCRT=Preoperative chemoradiotherapy; CEA= carcinoembryonic antigen; Gy=Gray; PPI=Protein-protein interaction; mRNA=messenger RNA; SSB=Single-strand breaks; DSB=Double-strand breaks; SNP=Single nucleotide polymorphism; HT=High throughput; CRT=Chemoradiotherapy; RIN=RNA integrity number; siRNA=Small interfering RNA;

Abstract

Preoperative chemoradiotherapy is widely used to improve local control of disease, sphincter preservation and to improve survival in patients with locally advanced rectal cancer. Patients enrolled in the present study underwent preoperative chemoradiotherapy, followed by surgical excision. Response to chemoradiotherapy was evaluated according to Mandard's Tumor Regression Grade (TRG). TRG 3, 4 and 5 were considered as partial or no response while TRG 1 and 2 as complete response. From pretherapeutic biopsies of 84 locally advanced rectal carcinomas available for the analysis, only 42 of them showed 70% cancer cellularity at least. By determining gene expression profiles, responders and non-responders showed significantly different expression levels for 19 genes ($P < 0.001$). We fitted a logistic model selected with a stepwise procedure optimizing the Akaike Information Criterion (AIC) and then validated by means of leave one out cross validation (LOOCV, accuracy D 95%). Four genes were retained in the achieved model:

ZNF160, XRCC3, HFM1 and ASXL2. Real time PCR confirmed that XRCC3 is overexpressed in responders group and HFM1 and ASXL2 showed a positive trend. In vitro test on colon cancer resistant/susceptible to chemoradiotherapy cells, finally prove that XRCC3 deregulation is extensively involved in the chemoresistance mechanisms. Protein-protein interactions (PPI) analysis involving the predictive classifier revealed a network of 45 interacting nodes (proteins) with TRAF6 gene playing a keystone role in the network. The present study confirmed the possibility that gene expression profiling combined with integrative computational biology is useful to predict complete responses to preoperative chemoradiotherapy in patients with advanced rectal cancer.

Introduction

Preoperative chemoradiotherapy (pCRT) is worldwide accepted as a standard treatment for locally advanced rectal cancer.[1-3] After pCRT the complete pathological response is approximately 20%, whereas in 20 to 40% of patients the response is poor or absent.[4,5] The prediction of response has the potential to spare unnecessary toxic treatments for non- responders and, in selected cases, to perform a less-radical surgery (e.g. local excision or a wait and see policy). Several studies have been performed to evaluate potential predictors of response after pCRT for rectal cancer, however findings are still unclear and controversial.[6,7] Discrepancies between studies are mainly related to patient selection, sample size, study design, treatments and definitions used for tumor response. Moreover, the only accepted marker to monitor colorectal cancer treatment, progression and relapse is the carcinoembryonic antigen (CEA).[8]

However, gene signatures using microarray technology may help to predict tumor response after pCRT. Recent studies using microarray technology have shown that

gene expression profiles of tumor cells can discriminate responders and non-responders patients after neoadjuvant or adjuvant chemotherapy.[9-13] The clinical value of these studies is to identify disease subtypes that represent distinct subphenotypes of rectal cancer in order to better approach opportunities for individualized therapeutics. Despite these advances, few studies have attempted to demonstrate the value in integrating genomic information with the traditional clinical risk factors to provide a more detailed assessment of clinical risk and an improved prediction of response to therapy. The results we present herein significantly improve the application of gene expression profiling, by biologically dissecting a commonly used clinical predictive classifier in rectal cancer. Using integrative computational biology, we combined multiple data to derive novel interpretations and identifying important players in the prediction of and in the response to treatment.

	Sample set		
Characteristic	**No.**	**%**	
Age	Median (range) yrs	60 (20–77)	
Sex	Male	24	57
	Female	18	43
Tumor distance from the anal verge	≤ 7 cm	23	55
	> 7 cm	19	45
Total radiotherapy dose delivered	≥ 50 Gy	38	90
	< 50 Gy	4	10
5-Fluorouracil administration	Continuous infusion	33	79
	Bolus	8	19
	Oral (capecitabine)	1	2
Other drugs	5-Fluorouracile alone	27	64
	Oxaliplatin	11	26
	Carboplatin	4	10
ypTNM	0	6	14
	I	13	31
	II	13	31
	III	4	10
	IV	6	14
	Not available	0	0
Radical surgery	Yes	34	81
	No	8	19
	Not available	0	0
Pre-chemotherapeutic CEA ($ng\,ml^{-1}$)	<5/ ≥5	30/ 7	71/17
	Not available	5	12

5-FU= 5-Fluorouracil; CEA= carcinoembryonic antigen

Table 1. Patient, tumor and treatment characteristics of the patients included in the study

Results

Patient, tumor and treatment characteristics

A total of 48 patients met all criteria for inclusion in this study. Six samples did not pass our microarray strict quality control standards and had to be excluded. Complete details of the patients, tumor and treatment characteristics are summarized in Table 1.

Gene Symbol	AffyID	Chromosome	Description
AGRN	217419_x_at	chr1	agrin
HFM1	241469_at	chr1	ATP-dependent DNA helicase homolog (S. cerevisiae)
CSTF3	203947_at	chr11	cleavage stimulation factor subunit 3 isoform 1
RAB6A	221792_at	chr11	RAB6A, member RAS oncogene family isoform a
PRKRIR	209323_at	chr11	protein-kinase, interferon-inducible double
C12orf32	225837_at	chr12	chromosome 12 open reading frame 32
XRCC3	216299_s_at	chr14	X-ray repair cross complementing protein 3
CDK10	203468_at	chr16	cyclin-dependent kinase 10 isoform b
CDK5R1	204996_s_at	chr17	cyclin-dependent kinase 5, regulatory subunit 1
IL12RB1	1552584_at	chr19	interleukin 12 receptor, β 1 isoform 1
BCKDHA	239158_at	chr19	branched chain keto acid dehydrogenase E1, α
ZNF160	1567031_at	chr19	zinc finger protein 160
ASXL2	231417_at	chr2	additional sex combs like 2
EIF3L	217719_at	chr22	eukaryotic translation initiation factor 3
PSMD6	232284_at	chr3	proteasome (prosome, macropain) 26S subunit,
MAGI1	232859_s_at	chr3	membrane associated guanylate kinase, WW and PDZ
RAB7A	1570061_at	chr3	RAB7, member RAS oncogene family
SPRY4	220983_s_at	chr5	sprouty homolog 4 isoform 1
CNKSR2	1554607_at	chrX	connector enhancer of kinase suppressor of Ras

Table 2. *List of 19 informative genes (adjusted p-value D 0.037) discriminating responders and non-responders groups*

Before the CRT, 91% and 88% of patients were clinically staged as T3–4 and lymph nodes positive, respectively; 38 (90%) patients received a total dose of radiotherapy higher than 50 Gy, and 15 out of these cases (36%), drugs other than 5-FU were administered (n = 11, Oxaliplatin; n D=4, Carboplatin). For 33 (79%) patients, 5-FU was administered by continuous venous infusion. The median (range) interval time between the completion of pCRT and surgery was 46 (30–66) days. With a median follow-up of 81 months, only 6 out of 42 patients had recurrent disease, 9 patients died from disease and 1 patient from unrelated causes. The following TRG distribution was found: TRG 1: n = 8; TRG 2: n = 11; TRG 3: n = 6; TRG 4: = D 10; and

TRG 5: n = 7. On the basis of the TRG distribution, 19 (45%) patients were considered responders (TRG 1 to 2), and 23 (55%) were considered non-responders (TRG 3 to 5).

Class comparison and Hierarchical clustering

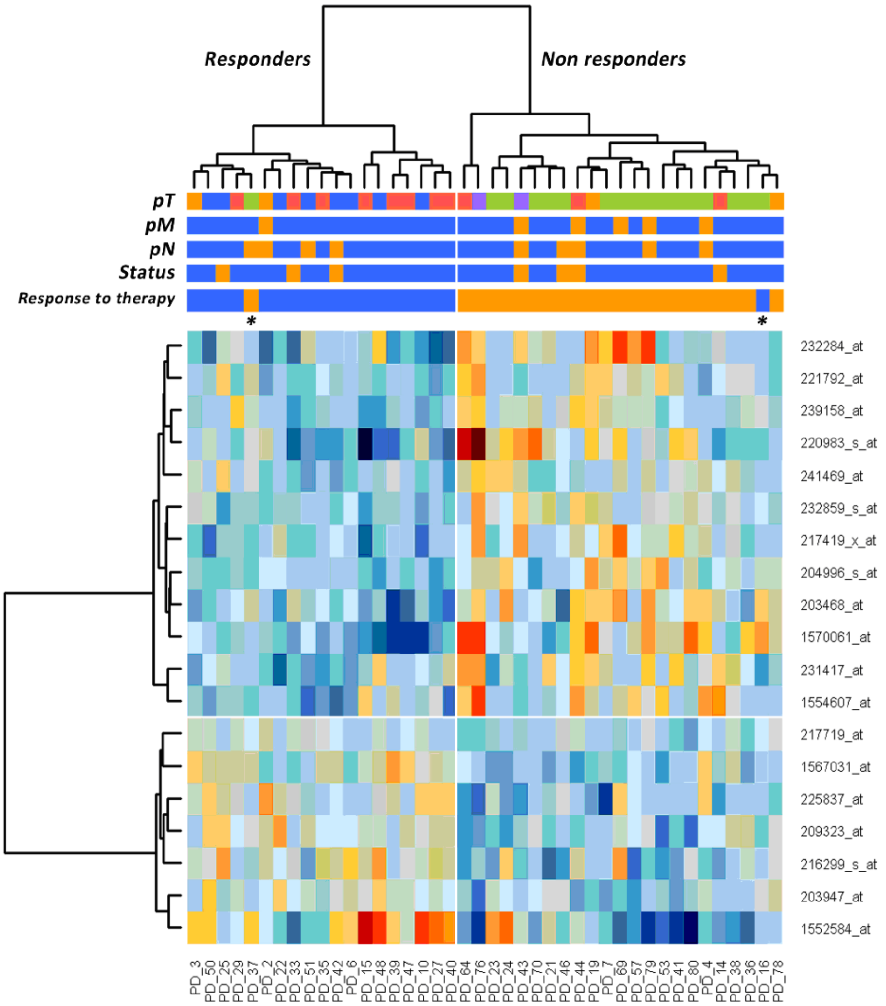

Figure 1. *Hierarchical clustering of 42 patients with rectal carcinomas based on significantly differentially expressed probe sets representing 19 genes (rows) between the subgroup of responders and non-responders (columns) to neoadjuvant chemoradiotherapy. Responders are located on the left branch, Non-responders are clustered on the right branch. Red depicts decreased gene expression; blue indicates increased expression. The two asterisks identify the outliers.*

A total of 45,868 out of 54,675 probe sets with RefSeq annotation were considered. We investigated different expression levels between the two groups of interest (responders and non-responders) by means of the modified F-test statistic with p-values computed by permutations, as described in experimental procedures.

Only 19 genes were found to be informative with an adjusted p-value = 0.037 (Table 2). Hierarchical cluster analysis using the 19 informative genes was able to clearly identify the two groups of interest with only two misclassified samples (Fig. 1, "Response to therapy" label). Left branch included 18/19 (94.7%) responders while right branch gathered 22/23 (95.7%) non-responders. Interestingly, non-responders branch correlated with 5/6 (83.3%) cases with pM event and 16/17 (94.1%) cases with a specific pT class.

The inspection of clinical data did not suggest any particular explanation about the two misclassified samples; further analyses will be performed to clarify the outliers.

The predictive 19 gene classifier from our study were entered into Ingenuity Pathway Analysis Software and, as previously described by Breettingham-Moore,[14] TNF signaling pathway was enriched in our network (Fig. S1).

Moreover, we tested the 19 genes classifier on patients treated with 5-FU alone (n D 27) and patients treated with other drugs alone (n = 15). Six out of 27 (22%) and 2 out of 15 (13%) outliers resulted in 5-FU alone and other drug association groups, respectively, suggesting similar trend for different treatment protocols.

Responders prediction

Considering all the probe sets, we further investigated the capability to predict the patient's outcome. To this aim we fitted a logistic model selected with a stepwise procedure optimizing the AIC and then validated by means of LOOCV. In this way we removed possible redundant information. Starting from the 19 probe-sets we selected the logistic model maximizing the Akaike Information Criterion. Performance was 95% accuracy by LOOCV. Four genes are representative of the

entire set: 1567031_at (ZNF160), 216299_s_at (XRCC3), 241469_at (HFM1) and 231417_at (ASXL2). The target sequence of the 231417_at probe is not defined but it matched 423/424 identities with “putative Polycomb group protein ASXL2” using NCBI BLASTN on all genome assemblies. These genes were included in the previously identified gene set and were able to correctly predict 40 out of 42 outcomes with one false responder and one false non-responder (LOOCV accuracy = 0.952, specificity = 0.9473, sensitivity = 0.9565, positive predictive value = 0.9565, negative predictive value = 0.9473).

Multivariate analysis

To exclude differences in gene expression between responders and non-responders was due to differences in other characteristics of the two groups (Table 1), we performed a multivariate analysis including both the four genes identified in their univariate analysis and the clinicopathological potential confounding factors.

We considered a linear model where the four identified genes represent the dependent variables while the confounding factors (sex, tumor distance from anal verge, radiotherapeutic dose delivered, ypTNM) represent the independent variables.

Multiplicity corrections have been performed using Holm-Bonferroni method. We found no significant results after multiplicity corrections, thus we can exclude putative associations between the 4 genes and possible confounding factors (data not shown).

Quantitative Real-time PCR analysis

In order to confirm data achieved with microarray analysis, we measured XRCC3, ZNF160, HFM1, and ASXL2 transcript levels, which alone are able to correctly predict 40 out of 42 outcomes, using Real Time quantitative polymerase chain reaction with TaqMan© Assay. XRCC3 gene showed a significant correlation between the array-based and quantitative PCR methods (Pearson = 0.85; r2 = 0.7),

with high expression on Affymetrix arrays corresponding to low delta threshold cycle (ΔCt) values from TaqMan© Assay. Also the expression with TaqMan© Assay of ZNF160, HFM1, and ASXL2 genes are in agreement with microarray results because they show the same expression pattern. Unfortunately, these three genes did not reach a sufficient significance to irrefutably confirm microarray results, probably due to a different resolution of the techniques. The authors anyhow, believes that such genes equally have a pivotal role on the determination of response to treatment, especially if we consider their indirect involvement in a complex protein interaction network, as described below for HFM1 and ASXL2.

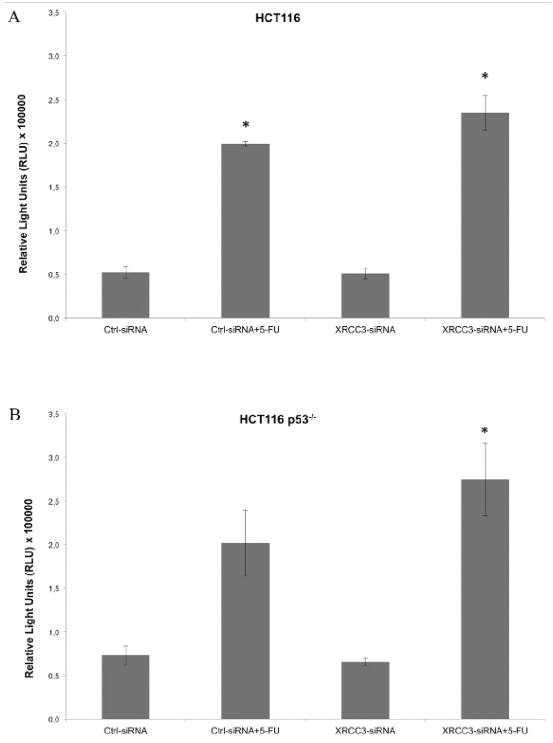

Figure 2. *Caspase activation assay on HCT116 and HCT116 p53$^{-/-}$ cells. (A) XRC33 knockdown does not influence caspase activation in HCT116 cells. (B) 5-FU, in combination with XRCC3 knockdown, causes a significant increase of caspase 3/7 activation as compared to control group in HCT116 p53$^{-/-}$ cells. Luminescence is expressed as Relative Light Units (RLU). *: p-value <0.05 compared to control group in t-test with Bonferroni's correction. Error bars represent standard errors of the mean.*

XRCC3 knockdown restores sensitivity to 5FU in chemoresistant colon cancer cells

In order to validate the relationship between XRCC3 expression and chemoresistance, we investigated the effect of XRCC3 knockdown on HCT116 and HCT116 p53$^{-/-}$ cells. HCT116 cells are known to be sensitive to 5-FU,

whereas HCT116 p53$^{-/-}$ are resistant to the 5-FU chemotherapeutic action.[15]

We performed a kinetic study of XRCC3 knockdown by siRNA, which revealed a significant decrease of XRCC3 protein levels 48 hours after transfection (Fig. S2), both in HCT116 and HCT116 p53$^{-/-}$cells.

We then evaluated the effect of XRCC3 knockdown on sensitivity of cells to 5-FU. HCT116 p53$^{-/-}$ (chemoresistant) and HCT116 (chemosensitive) cells were transfected with a control siRNA or with a XRCC3-siRNA, and cells were then treated with 5-FU 36 hours after transfection. XRCC3 knockdown in HCT116 cells had no effect on cell viability with or without administration of 5-FU. On the contrary, in HCT116 p53$^{-/-}$ cells the XRCC3 knockdown in combination with 5-FU treatment caused a relevant decrease of cell viability as compared to the control group (0,81 ± 0,09 vs. 2,05 ± 0,14 absorbance ratio respectively, p = 0.001). As expected, in all the other groups it was observed an increase in cell viability (Ctrl siRNA + 5-FU 1.22 ± 0.06 absorbance ratio; XRCC3-siRNA 1.80 ± 0.10 absorbance ratio). To further

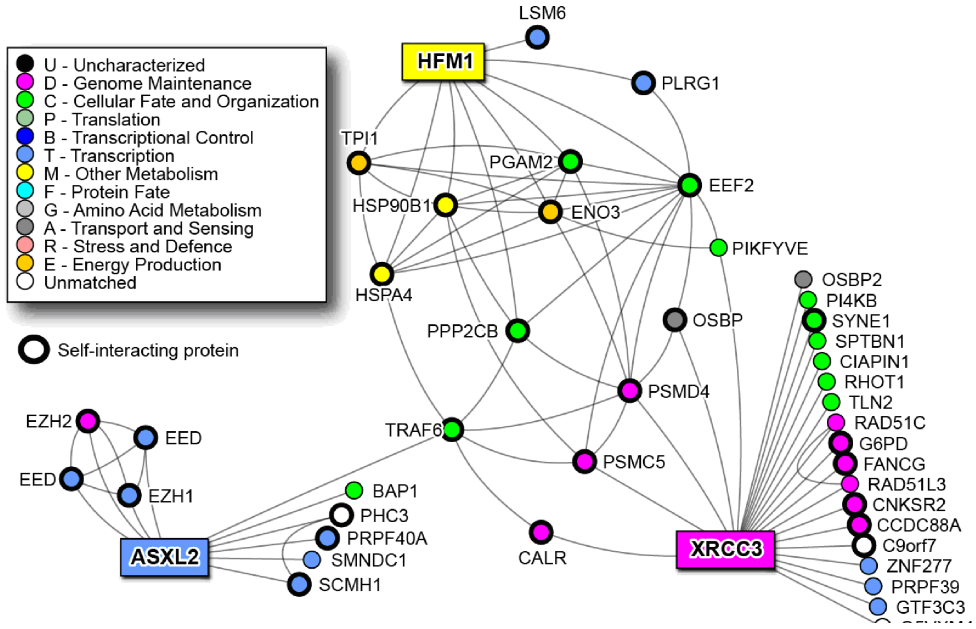

Figure 3. *NAViGaTOR PPI network for the 3 of the 4 predictor genes (rectangle nodes).*

characterize the response to 5-FU of the HCT116 or HCT116 p53$^{-/-}$ cells, we performed a caspase 3/7 activation assay which disclosed an increase of caspase activity in XRCC3- siRNA transfected HCT116 p53$^{-/-}$ cells treated with 5-FU. No effect of XRCC3-siRNA on caspase activation was revealed on HCT116 cells (Fig. 2).

p53 Immunohistochemistry

There are many different mechanisms at the basis of chemoresistance. Because XRCC3 in vitro testing was performed on HCT116 and HCT116 p53$^{-/-}$ cells, the result

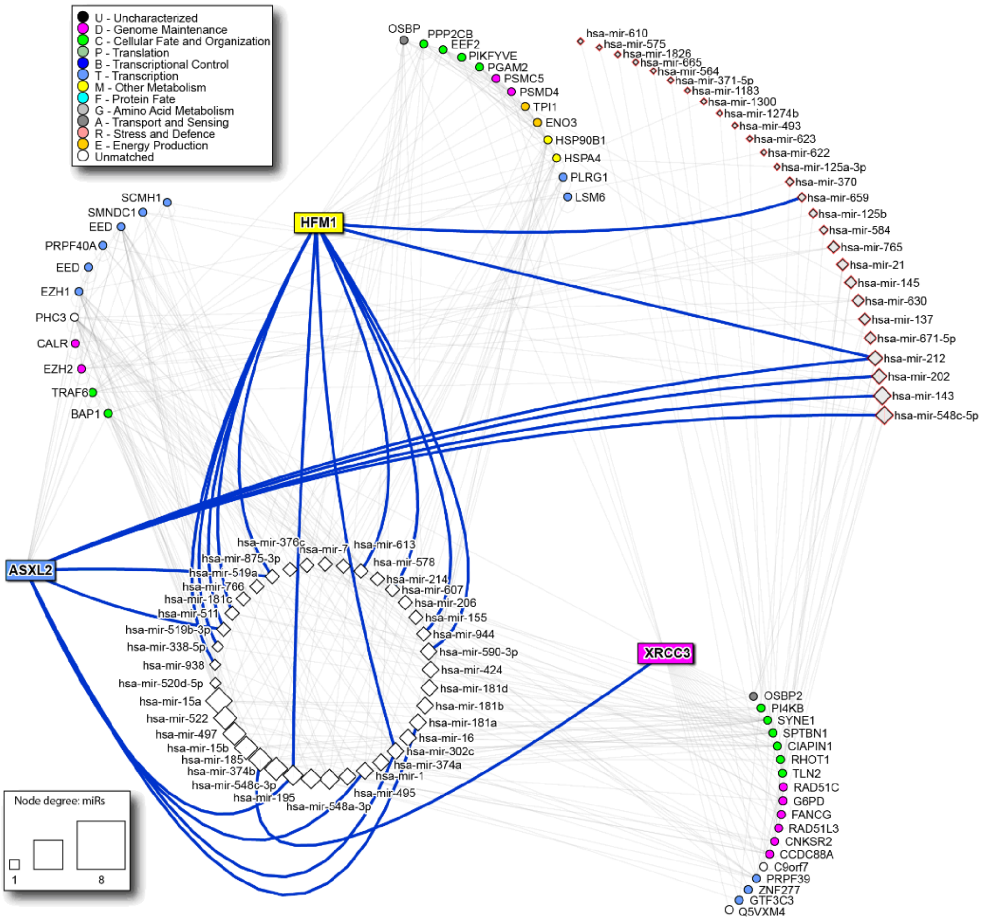

Figure 4. *microRNAs targeting the predictor genes PPI network. White squares: microRNAs shared by the 3 genes; pink squares: signature microRNAs described in the literature. The size of the microRNA node corresponds to number of target genes it has. Thick blue lines highlight direct links between predictor genes and corresponding microRNAs.*

showed above could be due to XRCC3 deregulation in a p53 mutated background cell line (HCT116 $p53^{-/-}$ cells), rather than to the XRCC3 over/under expression *per se*. We decided to address this issue characterizing p53 in patient tissues. In 42 preoperative biopsies analyzed, p53 protein expression was not detect in 23 samples (54.7%) whereas it showed different positive degree in 19 samples (45.3%): 4 samples with 11–25%, 4 samples with 26–75% and 11 samples with >75 % of immunostained tumor cells. (Fig. S3). No significant correlation was found between p53 expression and tumor response to therapy.

Network analysis

The analysis of the PPI network of the four genes revealed that ZNF160 is a protein with no described interactions while the remaining three are included in a network of 45 nodes (proteins).[16] In this network, our most significant protein XRCC3 not only interact with a relevant number of protein per se; but are also related to ASXL2 and HFM1 through indirect interactions. Interestingly, “the heart” of this network seems to be TRAF6 (not relevant by experimental data) that connects ASXL2 to the other two proteins (Fig. 3). The functional annotation and enrichment analysis show a major role of the proteins in the PPI network in DNA repair and recombination, mRNA processing, in sugar catabolic processes and in the organelle lumen organization (Fig. S1).

The microRNA target analysis using mirDIP shows 472 microRNAs targeting the nodes of the network. Thirty-nine of them are shared by the interactors of the three predictor genes. Twenty-seven have been already described as predictors of response in rectal cancer patients undergoing neoadjuvant therapy[17-20] (Fig. 4).

The analysis of drug targets using DrugBank highlighted 130 drugs targeting one or more proteins of the network. The drugs targeting many protein in the network (drug nodes with the highest degree) include cyclosporine, 7,8-Dihydro-7,8-

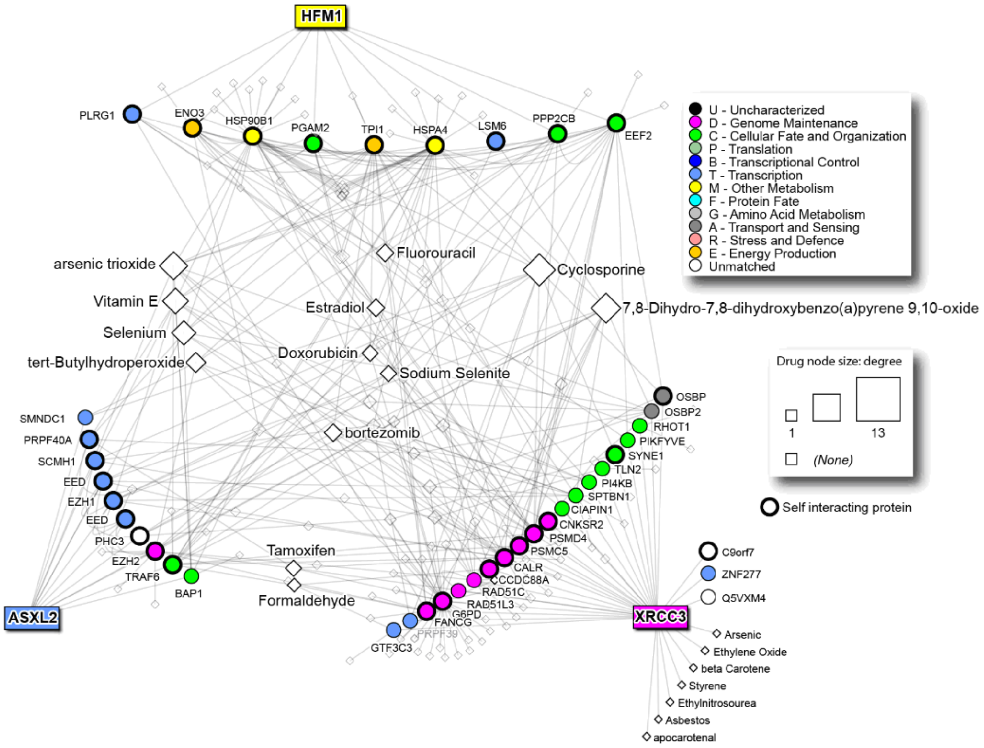

Figure 5. *Drugs targeting the predictor genes PPI network. The size of the node corresponds to number of proteins it targets.*

dihydroxybenzo(a)pyrene 9,10-oxide and arsenic trioxide. In this network, fluorouracil affects 6 proteins (PPP2CB, HSPA4, TPI1, PLRG1, PI4KB and FANCG), some of which have a central role. Oxaliplatin targets only one protein, SPTBN1, while carboplatin is not present in the network. Moreover, the central protein TRAF6 is targeted by Estradiol, Folic Acid, Aspirin, Curcumin, Formaldehyde, Hydrogen Peroxide, pirinixic acid and arsenic trioxide (Figure 5).

Discussion

Currently anti-tumor therapy is predominantly based on the use of chemotherapeutic drugs and leave aside the molecular basis of the disease.

Although these treatments have significantly improved the outcome of many patients, they are ineffective or even toxic for many other types of tumors and in case of metastasis. Recently, new drugs directed against cancer-specific molecular circuits, have been developed and introduced into clinical practice (so-called molecular drugs). However, only selected groups of patients respond to these drugs, and the molecular mechanisms underlying tumor resistance in unresponsive individuals remain to be fully elucidated. In this context, one of the priorities in the field of clinical oncology is the identification of genetic or phenotypic markers able to predict patient responsiveness to treatments. In an overall perspective of expanding our current capability to tailor personalized therapy, the integrated approach (gene profiling, proteomics, bioinformatics, *in vitro* and *ex-vivo* validation) would add an important piece to the puzzle.

Gene expression approach offers the opportunity to evaluate large sets of samples in parallel and has the potential to improve our understanding of tumorigenesis and patients treatment. However, molecular screening alone on different study groups has not achieved sufficient accuracy for the translation into clinical practice. An integrated approach aiming at the interpolation of data collected from protein biomarkers and genetic signatures might offer more reliable predictions. Recent advances in computational science allowed the processing, management and use of large sets of genomic and proteomic information that, properly analyzed, might address us to perform treatment selection and prediction of patient outcome. The molecular profiling of individual patient is a constitutive principle of personalized medicine and is the first step necessary to the clinicians for the selection of the

therapeutic regimen. This study provided a new set of genetic biomarkers associated with the prediction and monitoring of the response to therapy and of tumor chemoradioresistance. Although these tasks are of paramount importance for the development of personalized, mechanism-based anticancer therapies, currently anti-tumor therapy is predominantly based on the use of chemotherapeutic drugs that do not take into account the molecular basis of the disease. As shown in the current study, a crucial predictor gene is XRCC3 that codes for a protein involved in homologous recombination repair of DNA doublestrand breaks and is required for genomic stability. Ionizing radiation induces both DNA single-strand breaks (SSB) and double-strand breaks (DSB), with the DSBs generally considered the lethal event for cell homeostasis. XRCC3 polymorphisms have been implicated in radiosensitivity mechanisms,[21-27] but several studies on rectal cancer patients failed the link between them and sensitivity to radiation treatment. In our study, the expression of XRCC3 supports the importance of its role in the prediction of the response to treatment, suggesting that the mutational analysis limited to very few SNPs in the previous studies has been insufficient to highlight the role of the gene. The microRNA network reveals a central role of hsa-mir-185, directly targeting XRCC3. As hsa-mir-185 has been correlated with poor survival and metastasis in colorectal cancer,[28] the evaluation of the XRCC3 status should be performed not only considering SNPs but also its gene- targeting microRNA expression. To further investigate the role of XRCC3 gene in the chemoresistance in colon carcinoma, a siRNA-mediated knockdown of this gene was performed in a well-known in vitro model of 5-FU chemoresistance of colon carcinoma, the HCT116 $p53^{-/-}$cell line.[15] The down-regulation of XRCC3 in these cells re-sensitized the chemoresistant cells to 5-FU, suggesting a chemoprotective role of this gene in colon carcinoma settings and supporting the evidence of the up-regulation of this gene in non-responder colon carcinoma patients.

Interestingly another predictor gene, HFM1, is involved in DNA interaction by encoding a putative DNA helicase homolog (S. cerevisiae). Its probe was down regulated in responders group as well as the one related to ASXL2 gene. According to literature, the role of these genes in response to radiochemotherapies remains to be explored. Approaching to this new kind of study, we must consider that the increasing use of high-throughput (HT) assays shifted research from hypothesis-driven exploration to data-driven hypothesis generation. However, generating substantially more data, HT methods in turn led to shifting from predominantly using statistical tools to depending on computational biology approaches, especially data mining and machine learning algorithms, to aid data analysis and interpretation.[29,30] These theoretical paradigm is "on practice translate" in this study through the surprisingly identification of TRAF6 as protein with a pivotal role in XRCC3 network. In fact, basing on experimental data alone we have a partial vision on what really happen in the complex micro-world of cell signaling network. However, thanks to integrated HT approach, if we fall experimental data into a more complex scenario we can see the topics in a new prospective and identify that "hidden players" which better complete our model.

Through this approach, TRAF6 (Tumor necrosis factor (TNF) receptor associated factor 6) has been shown to play a central role in the PPI network of the predictor genes. TRAF6 is a crucial signaling molecule regulating a diverse array of physiological processes, including adaptive and innate immunity, bone metabolism and the development of several tissues including lymph nodes, mammary glands, skin and the central nervous system. [16] This protein mediates the signaling not only from the members of the TNF receptor superfamily, but also from the members of the Toll/IL-1 family. It also works as a signal transducer in the NF-kappaB pathway that activates IkappaB kinase (IKK) in response to pro-inflammatory cytokines. Interestingly, TRAF6 is targeted by aspirin, known to reduce risk of rectal cancer[31],

and by curcumin, a polyphenol known to affect the NFkappaB pathway in colorectal cancer cells, which is in phase II clinical trial for colorectal cancer prevention.[32,33.]
Afterward, TRAF6, activated by IL-1β or LPS, suppresses TGF-β1/Smad pathways through interaction with TβRIII upon TGF- β 1 stimulation. In general, inflammation is tightly regulated and resolved by the induction of anti-inflammatory cytokines.[34]
Once this regulatory balance is disturbed, non-specific stimulation and activation of inflammatory cells may lead to increased production and release of potently destructive immunological and inflammatory molecules. For instance, improper regulation of IL-1β signaling has been shown to potentiate neoplastic risk and ultimately induce tumor progression.[34]
In addition, decreased TbRIII expression was closely correlated with tumor progression in various human cancers including breast, lung, prostate, pancreatic, ovarian, and renal cancers,[35] supporting the idea that TβRIII-mediated regulation of normal epithelial cells may contribute to prevent tumor progression.
In conclusion, meta-analysis of published gene expression data will be performed to further validate our results and to allow the comparison of data retrieved by different platforms and work groups. Through a coordinated effort, our project could help us in identifying clinically useful biomarkers to predict tumor responsiveness to anti-cancer chemo/radiotherapies and to validate newly identified molecular circuits as potential targets for the development of mechanism-based therapeutic strategies.

Patients and Methods

Patients, samples, and treatment

Between 1998 and 2006, 186 patients with primary adenocarcinoma of the rectum underwent CRT followed by surgery. The pre-treatment evaluation of the patients

included a complete clinical history and physical examination, colonoscopy, complete blood cell count, transrectal ultrasound, pelvic computed tomography scan or magnetic resonance imaging, abdominal/chest CT and carcino-embryonic antigen test. The inclusion criteria for CRT were as follows: a) biopsy-proven adenocarcinoma of the mid-low rectum (< 11 cm from the anal verge); b) clinical stage T3–4 and/or node-positive; c) Eastern Cooperative Oncology Group performance status 0–2. Since most patients received the preoperative CRT elsewhere, only in 84 out of 186 patients who underwent surgery at our institution the pre CRT research biopsies (2–3 mm^3) were collected during the initial diagnostic endoscopy, immediately frozen and stored in a liquid nitrogen tank. Biopsies were divided into half, one piece undergoing independent histopathological examination and the other prepared for RNA extraction.

No statistically relevant differences were found between clinical and treatment characteristics of included and excluded patients.

The patients underwent to preoperative external beam radiotherapy using high-energy photons (> 6 MV) with conventional fractionation (≥ 50 Gy in 28 fractions, 1.8 Gy/day, 5 sessions per week) and 5-fluorouracil (5-FU)-based chemotherapy administered by bolus or continuous venous infusion. A standard total mesorectal excision was performed 4 to 8 weeks after the completion of pCRT. The study protocol was reviewed and approved by the local ethics committee (protocol number 740 P) and each patient provided written informed consent.

Evaluation of tumor response

The surgical specimens were assessed in a standardized way and reviewed by one pathologist (CM), who was unaware of the patient's outcome. The histopathology findings and definition of radical surgery were reported following the American Joint Committee on Cancer TNM (2002). The tumor response to CRT was defined as the tumor regression grade (TRG) and was scored following the criteria proposed

by Mandard et al. [36]: TRG-1, pathological complete response (pCR), i.e., absence of viable cancer cells in the resected specimen; TRG-2, presence of residual cancer cells; TRG-3, fibrosis outgrowing residual cancer cells; TRG-4, residual cancer cells outgrowing fibrosis; and TRG-5, absence of response. According to the TRG, the patients were classified as responders (TRG 1–2) and non-responders (TRG 3–5).[37,38]

RNA extraction

After independent histopathology review of sample set, in 52 out of 84 biopsies containing more than 70% tumor, RNA was extracted by phenol/chloroform extraction (TRIzol; Invitrogen) prior to further purification by column chromatography (RNeasy Mini kit; Qiagen). RNA integrity (RIN) was then assessed using the Agilent 2100 Bioanalyzer (Agilent Technologies); 4 samples showed evidence of RNA degradation (RIN<6) and were excluded from the analysis.

Microarrays preparation

Gene expression analysis was performed using the Affymetrix GeneChip Human Genome U133 Plus 2.0 Array Platform. Preparation of labeled and fragmented RNA targets, hybridization and scanning were carried out according to the manufacturer's protocol (Affymetrix). Briefly, 100 ng of total RNA for each sample was processed using the GeneChip 30 IVT Express Kit. RNA was reverse transcribed and then converted to double-stranded cDNA prior to biotin labeling during *in vitro* transcription. Fifteen micrograms of labeled aRNA was then fragmented, and quality control was carried out using the Agilent Bioanalyzer. Fragmented aRNA was then hybridized on Gene-Chip Human Genome U133 Plus 2.0 Arrays for 16 hours at 45°C. Arrays were then washed and stained using the GeneChip Hybridization, Wash, and Stain Kit on the GeneChip Fluidics Station 450. Chips were then scanned using the Affymetrix GeneChip Scanner 3000. Six out of 48 processed samples did not pass quality controls and were excluded from the analysis; thus, a total of 42 samples were used in the final analysis (19 responders and 23 non-responders).

Class comparison and class prediction analyses

The Affymetrix Human Genome U133 Plus 2.0 Array expressions were preprocessed and normalized using Robust Multiarray Average (RMA) procedure.39 A class-comparison analysis was applied to determine which genes were differentially expressed between responders and non-responders.

To this aim we used the Fss test statistic, which is a modified F test statistic that shrinks both the means and the variance. The Fss test has almost identical power as the Maximum Average Powerful test, but it is computationally less demanding and more powerful than the other modified F-type tests (for more details see Hwang, et al. [40]). P-values were computed by means of permutations, hence avoiding any distributional assumption. P-values adjustment for multiple testing was made using the Holm-Bonferroni method to control the family wise error rate. Adjusted p-values < 0.05 were considered significant.

We performed a cluster analysis on the interesting probe-sets to show the discriminant power of the profiles. To further investigate the predictive capability of genes expression, we selected the logistic model optimizing the Akaike Information Criterion (AIC) considering all the probe-sets.[41] LOOCV was then used to estimate the prediction accuracy for the selected model.[42,43]

Quantitative real-time PCR

The amount of starting RNA was normalized using 18S rRNA as a control transcript. To this end, a QuantumRNA 18S internal standard kit (Ambion) was utilized, followed by quantification of the electrophoretic bands by ImageQuant (Molecular-Dynamics). Real time PCR was performed on ABI PRISM 7300 (Applied Biosystems Foster City, California, USA) by using specific TaqMan© Gene Expression Assays (Applied Biosystems): XRCC3 (Hs00193725_m1), ASXL2 (Hs00827052_m1), HFM1

(Hs01651101_m1), ZNF160 (Hs00369142_m1). For the amplification, the qPCR core kit was utilized (Applied Biosystem). Real time PCR conditions were set as specified by the manufacturer. All samples were amplified in triplicate and results were analyzed by the $2^{-\Delta\Delta Ct}$ method.[44]

Cell Culture

HCT116 and HCT116 $p53^{-/-}$colon carcinoma cell lines were a kind gift of Prof. Bert Vogelstein (John Hopkins University, Baltimore, MD USA). Cells were maintained and cultured in a 37°C incubator at 5% CO2 and grown with McCoy's 5A-Glutamax medium with 10% FBS (Gibco, not Heat Inactivated), 100 U/ml Penicillin and 100 mg/ml Streptomycin.

siRNA mediated knockdown and cell treatments

For siRNA mediated knockdown, HCT116 and HCT116 $p53^{-/-}$ cells were transfected with control siRNA (Negative Control siRNA #1, Life Technologies, final concentration 10 nM) or siRNA against XRCC3 (s14946, Life Technologies, final concentration 10 nM), using Lipofectamine™ RNAiMax reagent (Life Technologies) and following manufacturer's protocol optimized for this cell lines.

5-Fluorouracil (5-FU, clinical grade) was administered to cells at the final concentration of 200 mM, 36 hours after transfection.

Cell viability assay and cell death evaluation

Cell viability was evaluated by the Crystal Violet (CV) assay and absorbance was measured with a microplate reader (Tecan Instruments). The cell viability data were calculated and expressed as the ratio between the absorbance read at the end of treatment and the absorbance read 24h after seeding. To test caspase 3/7 activity it was used the Caspase-Glo™ 3/7 Assay (Promega) following manufacturer's protocol. Statistical analysis was performed using IBM SPSS Statistics (version 19).

Significant differences between groups were determined by ANOVA with Bonferroni's post-hoc test for multiple comparisons (adjusted p-value <0.05 was considered as significant).

Protein extracts and Immunoblotting

Cells where harvested at determined time points and lysed with a modified RIPA buffer: Tris-HCl pH 8, 50 mM; NaCl 500 mM; IGEPAL 1% v/v; Sodium Deoxycholate 0.5% v/v; EGTA 1 mM; EDTA 1 mM; DTT 1 mM; Protease Inhibitor Cocktail (Sigma-Aldrich) 2% v/v. Quantification of protein lysates was performed using MicroBCA assay (Thermo Scientific). Protein extracts were separated by SDS-PAGE (NuPAGE, Life Technologies) and blotted on nitrocellulose membranes (iBlot system, Life Technologies). Membranes were then immunodecorated with the following primary antibodies: anti-XRCC3 (mouse monoclonal [10F1/6], Abcam) at a 1:1000 dilution and anti-vinculin (mouse monoclonal [V824], Sigma-Aldrich) at a 1:5000 dilution. The signal detection was performed with a HRP-conjugated secondary anti-mouse antibody (GE Healthcare) and images digitally acquired with G-BOX System (Syngene).

Immunohistochemistry

For each sample, we chosen one slide corresponding to the most representative part of the tumor in order to perform an immunohistochemical evaluation of p53 protein expression. Formalin-fixed, paraffin-embedded sections were deparaffinized and rehydrated and p53 was detected by the mouse monoclonal antibody anti-p53 Ab-2 (clone PAb 1801, Oncogene Research Products) as previously describe in Esposito et al.[45] p53 protein expression was graded as: (1) absent or present in ≤10% of tumor cells; (2) present in 11–25%; (3) present in 26 – 75%, or (4) present in >75% of tumor cells.

Network analysis

We further investigated the molecular pathways involving the predictive classifier using protein-protein interactions (PPIs) and enrichment analysis, as well as the possible common microRNAs and drugs targeting them. We first characterized one part of the classifier by retrieving physical PPIs from I2D database ver. 1.95[46] [http://ophid.utoronto.ca/i2d], creating a PPI network that we visualized and analyzed in NAViGaTOR 2.3 47 [http://ophid.utoronto.ca/navigator]. We then performed a functional annotation and enrichment analysis of all the proteins of the network using DAVID Bioinformatics resources 6.7 [48,49] [http://david.abcc.ncifcrf.gov/], a study of the microRNAs targeting the PPI network using mirDIP 1.1 [50] [http://ophid.utoronto.ca/mir-DIP], and a study of the drugs targeting the same network using DrugBank 3 [51] [http://www.drugbank.ca/]. Moreover, to prioritize microRNAs in the network, we collected data from published studies on response to neoadjuvant chemoradiotherapy and microRNA signatures. [17-19]

Disclosure of Potential Conflicts of Interest

No potential conflicts of interest were disclosed.

Acknowledgments

Some technical aspects and clinical work was supported by: Alessandro Ambrosi,[1] Gaspar C[2], Friso ML,[3] Lonardi S[4], ([1]University Center for Statistics in the Biomedical Sciences, Università Vita-Salute, San Raffaele Scientific Institute, Milan, Italy; [2]Department of Pathology, Josephine Nefkens Institute, Erasmus MC, Rotterdam, The Netherlands; [3]Radiotherapy and Nuclear Medicine Unit, Istituto Oncologico Veneto - IRCCS, Padua, Italy; [4]First Medical Oncology Unit, Istituto Oncologico

Veneto - IRCCS, Padua, Italy). Biological samples were provided by Surgical Clinic, Tumor Tissue Biobank.

Funding

This study was supported in part by grants from the CARIPARO, AIRC Foundation and AIRC Special Program Molecular Clinical Oncology, 5X1000 (No.12214), Fondazione Città della Speranza and MIUR (PON_02782 to ML). Computational analyses were supported in part by Ontario Research Fund (GL2-01-030), Canada Foundation for Innovation (CFI #12301 and CFI #203373), Canada Research chair Program (CRC #203373 and CRC #225404), and IBM to IJ. CP was funded in part by Friuli Exchange Program. This research was funded in part by the Ontario Ministry of Health and Long Term Care. The views expressed do not necessarily reflect those of the OMOHLTC.

References

1. Sauer R, Becker H, Hohenberger W, Rodel C, Wittekind C, Fietkau R, Martus P, Tschmelitsch J, Hager E, Hess CF, et al. Preoperative versus postoperative chemoradiotherapy for rectal cancer. N Engl J Med 2004; 351:1731-40; PMID:15496622; http://dx.doi.org/ 10.1056/NEJMoa040694

2. Bosset JF, Collette L, Calais G, Mineur L, Maingon P, Radosevic-Jelic L, Daban A, Bardet E, Beny A, Ollier JC. Chemotherapy with preoperative radiotherapy in rectal cancer. N Engl J Med 2006; 355:1114-23; PMID:16971718; http://dx.doi.org/10.1056/ NEJMoa060829

3. Roh MS, Colangelo LH, O'Connell MJ, Yothers G, Deutsch M, Allegra CJ, Kahlenberg MS, Baez-Diaz L, Ursiny CS, Petrelli NJ, et al. Preoperative multimodality therapy improves disease-free survival in patients with carcinoma of the rectum: NSABP R-03. J Clin Oncol 2009; 27:5124-30; PMID:19770376; http://dx.doi.org/10.1200/JCO.2009.22.0467

4. Minsky BD, Cohen AM, Kemeny N, Enker WE, Kelsen DP, Reichman B, Saltz L, Sigurdson ER, Frankel J. Enhancement of radiation-induced downstaging of rectal cancer by fluorouracil and high-dose leucovorin chemotherapy. J Clin Oncol 1992; 10:79-84; PMID:1727928

5. Mohiuddin M, Hayne M, Regine WF, Hanna N, Hagihara PF, McGrath P, Marks GM. Prognostic significance of postchemoradiation stage following preoperative chemotherapy and radiation for advanced/ recurrent rectal cancers. Int J Radiat Oncol Biol Phys 2000; 48:1075-80; PMID:11072165; http://dx.doi.org/10.1016/S0360-3016(00)00732-X

6. Smith FM, Reynolds JV, Miller N, Stephens RB, Kennedy MJ. Pathological and molecular predictors of the response of rectal cancer to neoadjuvant radiochemotherapy. Eur J Surg Oncol 2006; 32:55-64; PMID:16324817; http://dx.doi.org/10.1016/j.ejso.2005.09.010

7. Kuremsky JG, Tepper JE, McLeod HL. Biomarkers for response to neoadjuvant chemoradiation for rectal cancer. Int J Radiat Oncol Biol Phys 2009; 74:673-88; PMID:19480968; http://dx.doi.org/10.1016/j.ijrobp.2009.03.003

8. Desch CE, Benson AB, 3rd, Somerfield MR, Flynn PJ, Krause C, Loprinzi CL, Minsky BD, Pfister DG, Virgo KS, Petrelli NJ. Colorectal cancer surveillance: 2005 update of an American Society of Clinical Oncology practice guideline. J Clin Oncol 2005; 23:8512-9; PMID:16260687; http://dx.doi.org/10.1200/JCO.2005.04.0063

9. Watanabe T, Komuro Y, Kiyomatsu T, Kanazawa T, Kazama Y, Tanaka J, Tanaka T, Yamamoto Y, Shirane M, Muto T, et al. Prediction of sensitivity of rectal cancer cells in response to preoperative radiotherapy by DNA microarray analysis of gene expression profiles. Cancer Res 2006; 66:3370-4; PMID:16585155; http://dx.doi.org/10.1158/0008-5472.CAN-05-3834

10. Daemen A, Gevaert O, De Bie T, Debucquoy A, Machiels JP, De Moor B, Haustermans K. Integrating microarray and proteomics data to predict the response on cetuximab in patients with rectal cancer. Pac Symp Biocomput 2008:166-77; PMID:18229684

11. Ghadimi BM, Grade M, Difilippantonio MJ, Varma S, Simon R, Montagna C, Fuzesi L, Langer C, Becker H, Liersch T, et al. Effectiveness of gene expression profiling for response prediction of rectal adenocarcinomas to preoperative chemoradiotherapy. J Clin Oncol 2005; 23:1826-38; PMID:15774776; http://dx.doi.org/10.1200/JCO.2005.00.406

12. Rimkus C, Friederichs J, Boulesteix AL, Theisen J, Mages J, Becker K, Nekarda H, Rosenberg R, Janssen KP, Siewert JR. Microarray-based prediction of tumor response to neoadjuvant radiochemotherapy of patients with locally advanced rectal cancer. Clin Gastroenterol Hepatol 2008; 6:53-61; PMID:18166477; http://dx.doi.org/10.1016/j.cgh.2007.10.022

13. Kim IJ, Lim SB, Kang HC, Chang HJ, Ahn SA, Park HW, Jang SG, Park JH, Kim DY, Jung KH, et al. Microarray gene expression profiling for predicting complete response to preoperative chemoradiotherapy in patients with advanced rectal cancer. Dis Colon Rectum 2007; 50:1342-53; PMID:17665260; http://dx.doi.org/10.1007/s10350-007-277-7

14. Brettingham-Moore KH, Duong CP, Greenawalt DM, Heriot AG, Ellul J, Dow CA, Murray WK, Hicks RJ, Tjandra J, Chao M, et al. Pretreatment transcriptional profiling for predicting response to neoadjuvant chemoradiotherapy in rectal adenocarcinoma. Clin Cancer Res 17:3039-47; PMID:21224373; http://dx.doi.org/10.1158/1078-0432.CCR-10-2915

15. Bunz F, Hwang PM, Torrance C, Waldman T, Zhang Y, Dillehay L, Williams J, Lengauer C, Kinzler KW, Vogelstein B. Disruption of p53 in human cancer cells alters the responses to therapeutic agents. The Journal of clinical investigation 1999; 104:263-9; PMID:10430607; http://dx.doi.org/10.1172/JCI6863

16. Chung JY, Lu M, Yin Q, Lin SC, Wu H. Molecular basis for the unique specificity of TRAF6. Adv Exp Med Biol 2007; 597:122-30; PMID:17633022; http://dx.doi.org/10.1007/978-0-387-70630-6_10

17. Della Vittoria Scarpati G, Falcetta F, Carlomagno C, Ubezio P, Marchini S, De Stefano A, Singh VK, D'Incalci M, De Placido S, Pepe S. A Specific miRNA Signature Correlates with Complete Pathological Response to Neoadjuvant Chemoradiotherapy in Locally Advanced Rectal Cancer. Int J Radiat Oncol Biol Phys 2012; 83(4):1113-9; PMID:22172905

18. Drebber U, Lay M, Wedemeyer I, Vallbohmer D, Bollschweiler E, Brabender J, Monig SP, Holscher AH, Dienes HP, Odenthal M. Altered levels of the oncomicroRNA 21 and the tumor-supressor microRNAs 143 and 145 in advanced rectal cancer indicate successful neoadjuvant chemoradiotherapy. Int J Oncol 2011; 39:409-15; PMID:21567082

19. Garajova I, Svoboda M, Slaby O, Kocakova I, Fabian P, Kocak I, Vyzula R. ; Possibilities of resistance prediction to neoadjuvant concomitant chemoradiotherapy in the treatment algorithm of patients with rectal carcinoma. Klin Onkol 2008; 21:330-7; PMID:19382596

20. Agostini M, Pucciarelli S, Calore F, Bedin C, Enzo M, Nitti D. miRNAs in colon and rectal cancer: A consensus for their true clinical value. Clin Chim Acta 2010; 411:1181-6; PMID:20452339; http://dx.doi.org/10.1016/j.cca.2010.05.002

21. Cecchin E, Agostini M, Pucciarelli S, De Paoli A, Canzonieri V, Sigon R, De Mattia E, Friso ML, Biason P, Visentin M, et al. Tumor response is predicted by patient genetic profile in rectal cancer patients treated with neo-adjuvant chemo-radiotherapy. The pharmacogenomics journal 2011; 11:214-26; PMID:20368715; http://dx.doi.org/10.1038/tpj.2010.25

22. Pratesi N, Mangoni M, Mancini I, Paiar F, Simi L, Livi L, Cassani S, Buglione M, Grisanti S, Almici C, et al. Association between single nucleotide polymorphisms in the XRCC1 and RAD51 genes and clinical radiosensitivity in head and neck cancer. Radiotherapy and oncology : journal of the European Society for Therapeutic Radiology and Oncology 2011; 99:356-61; PMID:21704413; http://dx.doi.org/10.1016/j.radonc.2011.05.062

23. Mangoni M, Bisanzi S, Carozzi F, Sani C, Biti G, Livi L, Barletta E, Costantini AS, Gorini G. Association between genetic polymorphisms in the XRCC1, XRCC3, XPD, GSTM1, GSTT1, MSH2, MLH1, MSH3, and MGMT genes and radiosensitivity in breast cancer patients. International journal of radiation oncology, biology, physics 2011; 81:52-8; PMID:20708344; http://dx.doi.org/10.1016/j.ijrobp.2010.04.023

24. Vral A, Willems P, Claes K, Poppe B, Perletti G, Thierens H. Combined effect of polymorphisms in Rad51 and Xrcc3 on breast cancer risk and chromosomal radiosensitivity. Molecular medicine reports 2011; 4:901-12; PMID:21725594

25. Alsbeih G, El-Sebaie M, Al-Harbi N, Al-Hadyan K, Shoukri M, Al-Rajhi N. SNPs in genes implicated in radiation response are associated with radiotoxicity and evoke roles as predictive and prognostic biomarkers. Radiation oncology 2013; 8:125; PMID:23697595; http://dx.doi.org/10.1186/1748-717X-8-125

26. Curwen GB, Murphy S, Tawn EJ, Winther, JF, Boice, JD, Jr. A study of DNA damage recognition and repair gene polymorphisms in relation to cancer predisposition and G2 chromosomal radiosensitivity. Environmental and molecular mutagenesis 2011; 52:72-6; PMID:21113933; http://dx.doi.org/10.1002/em.20633

27. Farnebo L, Jerhammar F, Ceder R, Grafstrom RC, Vainikka L, Thunell L, Grenman R, Johansson AC, Roberg K. Combining factors on protein and gene level to predict radioresponse in head and neck cancer cell lines. Journal of oral pathology & medicine : official publication of the International Association of Oral Pathologists and the American Academy of Oral Pathology 2011; 40:739-46; http://dx.doi.org/10.1111/j.1600-0714.2011.01036.x

28. Akcakaya P, Ekelund S, Kolosenko I, Caramuta S, Ozata DM, Xie H, Lindforss U, Olivecrona H, Lui WO. miR-185 and miR-133b deregulation is associated with overall survival and metastasis in colorectal cancer. Int J Oncol 2011; 39:311-8; PMID:21573504

29. Stark C, Breitkreutz BJ, Reguly T, Boucher L, Breitkreutz A, Tyers M. BioGRID: a general repository for interaction datasets. Nucleic acids research 2006; 34: D535-9; PMID:16381927; http://dx.doi.org/10.1093/nar/gkj109

30. Kerrien S, Alam-Faruque Y, Aranda B, Bancarz I, Bridge A, Derow C, Dimmer E, Feuermann M, Friedrichsen A, Huntley R, et al. IntAct–open source resource for molecular interaction data. Nucleic acids research 2007; 35:D561-5; PMID:17145710; http://dx.doi.org/10.1093/nar/gkl958

31. Rothwell PM, Wilson M, Elwin CE, Norrving B, Algra A, Warlow CP, Meade TW. Long-term effect of aspirin on colorectal cancer incidence and mortality: 20-year follow-up of five randomised trials. Lancet 2010; 376:1741-50; PMID:20970847; http://dx.doi.org/10.1016/S0140-6736(10)61543-7

32. Carroll RE, Benya RV, Turgeon DK, Vareed S, Neuman M, Rodriguez L, Kakarala M, Carpenter PM, McLaren C, Meyskens FL, Jr., et al. Phase IIa clinical trial of curcumin for the prevention of colorectal neoplasia. Cancer Prev Res (Phila) 2011; 4:354-64; PMID:21372035; http://dx.doi.org/10.1158/1940-6207.CAPR-10-0098

33. Sandur SK, Deorukhkar A, Pandey MK, Pabon AM, Shentu S, Guha S, Aggarwal BB, Krishnan S. Curcumin modulates the radiosensitivity of colorectal cancer cells by suppressing constitutive and inducible NF-kappaB activity. Int J Radiat Oncol Biol

Phys,2009;75:534-42;PMID:19735878; http://dx.doi.org/10.1016/ j.ijrobp. 2009.06.034

34. Coussens LM, Werb Z. Inflammation and cancer. Nature 2002; 420:860-7; PMID:12490959; http://dx.doi.org/10.1038/nature01322

35. Gatza CE, Oh SY, Blobe GC. Roles for the type III TGF-beta receptor in human cancer. Cell Signal 2010; 22:1163-74; PMID:20153821; http://dx.doi.org/10.1016/j.cellsig.2010.01.016

36. Mandard AM, Dalibard F, Mandard JC, Marnay J, Henry-Amar M, Petiot JF, Roussel A, Jacob JH, Segol P, Samama G, et al. Pathologic assessment of tumor regression after preoperative chemoradiotherapy of esophageal carcinoma. Clinicopathologic correlations. Cancer 1994; 73:2680-6; PMID:8194005; http://dx.doi.org/10.1002/ 1097-0142(19940601)73:11%3c2680::AID-CNCR282 0731105%3e3.0.CO;2-C

37. Beddy D, Hyland JM, Winter DC, Lim C, White A, Moriarty M, Armstrong J, Fennelly D, Gibbons D, Sheahan K. A simplified tumor regression grade correlates with survival in locally advanced rectal carcinoma treated with neoadjuvant chemoradiotherapy. Ann Surg Oncol 2008; 15:3471-7; PMID:18846402; http://dx.doi.org/10.1245/s10434-008-0149-y

38. Ryan R, Gibbons D, Hyland JM, Treanor D, White A, Mulcahy HE, O'Donoghue DP, Moriarty M, Fennelly D, Sheahan K. Pathological response following longcourse

neoadjuvant chemoradiotherapy for locally advanced rectal cancer. Histopathology 2005; 47:141-6; PMID:16045774; http://dx.doi.org/10.1111/j.1365-2559.2005.02176.x

39. Irizarry RA, Bolstad BM, Collin F, Cope LM, Hobbs B, Speed TP. Summaries of Affymetrix GeneChip probe level data. Nucleic Acids Res 2003; 31:e15; PMID:12582260; http://dx.doi.org/10.1093/nar/gng015

40. Hwang JT, Liu P. Optimal tests shrinking both means and variances applicable to microarray data analysis. Stat Appl Genet Mol Biol 2010; 9:Article36; PMID:20887275

41. Marchet A, Mocellin S, Belluco C, Ambrosi A,DeMarchi F, Mammano E, DigitoM, Leon A, D'Arrigo A, Lise M, et al. Gene expression profile of primary gastric cancer: towards the prediction of lymph node status. Ann Surg Oncol 2007; 14:1058-64; PMID:17106627; http://dx.doi.org/10.1245/s10434-006-9090-0

42. Ntzani EE, Ioannidis JP. Predictive ability of DNA microarrays for cancer outcomes and correlates: an empirical assessment. Lancet 2003; 362:1439-44; PMID:14602436; http://dx.doi.org/10.1016/S0140-6736(03)14686-7

43. Simon R, Radmacher MD, Dobbin K, McShane LM. Pitfalls in the use of DNA microarray data for diagnostic and prognostic classification. J Natl Cancer Inst 2003; 95:14-8; PMID:12509396; http://dx.doi.org/ 10.1093/jnci/95.1.14

44. Livak KJ, Schmittgen TD. Analysis of relative gene expression data using real-time quantitative PCR and the 2(-Delta Delta C(T)) Method. Methods 2001; 25:402-8; PMID:11846609; http://dx.doi.org/ 10.1006/meth.2001.1262

45. Esposito G, Pucciarelli S, Alaggio R, Giacomelli L,Marchiori E, Iaderosa GA, Friso ML, Toppan P, Chieco-Bianchi L, Lise M. P27kip1 expression is associated with tumor response to preoperative chemoradiotherapy in rectal cancer. Annals of surgical oncology 2001; 8:311-8; PMID:11352304; http://dx.doi.org/10.1007/ s10434-001-0311-2

46. Brown KR, Jurisica I. Online predicted human interaction database. Bioinformatics 2005; 21:2076-82; PMID:15657099; http://dx.doi.org/10.1093/bioinformatics/bti273

47. Brown KR, Otasek D, Ali M, McGuffin MJ, Xie W, Devani B, Toch IL, Jurisica I. NAViGaTOR: Network Analysis, Visualization and Graphing Toronto. Bioinformatics 2009; 25:3327-9; PMID:19837718; http://dx.doi.org/10.1093/bioinformatics/btp595

48. Huang da W, Sherman BT, Lempicki RA. Systematic and integrative analysis of large gene lists using DAVID bioinformatics resources. Nat Protoc 2009; 4:44-57; PMID:19131956; http://dx.doi.org/10.1038/nprot. 2008.211

49. Huang da W, Sherman BT, Lempicki RA. Bioinformatics enrichment tools: paths toward the comprehensive functional analysis of large gene lists. Nucleic Acids Res 2009; 37:1-13; PMID:19033363; http://dx.doi. org/10.1093/nar/gkn923

50. Shirdel EA, Xie W, Mak TW, Jurisica I. NAViGaTing the micronome–using multiple microRNA prediction databases to identify signalling pathway-associated microRNAs. PLoS One 2011; 6:e17429; PMID:21364759; http://dx.doi.org/10.1371/journal. pone.0017429

51. Knox C, Law V, Jewison T, Liu P, Ly S, Frolkis A, Pon A, Banco K, Mak C, Neveu V, et al. DrugBank 3.0: a comprehensive resource for 'omics' research on drugs. Nucleic Acids Res 2011; 39:D1035-41; PMID:21059682; http://dx.doi.org/10.1093/nar/gkq1126

Supplementary Data

Supplementary Figure 1. Ingenuity Pathway Analysis on the 19 relevant gene set. The plot shows the correlation among the 19 genes and their location in the cell.

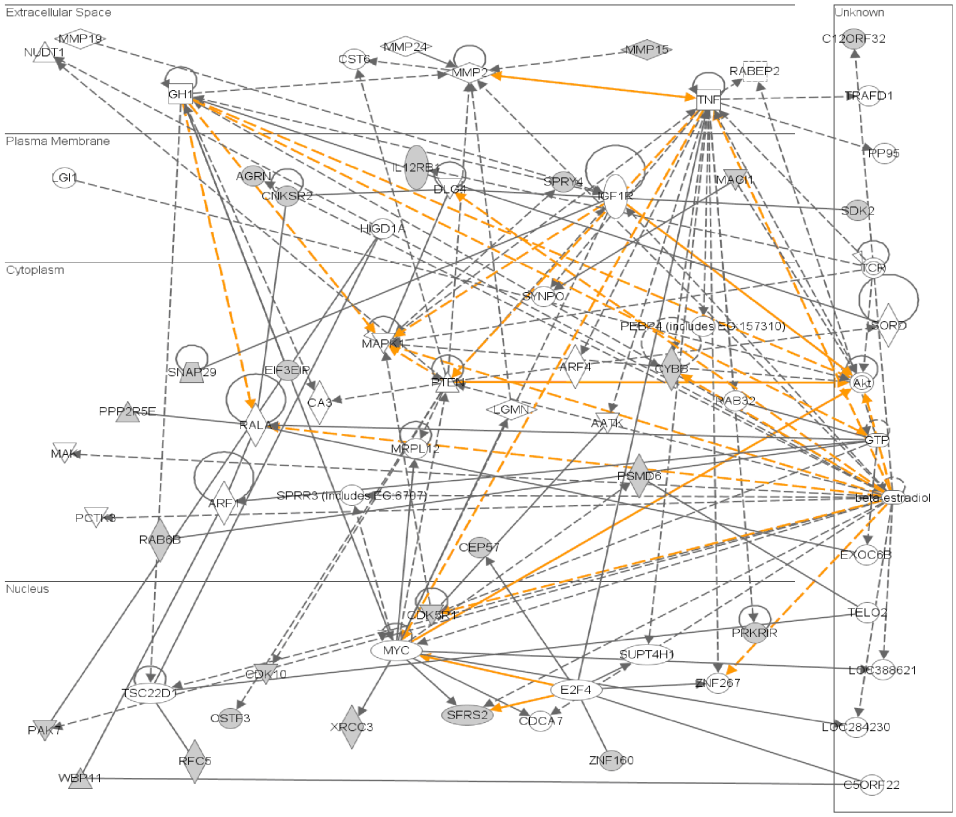

Supplementary Figure 2. siRNA mediated knockdown of XRCC3 in colon carcinoma cell lines. Effects of XRCC3-siRNA on the expression of the XRCC3 protein in HCT116 colon carcinoma 5-FU sensitive cell line at determined time-points after siRNA transfection (upper panel). Effects of XRCC3-siRNA on the

expression of the XRCC3 protein in HCT116 p53-/- colon carcinoma 5-FU resistant cell line at determined time-points after siRNA transfection (lower panel).

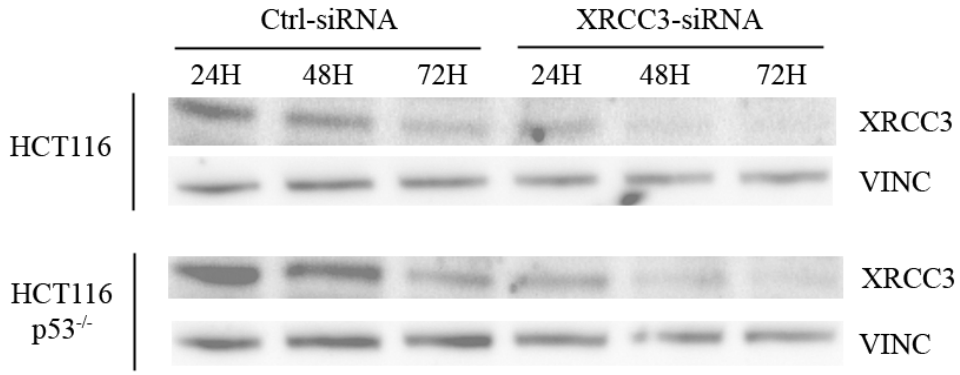

Supplementary Figure 3. A) p53 immunostaining shows overexpression of the oncoprotein in colon cancer cells (on the left of dotted line) compared to normal tissue (on the right of dotted line); B) Colorectal adenocarcinoma lacking p53 nuclear immunostaining.

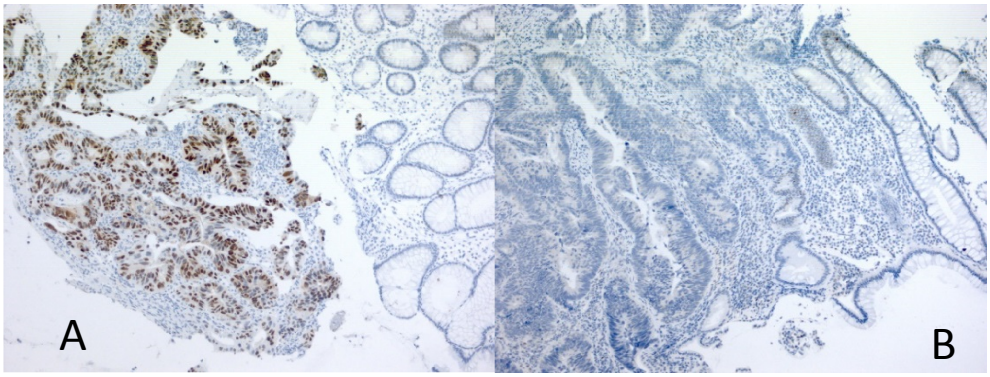

Chapter 4

Inhibition of GSK3B Bypass Drug Resistance of p53-null Colon Carcinomas by Enabling Necroptosis in Response to Chemotherapy

Emanuela Grassilli[1,2], Robert Narloch[1], Elena Federzoni[1], Leonarda Ianzano[1], Fabio Pisano[2], Roberto Giovannoni[1], **Gabriele Romano**[2], Laura Masiero[1], Biagio Eugenio Leone[1], Serena Bonin[3], Marisa Donada[3], Giorgio Stanta[3], Kristian Helin[4], Marialuisa Lavitrano[1,2]

Author's Affiliations: [1]Department of Surgery and Interdisciplinary Medicine, University of Milano-Bicocca, Milano, Italy; [2]BiOnSil srl, Milano; [3]Department of A.C.A.D.E.M., University of Trieste, Trieste, Italy; [4]Biotech Research and Innovation Centre (BRIC) and Centre for Epigenetics, University of Copenhagen, Copenhagen, Denmark.

Published in: **Clinical Cancer Research**; 19(14):3820-31; July 2013

Abstract

Purpose: Evasion from chemotherapy-induced apoptosis due to p53 loss strongly contributes to drug resistance. Identification of specific targets for the treatment of drug-resistant p53-null tumors would therefore increase the effectiveness of cancer therapy.

Experimental Design: By using a kinase-directed short hairpin RNA library and HCT116p53KO drug- resistant colon carcinoma cells, glycogen synthase kinase 3 beta (GSK3B) was identified as a target whose silencing bypasses drug resistance due to loss of p53. p53-null colon cancer cell lines with different sets of mutations were used to validate the role of GSK3B in sustaining resistance and to characterize cell death mechanisms triggered by chemotherapy when GSK3B is silenced. *In vivo* xenograft studies were conducted to confirm resensitization of drug-resistant cells to chemotherapy upon GSK3 inhibition. Colon cancer samples from a cohort of 50 chemotherapy-treated stage II patients were analyzed for active GSK3B expression.

Results: Downregulation of GSK3B in various drug-resistant p53-null colon cancer cell lines abolished cell viability and colony growth after drug addition without affecting cell proliferation or cell cycle in untreated cells. Cell death of 5-fluorouracil (5FU)–treated p53-null GSK3B-silenced colon carcinoma cells occurred via PARP1-dependent and AIF-mediated but RIP1-independent necroptosis. *In vivo* studies showed that drug-resistant xenograft tumor mass was significantly reduced only when 5FU was given after GSK3B inhibition. Tissue microarray analysis of colon carcinoma samples from 5FU-treated patients revealed that GSK3B is significantly more activated in drug-resistant versus responsive patients.

Conclusions: Targeting GSK3B, in combination with chemotherapy, may represent a novel strategy for the treatment of chemotherapy-resistant tumors.

Translational Relevance

DNA-damaging agents are among the most used drugs in the treatment of carcinomas. However, their efficacy is often hindered by development of drug resistance, usually derived from the alteration or misregulation of one or more apoptotic/antiapoptotic mechanisms. By studying a cohort of stage II colon carcinoma patients we found that glycogen synthase kinase 3 beta (GSK3B) is activated in almost half of all colon carcinomas and in two thirds of drug-resistant ones. Moreover, we show that upon GSK3B inhibition, DNA-damaging drugs bypass the need of p53 to induce cell death and tumor cells die by caspase-independent necroptotic death. Because p53 function is compromised in the vast majority of human cancers and caspase-dependent apoptosis is frequently impaired in tumors, GSK3B inhibition in combination with chemotherapy may represent a molecularly targeted approach to treat resistant tumors.

Introduction

Two main problems that affect the outcome of cancer therapy are the use of "poorly specific" drugs and, in a high percentage of patients, the lack of response due to drug resistance. Poor specificity is due to the fact that "classical" chemotherapeutic drugs act by inducing a generic damage (either to the DNA or the microtubuli) that cells recognize as an apoptotic trigger (1). However, several apoptotic mechanisms, or their regulation, are disabled during oncogenic transformation and progression, thus rendering a consistent percentage of tumors resistant to chemotherapy-induced cell death (2). To bypass the "poor specificity" issue, more rational approaches have been pursued by applying a molecularly

targeted approach, that is developing new drugs acting specifically by targeting a single molecule crucial for the survival of tumor cells. In the last decade, several kinases hyperactivated in different types of cancers have been successfully targeted and the corresponding specific inhibitors have entered therapy (3).

To increase the effectiveness of cancer therapy it could be appropriate to apply the molecular therapy approach, that is to find specific molecules to target, also in the case of drug resistance. Kinases are the best candidates for this approach for at least 2 reasons: (i) It is known that several kinases are usually coactivated by redundant inputs and participates in the pathogenesis of most solid tumors (4). Moreover, they often directly or indirectly contribute to render cancer cells more resistant to different types of stress (5, 6). (ii) Kinases are thought to be "druggable" targets.

Based on these premises, we conducted a phenotype screen using the kinase pools of the NKI short hairpin RNA (shRNA) library (7) and 5-fluorouracil (5FU)-resistant HCT116p53KO cells (8) as a model. We decided to use as a model a p53-null background because p53 activity is either lost or compromised in most tumors (9), which abolishes the apoptotic response to many anticancer agents (10). Here we report that the downregulation of glycogen synthase kinase 3 beta (GSK3B) abolishes growth after treatment with DNA-damaging drugs in the absence of p53 in resistant cells. Moreover, we show that GSK3B-depleted colon carcinoma cells undergo PARP1-dependent and AIF-mediated necroptosis. Accordingly, GSK3 inhibition by LiCl restores sensitivity to 5FU in xenograft experiments. Finally, studying a cohort of 50 colon carcinoma stage II patients we found that GSK3B is activated in 47% of all samples studied and in 63.6% of those from drug-resistant patients. Based on these results we propose that GSK3B is an interesting candidate target for the treatment of patients with 5FU-resistant tumors.

Materials and Methods

Drugs and reagents

5FU (Teva), oxaliplatin (OxPt; Sanofi-Aventis) were from San Gerardo Hospital (Monza, Italy). LiCl and necrostatin- 1 were from Sigma-Aldrich.

Cell lines and cell culture

DLD-1 and SW480 colon carcinoma cell lines were from the American Type Culture Collection (Manassas, VA). Isogenic p53 wild-type and p53 knockout HCT116 colon carcinoma cell lines were a kind gift of Dr. B. Vogelstein (Johns Hopkins University, Baltimore, MD). Upon arrival, cells were expanded and frozen as seed stocks of first or second passage. All cells were passaged for a maximum of 6 weeks, after which new seed stocks were thawed for experimental use. All cell lines were maintained in McCoy medium (Invitrogen) supplemented with 10% FBS (Invitrogen) and 1% penicillin–streptomycin at 37o C in 5% CO2. Cell lines stably interfered for each gene identified in the screen were obtained by retroviral infection and selection with the appropriate antibiotic as previously described (11). shRNAGSK3B target sequence GATGAGGTCTATCTTAATC (nt:1353-1371).

Cell viability

Cells were seeded overnight at 70% confluency and the next morning treated or not with the indicated drugs and inhibitors. Seventy-two hours later dead cells were counted—triplicate wells in each experiment—after Trypan blue staining. Graphs shown throughout the article represent the average of 3 to 5 independent experiments. Average ± SDs is plotted in the graphs.

Colony assay

A total of 3 x 10^5 cells/well were seeded in 6-well plate, let adhere overnight, and treated with 200 μmol/L 5FU for 12 hours. Cells were then trypsinized, counted, and reseeded at a low density (1,000 cells/well in 6-well plate) in triplicate. In

experiments without drug treatment, 1,000 cells/well were directly seeded in 6-well plates. In both cases, medium was replaced every 3 days, and after 2 weeks, colonies were fixed and stained in 1% crystal violet, 35% ethanol.

Caspase assay

A total of 4 x 10^4 cells/well were seeded in triplicate in 96-well plate, let adhere overnight, and treated with 200 µmol/L 5FU for 72 hours before evaluating active caspase-3/7 by the Caspase-Glo3/7 Assay System (Promega) according to the manufacturer's instructions.

Cell proliferation

A total of 1 x 104 cells/well were seeded in triplicate in 96- well plate and starting the following day (day 0) proliferation was evaluated each 24 hours by CellTiter 96 Aqueous Non-Radioactive Cell Proliferation Assay (Promega) according to the manufacturer's instructions.

Flow cytometric analysis

Exponentially growing cells were trypsinized, washed twice with cold PBS, fixed in ice-cold 96% ethanol, washed twice with cold PBS, and incubated overnight at 4°C with propidium iodide (10 mg/mL) and RNase A (12.5 mg/mL) in PBS. Fluorescence intensity of 1 x 10^4 cells/sample was determined with a FACSCalibur instrument and data analyzed using Modfit Cell Cycle Analysis (Becton Dickinson) as previously described (12).

Reporter assay

0.2 µg TopFlash + 0.2 µg pGL4.75 reporters were transfected in 5 x 10^4 cells/well seeded in triplicate in a 96-well plate and reporter activity was evaluated 48 hours later by Dual-Glo Luciferase Assay (Promega) according to the manufacturer's instructions. For a detailed description see Supplementary Data.

Western blot analysis

Cells were lysed in high-salt lysis buffer (Hepes 50 mmol/L, pH 7.5, NaCl 500 mmol/L, DTT 1 mmol/L, EDTA 1 mmol/L, 0.1% NP40) supplemented with 1% protease inhibitor cocktail (PIC; Sigma-Aldrich) and Western blots performed as described previously (11) using the following antibodies: anti-actin (A1978; Sigma-Aldrich), anti-cleaved Caspase-3 (#9661), anti-pSer9-GSK3B (clone D85E12), anti-pSer21- GSK3A (clone 36E9) were from Cell Signaling; anti- GSK3A/B sc-56913), anti–caspase-3 (total; sc-6549) were from Santa Cruz Biotechnology.

Immunofluorescence

Cells were fixed with 4% paraformaldehyde in PBS. Permeabilization and staining with anti-PAR (clone mAb 10H, Alexis), anti-AIF (sc-13116; Santa Cruz Biotechnology), anti-g H2AX (Ab 22551; Abcam), anti-RPA70 (clone 2H10; Sigma-Aldrich) was conducted as described (11). Cells were counterstained with DAPI before microscopic examination using 60x magnification and a Nikon Eclipse 80i microscope. Images were acquired using Genikon (Nikon) software and processed with Adobe Photoshop.

Patients

The case study was composed of 50 patients with a clinical diagnosis of colon cancer who received 5FU adjuvant chemotherapy after surgery. All samples were classified by a pathologist as stage II. At the first diagnosis of colon cancer, patients had no other cancers and they were followed up until December 31, 2010 or death, whichever came first. The median duration of overall follow-up was 9.2 years (25th–75th percentile = 3.8–12.7 years). Overall survival was defined as the time from surgery to colon cancer–specific death. Log-rank test was used to check the dependence of patients' survival on single variables or on combinations of variables. All P values are two-sided with values <0.05 regarded as statistically

significant. Statistical analyses were conducted with the Stata/SE 12 package (Stata).

Immunohistochemistry

Sample triplicates were arrayed using BioRep Tissue MicroArray System and antibody against pTyr216-GSK3B (sc-135653, Santa Cruz Biotechnology) was used as described (13). pTyr216-GSK3B staining was graded accordingly to an increasing intensity by blind reading by 2 experienced operators.

In vivo xenograft studies

All the experiments involving animals were carried out in accordance with Italian law (DDL 116/92) and European Guidelines for use and care of laboratory animals, according to a protocol approved by the local ethical committee of BIOGEM Institute (where the experiments have been con- ducted). Tumors were established by s.c. injecting 1 x 10^6 cells (in 100 µL of a 50% PBS and 50% Matrigel solution), HCT116p53KO cells into the left flanks and HCT116 into the right flanks, of 5 to 7 weeks old female CD-1 nude mice (Charles River Laboratories). When HCT116p53KO tumors reached the average volume of 100 mm^3 (day 7 post-engraftment), animals were randomized and given vehicle, 5FU [via intraperitoneal (i.p.) injection, 75 mg/kg, twice a week], LiCl (via i.p. injection, 80 mg/kg, twice a day for 5 days a week), or a combination thereof. 5FU treatment started at day 8 post-engraftment, whereas LiCl treatment started at day 7 post-engraftment. Mice that received LiCl were also given additional NaCl to prevent electrolyte imbalance. Control mice received i.p. injections of vehicle (0.9% NaCl solution) with the same schedule of the other groups. Tumors were measured with caliper twice/week. Statistical significance was determined with a Kruskal–Wallis non parametric test (normal distribution not assumable), followed by Nemenyi–Damico–Wolfe–Dunn test for multiple pairwise comparisons between groups. In all cases, a P value < 0.05 was considered as significant. Resected tumors were weighed then fixed in 4%

paraformaldehyde and processed for hystological and immunohistochemistry analysis. Tumor biopsies were removed from formalin, dehydrated, diafanized with xylene, put in paraffin, sectioned with microtome, put on slides, and stained with hematoxylin/eosin following standard procedures. Anti- p53 [mouse monoclonal (DO-7); Ventana Medical) was used at a 1:500 dilution. Hystological and immunohistochemistry slides were then digitally acquired using Scan- Scope (Aperio) system.

Results

GSK3B silencing abolishes drug resistance of p53-null colon carcinoma cell lines

HCT116p53KO colon carcinoma cell line is resistant to many genotoxic drugs due to lack of p53 (8). To identify kinases whose activation sustain resistance to DNA-damaging chemotherapy, we conducted a phenotype screen using the kinase pools of the NKI shRNA library (7) and 5FU-resistant HCT116p53KO cells as a model system (Supplementary Fig. S1A). After having validated several of the hits (Supplementary Fig. S1B–S1D), we focused on one of these, GSK3B. In epithelial cells, this kinase, by phosphorylating β-catenin, negatively regulates proliferation (14); in addition, it is widely accepted that GSK3B suppresses cancer-associated signaling pathways via negative regulation of the Wnt/β-catenin pathway that support both invasive and metastatic processes (14, 15). However, HCT116p53KO cells express mutated, nonphosphorylatable β-catenin, that is constitutively active and not regulatable by GSK3B (16) suggesting that in our model system the effect of GSK3B inhibition is independent of its known antiproliferative role. To test this hypothesis, we first established stable cell lines expressing low-to-undetectable levels of GSK3B by transducing HCT116p53KO, as well as DLD-1 and SW480, with retroviruses

expressing shRNAs to GSK3B (Fig. 1A). DLD-1 and SW480 express mutated p53 and constitutively active β-catenin due to an APC truncation (16 and Supplementary Table S1) that prevents GSK3B-mediated regulation. Next, we analyzed several parameters related to cell cycle and proliferation in cells stably silenced for GSK3B. Notably, downregulation of GSK3B does not change the proliferation of these cells as assessed either by colony assay (Fig. 1B) or by growth curve (Fig. 1C). Also cell- cycle distribution is not affected by lack of GSK3B (Fig. 1D). Finally, as expected, the decrease in GSK3B expression does not alter β-catenin activity, as shown by the reporter assay experiment in Fig. 1E.

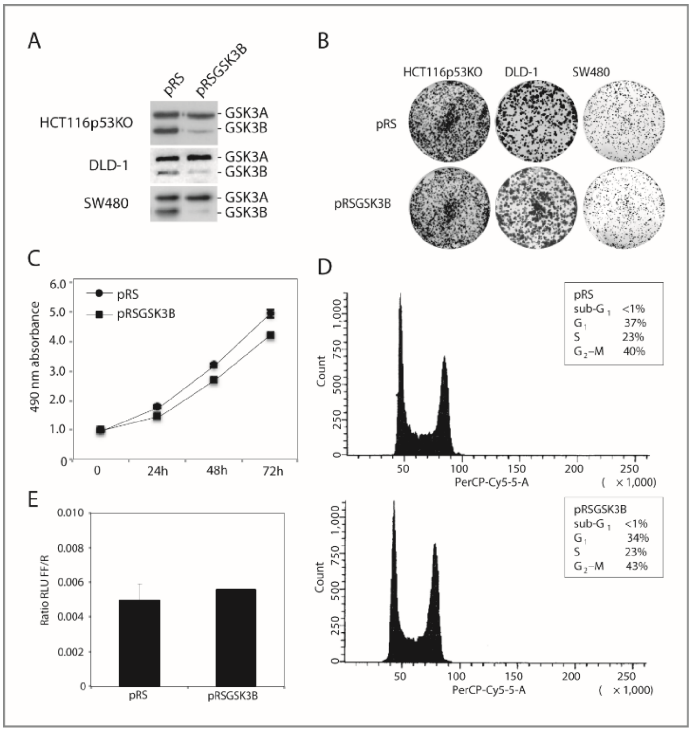

*Figure 1. GSK3B silencing in p53-null colon carcinoma cell lines does not affect proliferation or cell cycle. **A**, decreased expression of GSK3B in HCT116p53KO, SW480, and DLD-1 cells stably infected with empty (pRS) and GSK3B shRNA encoding vector (pRSGSK3B). An antibody recognizing both GSK3A and GSK3B was used: GSK3A levels served as an internal loading control. **B**, the indicated cell lines were seeded at low density and grown for 2 weeks before staining. **C**, growth curve of HCT116p53KO stably infected with pRS and pRSGSK3B. **D**, DNA content of HCT116p53KO stably infected with pRS and pRSGSK3B in the logarithmic phase of growth was evaluated after propidium iodide staining and flow cytometric analysis; percentage of cells in sub-G1, G1, S phase, andG2–M are indicated as an inset inside the graph. **E**, β-catenin activity in HCT116p53KO-pRS and -pRSGSK3B was evaluated 48 hours after cotransfection of firefly (FF) luciferase under the control of a responsive reporter together with constitutively expressed renilla (R) luciferase used as a normalizator. RLU, relative light units.*

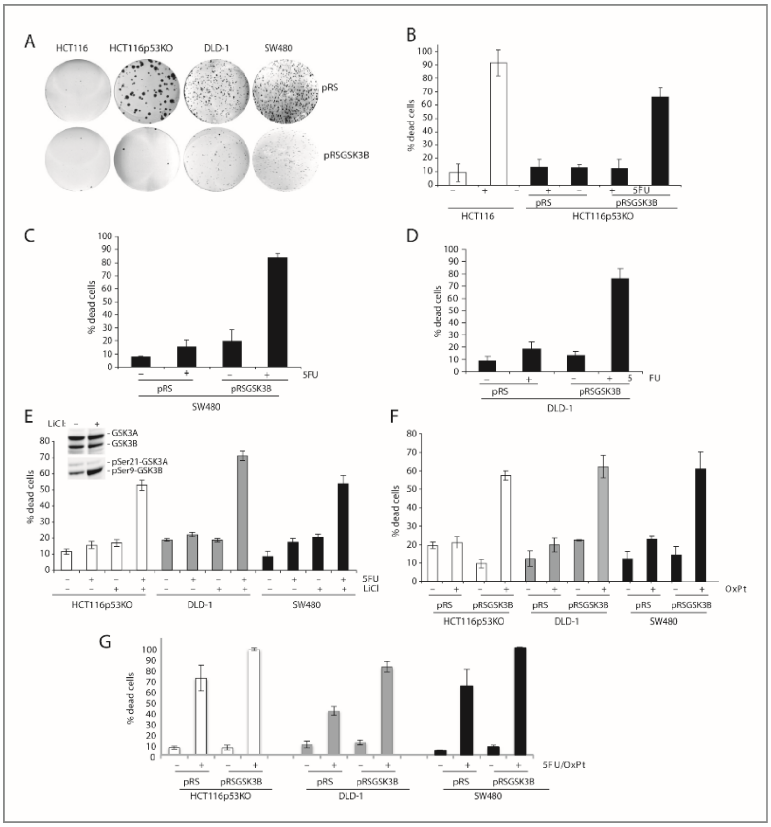

Altogether these data show that GSK3B silencing in colon carcinoma cells does not affect cell cycle or proliferation. Next, we studied the role of GSK3B in the response to chemotherapy and found that GSK3B stable silencing in p53-null drug-resistant colon carcinoma cells abolishes growth of colonies after drug exposure (Fig. 2A) and resensitize cells to drug-induced cytotoxicity (Fig. 2B–D). To further confirm

Figure 2. *GSK3B silencing or inhibition abolishes drug resistance of p53-null colon carcinoma cell lines.* ***A****, the indicated cell lines were trypsinized and reseeded at low density 12 hours after 5FU treatment. Colony formation was assessed 2 weeks after the reseeding. Cell death 72 hours after 200 μmol/L 5FU treatment of (****B****) HCT116p53KO, (****C****) SW480, and (****D****) DLD-1 cells stably infected with empty (pRS) and GSK3B shRNA-encoding vector (pRSGSK3B). HCT116 cells were used as a positive control.* ***E****, cell death 72 hours after 200 μmol/L 5FU treatment of HCT116p53KO, SW480, and DLD-1 cells in the presence or absence of 10 mmol/L LiCl. Insert, increased levels of inhibitory pSer-GSK3B (but not of pSer21-GSK3A) upon LiCl treatment of HCT116p53KO cells were assessed by incubating the blot with a mix of pSer9-GSK3B and pSer21-GSK3A antibodies.* ***F****, cell death of HCT116p53KO, DLD-1, and SW480 cells stably infected with empty pRS and pRSGSK3B 72 hours after treatment with 50 μmol/L OxPt.* ***G****, as in* ***F*** *after treatment with 200 μmol/L 5FU + 50 μmol/L OxPt.*

the role of GSK3B in drug resistance, we inhibited its function by 2 more different means (17).

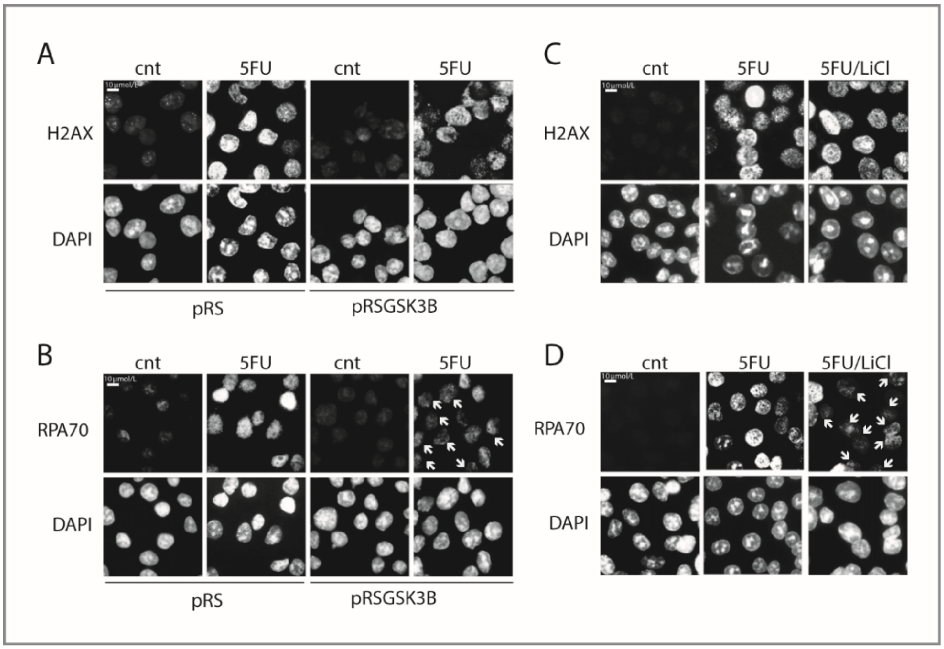

Figure 3. *GSK3B inhibition abolishes drug resistance of p53-null colon carcinoma cells by affecting the response to DNA damage. HCT116p53KO cells stably infected with empty (pRS) and GSK3B shRNA-encoding vector (pRSGSK3B) untreated (cnt) or treated for 18 hours with 200 μmol/L 5FU (5FU) and stained with anti-gH2AX antibody (**A**) or anti-RPA70 antibody (**B**) and counterstained with DAPI. HCT116p53KO untreated (cnt), treated for 18 hours with 200 μmol/L 5FU (5FU) or with 200 μmol/L 5FU + 10 mmol/L LiCl and stained with anti-gH2AX antibody (**C**) or anti-RPA70 antibody (**D**) and counterstained with DAPI. White arrows indicate cells with very few or no RPA70 foci.*

Transient GSK3B protein depletion by use of siRNA restored cell death in response to 5FU (Supplementary Fig. S2). We confirmed these findings by treating HCT116p53KO, DLD- 1, and SW480 cells with 5FU in the presence of LiCl (a GSK3B inhibitor approved by FDA for the treatment of bipolar disorder; ref. 14; Fig. 2E). We further tested the role of GSK3B in drug resistance by treating colon cancer cells with OxPt, another DNA-damaging drug commonly used in colon carcinoma therapy, usually given in combination with 5FU and found that inhibition of GSK3B expression reverts resistance to OxPt treatment (Fig. 2F). In particular genetic

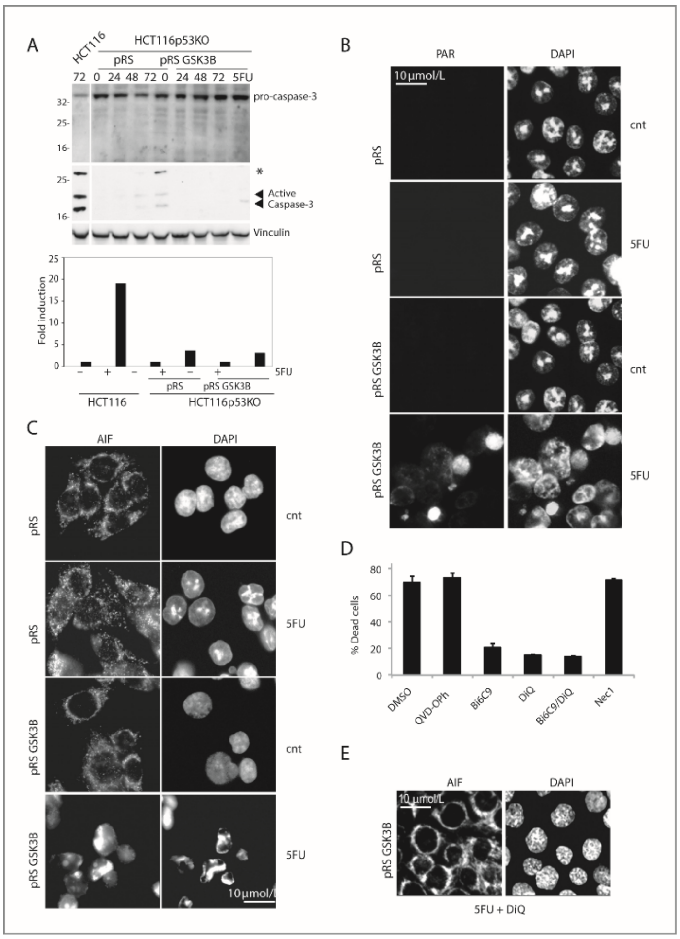

settings, inhibition of GSK3B expression is also able to lower resistance to the concomitant addition of 5FU and OxPt, which is significant in DLD-1 cells (Fig. 2G). Finally, we investigated whether GSK3B inhibition might also abolish the resistance to targeted drugs currently used for colon carcinomas and found that GSK3B inactivation did not sensitize resistant cells to

Figure 4. *p53-null, GSK3B-silenced colon carcinoma cells treated with 5FU die via RIP1-independent necroptosis.* ***A****, HCT116p53KO-pRS and HCT116p53KO-pRSGSK3B were treated for the indicated times with 200 µmol/L 5FU and total cell lysates blotted with antibodies recognizing pro-caspase-3 (upper) or the cleaved forms of caspase-3 (central); lysates from 5FU-treated HCT116 cells (72 hours) were also loaded on the same gel as a control; the lane after the control (containing the molecular weight marker) has been cut out; solid arrows indicate active forms of caspase-3, asterisk indicates intermediate forms produced during proteolytic activation; an aliquot of the same samples at 72 hours after treatment was used for a luminometric caspase-3/-7 assay (lower).* ***B****, HCT116p53KO-pRS and HCT116p53KO-pRSGSK3B untreated (cnt) and treated for 18 hours with 200 µmol/L 5FU and stained with anti-PAR antibody as well as DAPI.* ***C****, HCT116p53KO-pRS and HCT116p53KO-pRSGSK3B untreated (cnt) and treated for 30 hours (when 40–50% cells are dead) with 200 µmol/L 5FU and stained with anti-AIF antibody as well as DAPI: > 80% 5FU-treated HCT116p53KO-pRSGSK3B showed nuclear AIF. D, HCT116p53KO-pRSGSK3B were preincubated for 2 hours with pan-caspase inhibitor QVD-OPh (10 µmol/L), BID inhibitor (20 µmol/L Bi6C9), PARP1 inhibitor (100 µmol/L DiQ), Bi6C9þDiQ, or Necrostatin-1 (20 µmol/L Nec1) before adding 200 µmol/L 5FU and counted 72 hours later. E, HCT116p53KOpRSGSK3B were treated for 30 hours with 200 µmol/L 5FU in the presence of 100 µmol/L DiQ and stained with anti-AIF antibody as well as DAPI.*

cetuximab, panitumumab, and bevacizumab (Supplementary Fig. S3).

Thus, our findings indicate that, in the absence of p53, GSK3B depletion or inhibition restores the response of colon carcinoma drug-resistant cells only to DNA-damaging chemotherapy.

GSK3B inhibition abolishes drug resistance of p53-null colon carcinoma cell lines by affecting the response to DNA damage.

To investigate whether GSK3 inhibition influences DNA damage response/repair systems, we analyzed γH2AX foci formation as markers of the DNA damage response and RPA70 foci formation as markers of DNA repair (18, 19). To this end, we immunostained cells stably silenced for GSK3B and control cells, in presence and absence of 5FU (Fig. 3A): DNA damage is sensed upon 5FU treatment, even in absence of p53, as showed by γH2AX foci formation and this step is not impaired by GSK3B silencing. Also RPA70 foci are formed in p53-null cells (Fig. 3B), indicating that DNA repair is initiated: this process seems to be dependent on GSK3B activity, because silenced cell have very few or no RPA70 foci. We further confirmed these findings by inhibiting GSK3B activity in HCT116p53KO cells with LiCl (Fig. 3C and D). Taken together these results suggest that, in the absence of p53, GSK3B activity allows cells to survive despite treatment with DNA-damaging drugs by sustaining DNA repair.

GSK3B silencing enables RIP1-independent necroptosis in response to 5FU in p53-null colon carcinoma cells

To investigate the mechanisms of cell death induced by 5FU when GSK3B is silenced, we measured typical hall- marks of apoptosis, such as caspase activation. 5FU-treated GSK3B-silenced HCT116p53KO cells did not show appreciable levels of

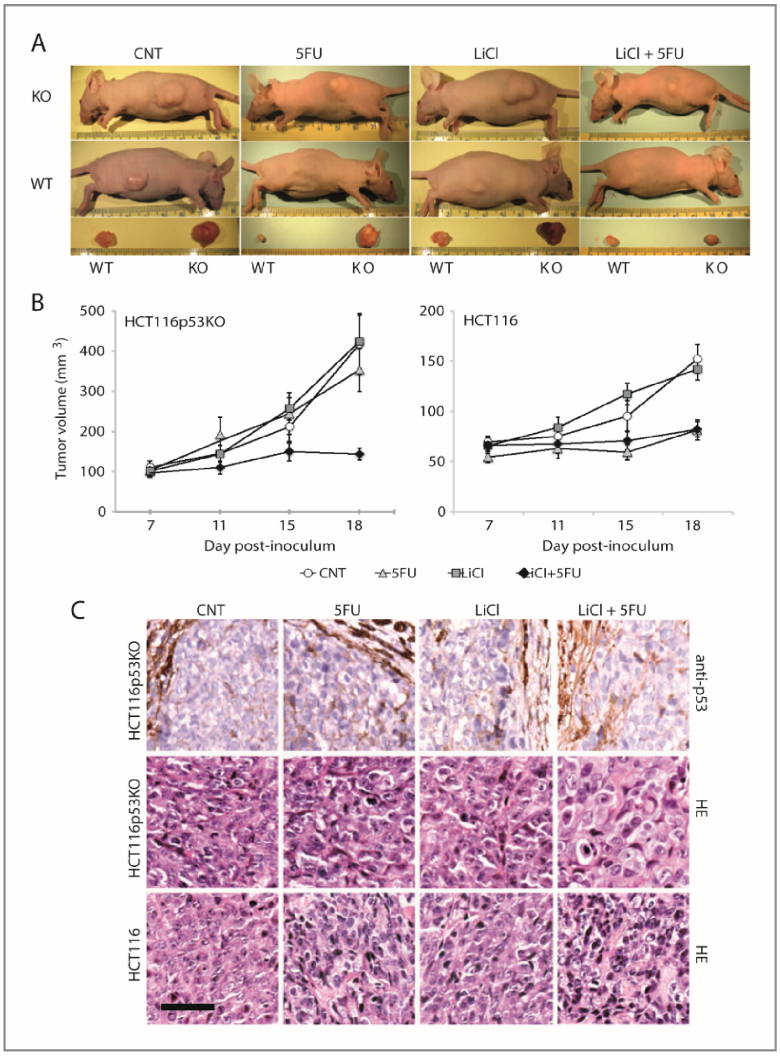

Figure 5. *GSK3 activation influences the therapeutic response to 5FU in vivo.* ***A****, representative pictures taken at the moment of sacrifice of mice, and relative tumoral masses, treated with vehicle only (CNT), 5FU, LiCl, and 5FU+LiCl as described in Materials and Methods.* ***B****, graph representing the average relative tumor volume (in mm^3) of xenografted tumors in the different treatment groups. Statistical analysis of the results was conducted using the Kruskal-Wallis test, followed by Nemenyi- Damico-Wolfe-Dunn test for multiple pairwise comparisons between groups. A P-value < 0.05 was considered significant.* ***C****, immunohistochemical staining for p53 on slides of HCT116p53KO xenograft tumors, showing positivity only for stromal murine cells (upper row) and hematoxylin and eosin staining (central and lower rows) of representative sections of xenografted tumors taken from vehicle only (CNT), 5FU, LiCl, and 5FU + LiCl-treated mice at the moment of sacrifice. Bar, 50 micron.*

processed caspases (Supplementary Fig. S4) and only showed minor caspase-3 activation (Fig. 4A); moreover, QVD-OPh addition did not prevent cell death (Fig. 4D).

These data collectively suggest that GSK3B participates in the regulation of caspase-independent cell death (20). PARP1 is an important activator of caspase-independent necroptosis: DNA damage-induced PARP1 activation leads to Calpain activation which in turn, via BID cleavage, activates BAX, thus facilitating the release from the mitochondria of a truncated form of AIF (tAIF) produced by Calpain (21). Once liberated in the cytosol tAIF translocates to the nucleus, where it promotes large-scale fragmentation of DNA, peripheral chromatin condensation, and, ultimately, cytotoxicity (22). We conducted several experiments to assess a possible role of GSK3B as a modulator of PARP1 and AIF in drug-induced caspase-independent necroptosis. First, we found that polymers of PAR, whose formation depends on PARP activation (23), accumulated only when 5FU was added to GSK3B-depleted cells and not to controls (Fig. 4B). Second, we showed that tAIF was released into the cytosol (Supplementary Fig. S5A) and relocalized to cell nuclei upon 5FU exposure of GSK3B-depleted cells (Fig.4C). Third, to test whether AIF relocalization was dependent on tBID and PARP-1, we pretreated cells with tBID and PARP1-specific inhibitors (Bi6C9 and DiQ, respectively) before drug addition and we showed that both inhibitors prevented 5FU cytotoxicity as well as tAIF nuclear translocation (Fig. 4D and E). Accordingly, we also showed that silencing AIF in GSK3B-depleted HCT116p53KO cells reduced 5FU cytotoxicity (Supplementary Fig. S5B). Finally, because TNF-α–mediated necroptosis is dependent on the activation of RIP1 kinase (24), we tested its involvement in our model by preincubating GSK3B-depleted cells with the RIP1 specific inhibitor necrostatin-1 (25) before adding 5FU. Cell death was not prevented by necrostatin-

1 (Fig. 4D) indicating that, at variance with TNF-α, DNA damage does not require RIP1 activity to trigger necroptosis.

Therefore, our data indicate that, in the absence of functional p53, GSK3B regulates a necroptotic response to DNA-damaging chemotherapy.

GSK3 inhibition restores the therapeutic response to 5FU in a xenograft model

To test whether GSK3B inhibition restores sensitivity to chemotherapy of p53-null colon carcinoma cells also *in vivo*, we conducted xenograft experiments. HCT116p53KO cells (left flank), and HCT116 cells as a control (right flank), were subcutaneously inoculated into CD-1 nude mice and treated with vehicle, 5FU only, LiCl only, and LiCl + 5FU. We observed that, 5FU, as well as LiCl given alone, had little or no effect on xenografted HCT116p53KO tumors, whereas GSK3B inhibition by LiCl prior 5FU administration significantly decreased the tumor burden (Fig. 5A and B). As expected, in HCT116 control tumors, 5FU alone significantly decreased the tumor burden. Histology of tumor masses is shown in Fig. 5C, where murine stromal cells were identified as positive to p53 staining whereas HCT116p53KO tumor cells tested negative (upper row). Different morphology and tissue organization, are evident in untreated, 5FU- and LiCl-treated versus LiCl + 5FU- treated HCT116p53KO xenografts (central row). In the latter, the significant decrease of the tumor masses is not paralled by the massive appearance of hyperchromatic, pyknotic nuclei (consistent with massive apoptosis) that are at variance visible in regressing 5FU- and LiCl + 5FU- treated HCT116 xenografts (lower row). On the whole, our results confirm that GSK3B inhibition resensitizes drug-resistant tumors to chemotherapy also *in vivo*.

GSK3B is activated in colon carcinoma samples from patients

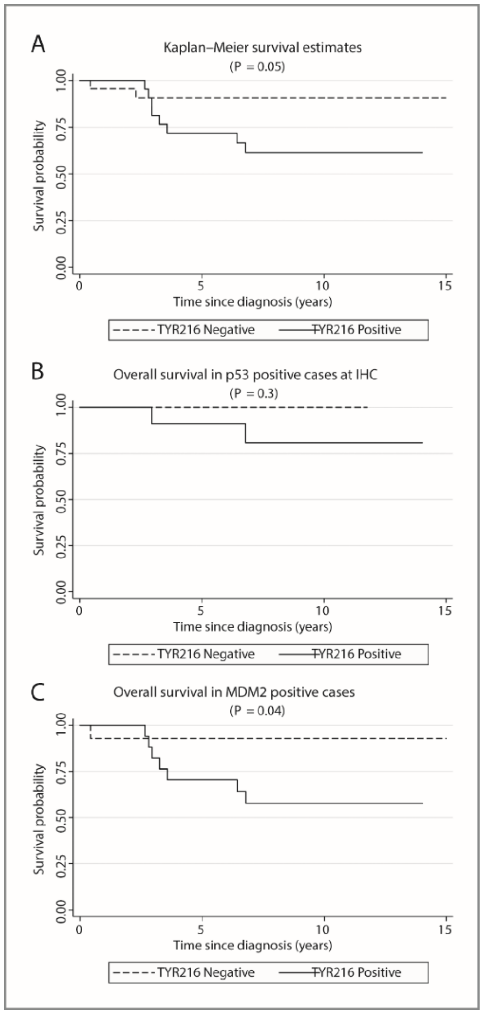

Figure 6. *GSK3 activation correlates with poorer outcome after adjuvant chemotherapy.* ***A****, Kaplan-Meier plot of the survival probability of 5FU-treated patients stratified by pTyr216-GSK3B positivity.* ***B****, Kaplan-Meier plot representing overall survival of 5FU-treated p53-positive patients stratified by pTyr216-GSK3B positivity.* ***C****, Kaplan-Meier plot representing overall survival of 5FU-treated MDM2-positive*

Preliminary data from 2 different laboratories reported high expression of active GSK3B in cell lysates from small groups of colon carcinoma samples (26, 27). Because our data indicated an important functional role for GSK3B in restoring sensitivity to 5FU both in vitro and in vivo, we decided to assess whether GSK3B was activated in a case study of colon carcinoma stage II 5FU-treated patients (n= 50) with long follow up. By the end of the follow-up, 11 5FU-treated patients (22%) relapsed. All tumor samples were also characterized for MLH1, p53, p21, MDM2, pTyr216-GSK3B expression by IHC on tissue microarrays (TMA; Supplementary Table S2). As a control, we analyzed also a TMA of 24 colonic biopsies taken from patients undergoing surgery for pathologies different than cancer (i.e., diverticulosis). Phosphorylation on Tyr216 allows the activation of GSK3B (14). Using a commercial phospho-specific antibody, we observed no or very low anti-pTyr216 reactivity in peritumoral samples or diverticulosis colonic

mucosa, whereas 52% (26/50) of cancer patients samples were positive (Supplementary Fig. S6 and Tables S2 and S3). Notably, the percentage of active GSK3B was significantly higher in samples from patients who relapsed after 5FU treatment than in patient who responded to therapy being 63.6% (7/11) versus 48.7% (19/50; P = 0.002599; McNemar test). Moreover, the log-rank test confirmed that active GSK3B is associated with cancer progression, poor response to therapy and worse overall survival. In particular, survival probability is significantly higher in colon cancers with inactive GSK3B, tested as immunohistochemically negative to pTyr216 (Fig. 6A). When patients are stratified for p53, again inactive GSK3B correlate with better survival probability, which is significant in the subset of MDM2 positive patients (Fig. 6B and C).

Altogether, our data indicate that colon cancers with active GSK3B, compared to those where GSK3B is not activated, have a worse outcome and are more prone to develop drug resistance.

Discussion

So far GSK3B has been described to be involved in modulating biological processes as opposite as proliferation or apoptosis, depending on the cellular, molecular, and developmental context (28–37). In fact, GSK3B is known to play an antiproliferative role by promoting APC-dependent phosphorylation—and hence proteosome-mediated degradation—of β-catenin, a transcription factor positively regulating Myc and cyclin D1 expression (14). In HCT116 colon carcinoma cell line it has been showed that GSK3B inhibition leads to apoptosis via p53 activation (38, 39). Here we present a novel role for GSK3B in colon carcinomas showing that its inhibition resensitizes drug-resistant p53-null colon cancer cells to chemotherapy both *in vitro* and *in vivo* and that GSK3B negatively regulates RIP1-

independent necroptosis in response to chemotherapy. Moreover, in accordance with *in vitro* and *in vivo* data, we showed that GSK3B is activated in a high percentage (63.6%) of samples from 5FU-treated stage II colon carcinoma patients relapsed after 5FU-based therapy and that positivity for active form of GSK3B correlates with worse outcome and survival probability after adjuvant chemotherapy.

All the cell lines we used for the experiments express either mutated, nonphosphorylatable β-catenin or mutated APC (see Supplementary Table S1), thus rendering β-catenin activation constitutive and GSK3B-independent (16). Consistently, no proliferative defects were evident in cell lines stably silenced for GSK3B (Fig. 1). Being all the cell lines p53-null, we found particularly intriguing that GSK3B silencing had such a dramatic effect on the response to chemotherapy and reasoned that in this setting hitherto unrecognized pathways are likely to be crucially regulated by GSK3B-mediated phosphorylation. Our data suggest that GSK3B plays a relevant role in drug resistance. In fact, we have shown that when GSK3B is expressed, p53-null colon carcinoma cells survive and proliferate despite chemotherapy and its silencing or inhibition abolishes cell growth after anticancer therapy both *in vitro* (Fig. 2A) and *in vivo* (Fig. 5). Therefore, GSK3B inhibition is sufficient to allow a cell death response to DNA-damaging drugs in resistant cells even in absence of p53 (Fig. 2). In particular, our results suggest that GSK3B modulates the response to DNA damage by affecting DNA repair (Fig. 3B) and negatively regulating PARP1 activity (Fig. 4B). Notably, PARP1 is involved in 3 pathways of DNA repair that are differently affected by p53 absence (40) and directly or indirectly activated by 5FU treatment (41): base excision repair (BER), nonhomologous end joining (NHEJ), and homologous recombination. In fact, in absence of wild type p53, activation of BER is suppressed whereas NHEJ and homologous recombination are active leading to aberrant double strand breaks

repair. Accordingly, it has been reported that after severe genotoxic damage, p53 mutant cells can recover from a G2 arrest and resume proliferation following aberrant DNA repair (42). Our data indicates that GSK3B-regulated PARP1 activity is important for modulating DNA repair and tilting the balance toward cell death when too much damage occurs. Moreover, we showed that in p53 null cells, where drug-induced apoptosis is defective, the inhibition of GSK3B enables necroptosis as a response to chemotherapy (Fig. 4). RIP1 has been shown to mediate necroptosis in response to TNF receptor engagement (43), radiations (44), a few drugs (45) and so far its activation is thought to be central for the modulation of the necroptotic response. Intriguingly, in our model, RIP1 kinase is not involved in mediating the necroptotic response as showed by a lack of protection when using necrostatin-1 (Fig. 4D). In addition, our results suggest that DNA damage triggered a RIP1-independent pathway negatively regulated by GSK3B.

Consistently with the role of GSK3B in drug resistance showed in *in vitro* (Fig. 2) and *in vivo* in xenograft experiments (Fig. 5), we observed expression of active GSK3B in 63.6% of biopsies from colon carcinoma stage II patients not responsive to 5FU-based therapy (Supplementary Tables S2 and S3 and Fig. S6). Accordingly, survival probability is significantly higher in colon cancers with inactive GSK3B (Fig. 6A). When patients are stratified for p53, again, inactive GSK3B correlate with better survival probability, which is significant in the subset of MDM2-positive patients (Fig. 6B and C). These findings are particularly relevant taking into account that the treatment for stage II primary colon cancer remains controversial. Although chemotherapy is often recommended for high-risk stage II disease, many tumors with similar histopathologic features will relapse, even after chemotherapy (46). Finding molecular markers with predictive value for the response to therapy in stage II colon cancer would therefore help clinicians with information to decide whether and how to treat these patients with adjuvant chemotherapy (47).

The strong correlation of GSK3B activation with drug resistance, worse survival probability, and clinical outcome in 5FU-treated patients (Fig. 6A) suggests that GSK3B may be considered a candidate prognostic/predictive biomarker. Further studies on larger cohorts, stratified for both p53 and MDM2 are awaited to confirm these findings.

On the whole, our results add further support to previous data suggesting that GSK3B is a good candidate target for anticancer therapy and are particularly relevant for 2 main reasons. First, when GSK3B is inhibited DNA-damaging drugs bypass the need of p53 to induce cell death: triggering p53-independent cell death mechanisms is therefore an effective way to bypass one of most relevant causes of drug resistance. Therefore, the addition of GSK3B inhibitors to standard chemotherapy might be beneficial to a large number of colon carcinomas. Second, in a large number of tumors, classical apoptotic mechanisms are altered and such defects render treatment with traditional chemotherapeutic agents ineffective. Our findings that GSK3B inhibition in combination with chemotherapy unleashes a necroptotic response would therefore represent an alternative strategy to selectively treat otherwise nonresponsive tumors.

In conclusion, our study showed that GSK3B: (i) is a target whose inhibition restores the sensitivity to DNA- damaging agents in p53-null tumors; (ii) *in vitro* modulates a necroptotic response to chemotherapy; (iii) its inhibition bypasses drug resistance in *in vivo* tumor xenografts; (iv) its activation correlates with worse survival probability and clinical outcome in colon cancer stage II patients treated with adjuvant therapy. Altogether our findings suggest that GSK3B may be a potential teranostic marker in colon cancer.

Disclosure of Potential Conflicts of Interest

No potential conflicts of interest were disclosed.

Authors' Contributions

Conception and design: E. Grassilli, R. Giovannoni, G. Romano, B.E. Leone, K. Helin, M. Lavitrano

Development of methodology: R. Narloch, L. Ianzano, B.E. Leone

Acquisition of data: (provided animals, acquired and managed patients, provided facilities, etc.): E. Grassilli, R. Narloch, E. Federzoni, F. Pisano, R. Giovannoni, B.E. Leone, S. Bonin, M. Donada, G. Stanta

Analysis and interpretation of data: (e.g., statistical analysis, biosta- tistics, computational analysis): E. Grassilli, R. Narloch, E. Federzoni, L. Ianzano, R. Giovannoni, G. Romano, G. Stanta, M. Lavitrano

Writing, review, and/or revision of the manuscript: E. Grassilli, R. Giovannoni, B.E. Leone, S. Bonin, K. Helin, M. Lavitrano

Administrative, technical, or material support: (i.e., reporting or organizing data, constructing databases): G. Romano, L. Masiero, B.E. Leone, M. Donada

Study supervision: E. Grassilli, B.E. Leone, G. Stanta, K. Helin, M. Lavitrano

Acknowledgments

The authors thank L. Dalprà for helpful discussion and critical reading of the manuscript; B. Vogelstein for the gift of HCT116p53KO cells; R. Bernards for the pRS-shRNA library; and A. Affuso and D. Consolante for the precious assistance with

the xenograft experiments. The authors are grateful to the Department of Experimental Oncology, European Institute of Oncology for the use of its laboratory resources for the infections and screen phases of this work and BIOGEM Institute for the use of its facilities for the xenograft experiments.

Grant Support

This work was supported by F.A.R. grants from the University of Milano- Bicocca, Ministry of Health Grant RF-2010-2305526-N3, and PON 01_02782/7 grant to M. Lavitrano; from the European Union Framework 6 programme (INTACT) and from the Italian Cancer Society (AIRC) grants to K. Helin.

References

1. Fulda S, Debatin KM. Extrinsic versus intrinsic apoptosis pathways in anticancer chemotherapy. Oncogene 2006;25:4798–811.

2. Won RSY. Apoptosis in cancer: from pathogenesis to treatment. J Exp Clin Cancer Res 2011;30:87–101.

3. Palazzo A, Iacovelli R, Cortesi E. Past, present and future of targeted therapy in solid tumors. Curr Cancer Drug Targets 2010;10:433–61.

4. Brognard J, Hunter T. Protein kinase signaling networks in cancer. Curr Opin Genet Dev 2011;21:4–11.

5. Wouters BG, Koritzinsky M. Hypoxia signalling through mTOR and the unfolded protein response in cancer. Nat Rev Cancer 2008;8:851–64.

6. Wek RC, Jiang HY, Anthony TG. Coping with stress: eIF2 kinases and translational control. Biochem Soc Trans 2006;34:7–11.

7. Berns K, Hijmans EM, Mullenders J, Brummelkamp TR, Velds A, Heimerikx M, et al. A large-scale RNAi screen in human cells identifies new components of the p53 pathway. Nature 2004;428:431–4.

8. Bunz F, Hwang PM, Torrance C, Waldman T, Zhang Y, Dillehay M, et al. Disruption of p53 in human cancer cells alters the responses to therapeutic agents. J Clin Invest 1999;104:263–9.

9. Toledo F, Wahl GM. Regulating the p53 pathway: in vitro hypotheses, in vivo veritas. Nat Rev Cancer 2006;6:909–23.

10. Seemann S, Maurici D, Olivier M, de Fromentel CC, Hainaut P. The tumor suppressor gene TP53: implications for cancer management and therapy. Crit Rev Clin Lab Sci 2004;41:551–83.

11. Grassilli E, Ballabeni A, Maellaro E, Del Bello B, Helin K. Loss of MYC confers resistance to doxorubicin-induced apoptosis by preventing the activation of multiple serine protease- and caspase-mediated pathways. J Biol Chem 2004;279:21318–26.

12. Rigolio R, Miloso M, Nicolini G, Villa D, Scuteri A, Simone M, et al. Resveratrol interference with the cell cycle protects human neuroblastoma SH-SY5Y cell from paclitaxel-induced apoptosis. Neurochem Int 2005;46:205–11.

13. Busnelli M, Froio A, Bacci ML, Giunti M, Cerrito MG, Giovannoni R, et al. Pathogenetic role of hypercholesterolemia in a novel preclinical model of vascular injury in pigs. Atherosclerosis 2009;207:384–90.

14. Beurel E, Jope RS. The paradoxical pro- and anti-apoptotic actions of GSK3 in the intrinsic and extrinsic apoptosis signaling pathways. Prog Neurobiol 2006;79:173–89.

15. Le Floch N, Rivat C, De Wever O, Bruyneel E, Mareel M, Dale T, et al. The proinvasive activity of Wnt-2 is mediated through a noncanonical Wnt pathway coupled to GSK-3beta and c-Jun/AP-1 signaling. FASEB
J 2005;19:144–6.

16. Morin PJ, Sparks AB, Korinek V, Barker N, Clevers H, Vogelstein B, et al. Activation of β-catenin—Tcf signaling in colon cancer by mutations in β-catenin or APC. Science 1997;275:1787–90.

17. Sigoillot FD, King RW. Vigilance and validation: keys to success in RNAi screening. ACS Chem Biol 2011;6:47–60.

18. Bonner WM, Redon CE, Dickey JS, Nakamura AJ, Sedelnikova OA, Solier S, et al. GammaH2AX and cancer. Nat Rev Cancer 2008;8:957–67.

19. Oakley GG, Patrick SM. Replication protein A: directing traffic at the intersection of replication and repair. Front Biosci 2010;15:883–900.

20. Bröker LE, Kruyt FAE, Giaccone G. Cell death independent of caspases: a review. Clin Cancer Res 2005;11:3155–62.

21. Cabon L, Gal_an-Malo P, Bouharrour A, Delavall_ee L, Brunelle-Navas MN, Lorenzo HK, et al. BID regulates AIF-mediated caspase-independent necroptosis by promoting BAX activation. Cell Death Differ 2012; 19:245–56.

22. Hong SJ, Dawson TM, Dawson VL. Nuclear and mitochondrial conversations in cell death: PARP-1 and AIF signaling. Trends Pharmacol Sci 2004;25:259–64.

23. Luo X, Kraus WL. On PAR with PARP: cellular stress signaling through poly(ADP-ribose) and PARP-1. Genes Dev 2012;26:417–32.

24. Dunai Z, Bauer PI, Mihalik R. Necroptosis: biochemical, physiological and pathological aspects. Pathol Oncol Res 2011;17:791–800.

25. Degterev A, Hitomi J, Germscheid M, Ch'en IL, Korkina O, Teng X, et al. Identification of RIP1 kinase as a specific cellular target of necrostatins. Nat Chem Biol 2008;4:313–21.

26. Shakoori A, Ougolkov A, Yu ZW, Zhang B, Modarressi MH, Billadeau DD, et al. Deregulated GSK-3b activity in colorectal cancer: its association with tumor cell survival and proliferation. Biochem Biophys Res Commun 2005;334:1365–73.

27. Wang HL, Hart J, Fan L, Mustafi R, Bissonnette M. Upregulation of glycogen synthase kinase 3b in human colorectal adenocarcinomas correlates with accumulation of CTNNB1. Clin Colorectal Cancer 2011;10:30–6.

28. Forde JE, Dale TC. Glycogen synthase kinase 3: a key regulator of cellular fate. Cell Mol Life Sci 2007;64:1930–44.

29. Wang Z, Smith KS, Murphy M, Piloto O, Somervaille TC, Cleary ML. Glycogen synthase kinase 3 in MLL leukaemia maintenance and targeted therapy. Nature 2008;455:1205–9.

30. Kunnimalaiyaan M, Vaccaro AM, Ndiaye MA, Chen H. Inactivation of glycogen synthase kinase-3b, a downstream target of the raf-1 pathway, is associated with growth suppression in medullary thyroid cancer cells. Mol Cancer Ther 2007;6:1151–58.

31. Mazor M, Kawano Y, Zhu H, Waxman J, Kypta RM. Inhibition of glycogen synthase kinase-3 represses androgen receptor activity and prostate cancer cell growth. Oncogene 2004;23:7882–92.

32. Liao X, Zhang L, Thrasher JB, Du J, Li B. Glycogen synthase kinase-3b suppression eliminates tumor necrosis factor-related apoptosisinducing ligand resistance in prostate cancer. Mol Cancer Ther 2003;2:1215–20.

33. Ougolkov AV, Bone ND, Fernandez-Zapico ME, Kay NE, Billadeau DD. Inhibition of glycogen synthase kinase-3 activity leads to epigenetic silencing of nuclear factor kappaB target genes and induction of
apoptosis in chronic lymphocytic leukemia B cells. Blood 2007;110: 735–42.

34. Erdal E, Ozturk N, Cagatay T, Eksioglu-Demiralp E, Ozturk M.Lithium-mediated downregulation of PKB/Akt and cyclin E with growth inhibition in hepatocellular carcinoma cells. Int J Cancer 2005;115:903–10.

35. Ougolkov AV, Fernandez-Zapico ME, Savoy DN, Urrutia RA, Billadeau DD. Glycogen synthase kinase-3b participates in nuclear factor kappaB- mediated gene transcription and cell survival in pancreatic cancer
cells. Cancer Res 2005;65:2076–81.

36. Wilson W, Baldwin AS. Maintenance of constitutive IKB kinase activity by glycogen synthase kinase-3A/B in pancreatic cancer. Cancer Res 2008;68:8156–63.

37. Mai W, Kawakami K, Shakoori A, Kyo S, Miyashita K, Yokoi K, et al. Deregulated GSK3b sustains gastrointestinal cancer cell survival by modulating human telomerase reverse transcriptase and telomerase. Clin Cancer Res 2009;15:6810–9.

38. Ghosh JC, Altieri DC. Activation of p53-dependent apoptosis by acute ablation of glycogen synthase kinase3beta in colorectal cancer cells. Clin Cancer Res 2005;11:4580–8.

39. Tan J, Zhuang L, Leong HS, Iyer NG, Liu ET, Yu Q. Pharmacologic modulation of glycogen synthase kinase-3beta promotes p53-dependent apoptosis through a direct Bax-mediated mitochondrial pathway in colorectal cancer cells. Cancer Res 2005; 65:9012–20.

40. Gatz SA, Wiesmüller L. p53 in recombination and repair. Cell Death Differ 2006;13:1003–16.

41. Thorn CF, Marsh S, Carrillo MW, McLeod HL, Klein TE, Altman RB. PharmGKB summary: fluoropyrimidine pathways. Pharmacogenet Genomics 2011;21:237–42.

42. Ivanov A, Cragg MS, Erenpreisa J, Emzinsh D, Lukman H, Illidge TM. Endopolyploid cells produced after severe genotoxicdamage have the potential to repair DNA double strand breaks. J Cell Sci 2003;116: 4095–106.

43. Vandenabeele P, Declercq W, Van Herreweghe F, Vanden Berghe T. The role of the kinases RIP1 and RIP3 in TNF-induced necrosis. Sci Signal 2010;3:115–21.

44. Nehs MA, Lin CI, Kozono DE, Whang EE, Cho NL, Zhu K, et al. Necroptosis is a novel mechanism of radiation-induced cell death in anaplastic thyroid and adrenocortical cancers. Surgery 2011;150:1032–9.

45. Han W, Li L, Qiu S, Lu Q, Pan Q, Gu Y, et al. Shikonin circumvents cancer drug resistance by induction of a necroptotic death. Mol Cancer Ther 2007;6:1641–9.

46. Benson AB 3rd, Schrag D, Somerfield MR, Cohen AM, Figueredo AT, Flynn PJ, et al. American Society of Clinical Oncology recommendations on adjuvant chemotherapy for stage II colon cancer. J Clin Oncol 2004;22:3408–19.

47. Chun P, Wainberg ZA. Adjuvant chemotherapy for stage II colon cancer: the role of molecular markers in choosing therapy. Gastrointest Cancer Res 2009;3:191–6.

Supplementary Data

Supplementary Materials and Methods

Materials. Cetuximab (Erbitux, Ely Lilly), panitumumab (Vectibx, Amgen), bevacizumab (Avastin, Genentech) were from San Gerardo Hospital, Monza. SB216763, SB415286, were from Sigma-Aldrich. anti-p53 (DO-1, sc-126), anti-caspase-9 sc-56073, anti- caspase-8 sc-70503 were from SantaCruz Biotechnology; anti-p21 (clone EA10) and anti-MDM2 (clone IF2) were from Merck Chemicals; anti-caspase-2 was a kind gift of Prof. Claudio Brancolini (Dept. Medical and Biological Sciences, University of Udine, Italy) .

Reporter assay. 5 x 10^4 cells/well in a 96-well plate were seeded in triplicate the day before transfection. 0.2 µg TopFlash (containing two sets of three copies of the TCF binding site upstream of the Thymidine Kinase minimal promoter and Luciferase open reading frame) + 0.2 µg pGL4.75 (encoding for Renilla luciferase, used as an internal control for transfection efficiency) reporters were transfected in each well using Lipofectamine2000 following the manufacturer's protocol. 48 hrs later cells were washed, lysed and assayed for Luciferase signals directly in the well by using the Dual-Glo Luciferase Assay System (Promega), according manufacturer's instructions. Firefly luciferase intensity was normalized over Renilla luciferase signal. siRNA transfection. Transient siRNA transfection were performed using Lipofectamine 2000 (Invitrogen) according to the manufacturer's instructions. Commercial siRNAs targeting GSK3B sequence GCTAGATCACTGTAACATA (#4390824 Ambion Applied Biosystems covering nt 1292-1310); GSK3A (#S100288554 Qiagen); luc (Luciferase GL2 Eurofins MWG Operon); siRNA AIF: AUGUCACAAAGACACUGCA were used.

Fractionation. Cells were washed once with cold PBS buffer before lysis and pellet resuspended in 900 µl fractionation buffer (10 mM Hepes, 250 mM sucrose, 1mM

EDTA, 1mM EGTA, 1mM DTT,1% PIC) and left on ice 1h. The suspension was then passed 3x10times through a 25g needle and then 3x10times through a 27g needle and centrifuged using a microcentrifuge at 4000 rpm 4°C, 10 min. The pellets (formed by unbroken cells, nuclei, high molecular wieght membranes) were discarded and the supernatants centrifuged using a microcentrifuge at maximum speed, 4°C, 20min. Supernatants (cytoplasms) were saved and freezed as such. Pellets (mitochondria) were resuspended in 65 µl RIPA buffer + inhibitors and freezed until further processing.

Supplementary Tables

cell line	MMR status	MLH1	MSH2	MSH6	BRCA2	p53	EGFR	PIK3CA	PTEN	AKT	KRAS	BRAF	APC	CTNNB1
HCT-116p53KO	MMR deficient	mt			insertion	KO	wt	H1047R	wt	wt	G13D	wt		deletion
DLD-1	MMR deficient			truncated		mt	wt	E545K	wt	wt	G13D	wt	deletion	wt
SW480	MMR proficient	wt	wt			mt	wt	wt	low expression	wt	G12V	wt	deletion	wt

Supplementary Table 1. Known genetic alterations characterizing the different colon carcinoma cell lines used in the paper. Information about genetic defects were retrieved from the database of the Wellcome Trust Sanger Institute Catalogue Of Somatic Mutations In Cancer (COSMIC, http://www.sanger.ac.uk/genetics/CGP/cosmic).

Patient Id	Age	Sex	OS	DFS	Grade	Relapse	MHL1	p53	MDM2	p21	pTyr216 GSK3B
t5	72	M	12.83	12.83	2	no	+	-	weak	+ weak	-
t6	46	F	11.78	11.78	2	no	+	-	+	+/-	++
t7	59	F	3.26	1.25	2	yes	+	-	weak	+	+
t9	49	F	11.70	11.70	2	no	+	+	+	+	+
t12	72	M	2.94	2.55	2	yes	+	+	weak	+ weak	++
t16	66	F	10.87	10.87	1	no	+	-	++	+	+
t19	68	F	2.87	2.87	2	no	+	+	-	+	+
t20	59	M	11.04	11.04	2	no	-	-	weak	+	-
t22	68	M	11.16	11.16	2	no	+	-	weak	-	+
t24	65	M	11.78	11.78	2	no	+	+	weak	+	-
t25	59	F	10.81	10.81	2	no	+	+	+	+	+
t26	64	M	11.52	11.52	2	no	+	+	+	+	+
t28	77	F	2.65	0.66	2	yes	+	-	+	+	+
t30	69	M	11.38	11.38	2	no	+	+	+	+	+
t31	67	M	11.19	11.19	2	no	+	-	-	-	-
t32	79	M	2.81	1.19	2	yes	+	-	+	+	+
t34	71	M	11.18	11.18	2	no	+	-	-	+	-
t35	58	M	5.00	5.00	2	no	+	+	-	+ weak	-
t36	65	M	10.92	10.92	2	no	+	+	NA	NA	-
t37	56	F	10.64	10.64	2	no	+	+	-	-	+
t39	63	M	9.98	9.98	2	no	+	+	weak	+/-	-
t41	58	M	10.67	10.67	2	no	+	-	weak	+/-	-
t42	60	F	9.48	9.48	2	no	-	-	-	+	-
t45	67	F	7.57	7.57	2	no	+	-	+	+/-	-
t47	69	F	10.39	10.39	2	no	+	-	++	+/-	+
t53	70	F	6.44	3.11	2	no	+	-	+	+/-	++
t58	68	F	14.03	14.03	2	no	+	+	weak	+/-	+
t59	44	M	6.78	2.30	2	yes	+	+	+	+/-	+
t60	68	M	6.42	6.12	3	yes	-	+	weak	+	-
t63	66	M	2.94	1.41	2	yes	+	-	-	+/-	+
t64	60	M	11.12	11.12	1	no	+	-	+	+	-
t67	64	M	0.17	0.17	1	no	+	-	+	+	+
t68	86	M	0.44	0.44	3	no	-	-	NA	+	-
t69	57	M	10.34	10.34	2	no	+	+	+	+ weak	+
t70	74	F	10.51	10.51	1	no	+	-	+	+	-
t71	75	F	10.67	10.67	2	no	+	+	weak	+	+
t72	86	F	0.03	0.03	3	no	+	-	++	+	++
t73	77	F	0.65	0.65	2	yes	+	+	-	+ weak	-
t75	76	F	15.00	15.00	2	no	-	-	weak	+	-
t76	89	F	2.14	2.14	2	no	+	-	+	+	+
t77	70	F	4.29	4.29	2	no	+	+	weak	+	+
t78	71	F	9.15	9.15	1	no	+	-	weak	+	-
t79	66	M	9.45	9.45	2	no	+	+	+	+	-
t80	83	F	0.00	0.00	2	no	+	+	-	-	+
t81	54	F	9.24	9.24	2	no	+	-	++	-	-
t82	85	F	2.30	2.14	1	yes	+	-	-	NA	-
t83	62	F	0.42	0.33	2	yes	+	-	+	+/-	-
t85	65	M	3.57	1.22	2	yes	+	-	+	+	+
t86	90	F	0.21	0.21	2	no	+	+	+	+	++
t87	74	F	7.13	7.13	2	no	-	-	weak	NA	-

Supplementary Table 2. *Cohort of patients characterization. Expression of MHL1, p53, MDM2, p21, pTyr216-GSK3B were studied by IHC staining on TMA. In the table are also shown: age, sex, overall survival, disease-free survival, tumor grade, and clinical outcome (relapse). Sample triplicates arrayed in tissue microarray were stained with specific antibodies and graded accordingly to an increasing intensity by blind reading by two experienced operators.*

	number of patients	number of patients pTyr216GSK3B positive	%
FU-treated patients	50	26	52%
Non relapsed after 5FU-based adjuvant therapy	39	19	48.7% *
Relapsed after 5FU-based adjuvant therapy	11	7	63.6% *

* 48.7% vs 63.6% P(two-sided) = 0.002599 McNemar's test
OR = 0.2105; 95% CI (0.05209, 0.6335)

Supplementary Table 3. *Correlation between activated GSK3B and patients outcome. The cohort of 50 patient was analyzed for the expression of active GSK3B, expressed as immuno-histochemically pTyr216 positive, in correlation with the relapse of the tumor disease. pTyr216-GSK3B was significantly higher in samples from patients that relapsed after 5FU treatment than in patient that responded to therapy.*

Supplementary Figures

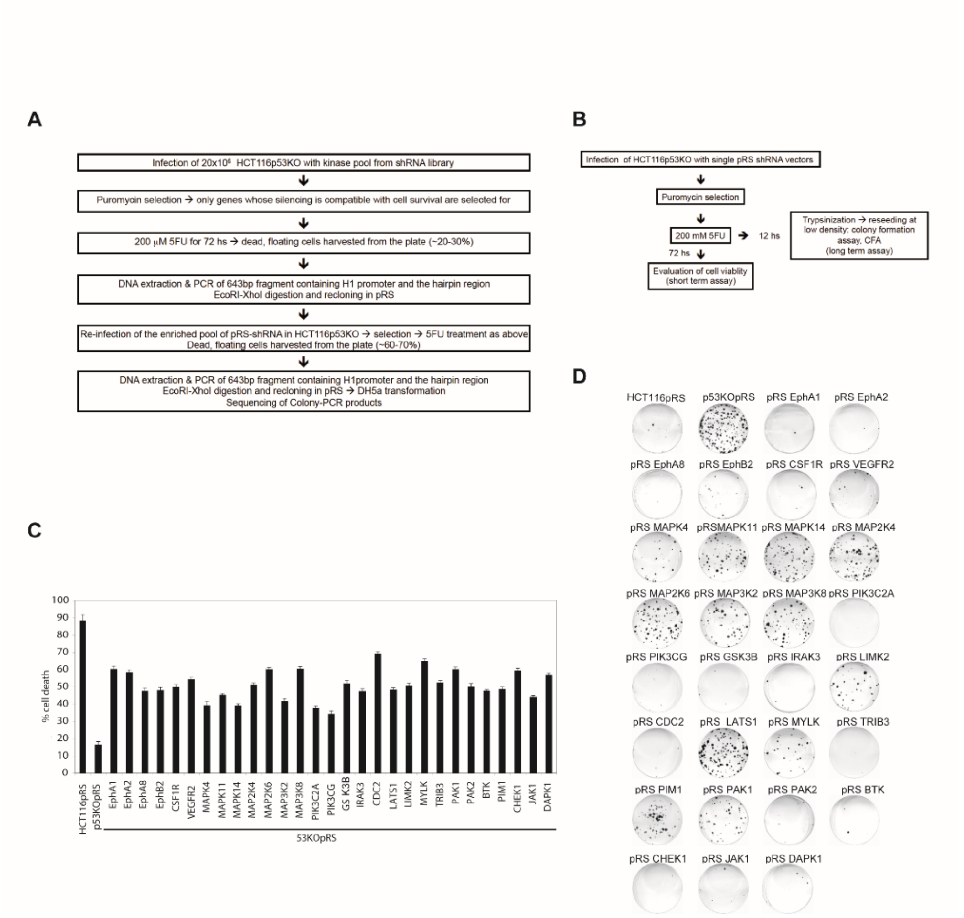

Supplementary Figure 1. *Identification and validation of the genes supporting drug resistance by shRNA-mediated phenotype screen. (**A**) Diagram explaining how the phenotype screen was performed. (**B**) Diagram explaining how the validation phase of the screen was performed. (**C**) HCT116p53KO cells singularly infected with viral stocks of each shRNA plasmid recovered in the screen and puromycin selected were treated 72hs with 200 μM 5FU before counting. Each batch of infected cells is labeled as KO53pRS followed by the name of the silenced gene. In parallel, as a positive control, also empty vector-infected HCT116 (WTpRS) have been treated. A representative experiment out of 3 is shown. (**D**) An aliquot of each batch on infected cells from (**C**) was used for colony assay performed as described in Materials and Methods. A representative experiment out of 5 is shown.*

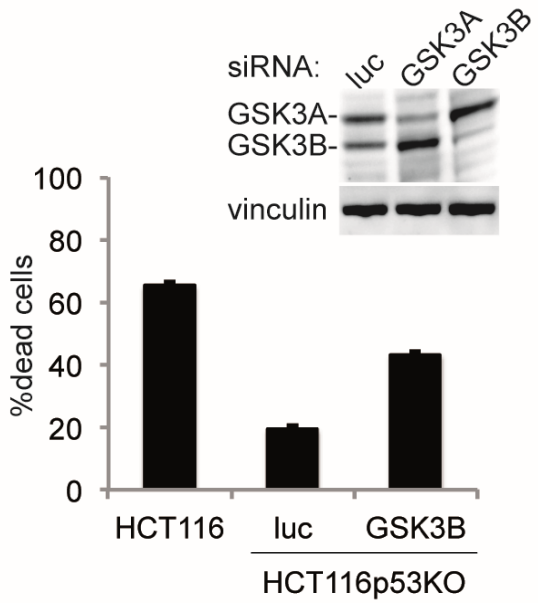

Supplementary Figure 2*. GSK3B silencing by siRNA abolishes drug resistance of p53-null colon carcinoma cell lines. siRNA transfection was performed using 100nM commercial oligos for the indicated genes; oligos targeting luciferase (luc) were used as a control. 24 hs after transfection medium was replaced with complete medium containing 200μM 5FU and cells were harvested 48hs later for analyzing GSK3B levels by western blot and counting dead cells after Trypan blue staining.*

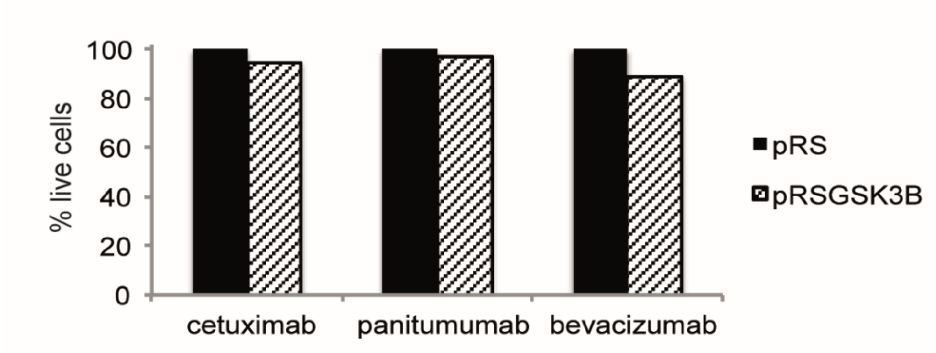

Supplementary Figure 3. *GSK3B depletion do not alter the response of HCT116p53KO resistant cells to targeted drugs. Cell death 72 hrs after treatment of HCT116p53KO-pRS and -pRSGSK3B with 10 μg/ml cetuximab, 75 μg/ml panitumumab, 25 μg/ml bevacizumab was evaluated by Trypan blue staining.*

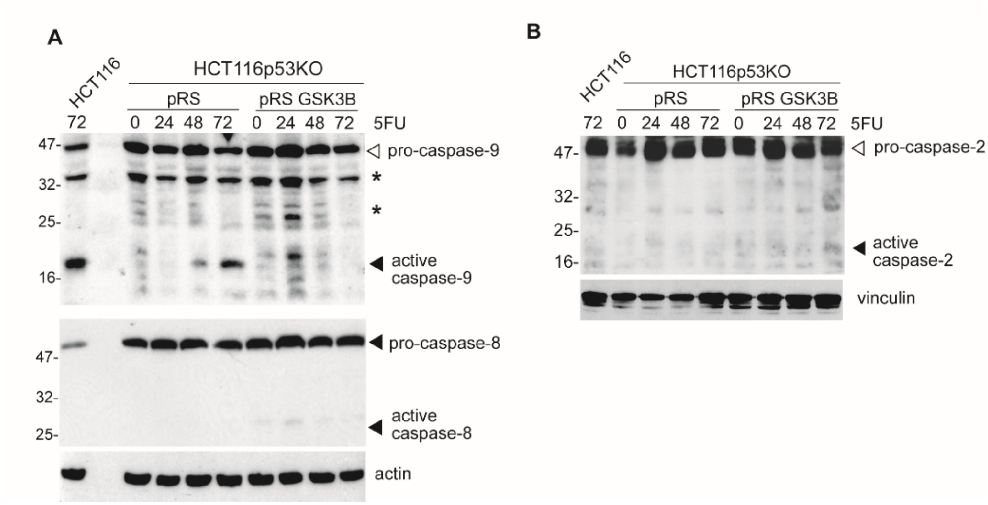

Supplementary Figure 4. *Caspases are not activated after 5FU treatment in GSK3B-silenced cells. HCT116p53KO-pRS and HCT116p53KO-pRSGSK3B were treated for the indicated times with 200 μM 5FU and total cell lysates blotted with antibodies recognizing: (**A**) total and cleaved form of caspase-9 and -8; (**B**) total and cleaved form of caspase-2; Notably no (or barely visible) processing of the caspase enzymes is evident. Actin and vinculin levels served as loading controls. Solid arrows indicate active caspase cleaved fragment; white arrows indicate pro-caspase; asterisks indicate intermediate fragments derived from proteolytic processing of the caspases.*

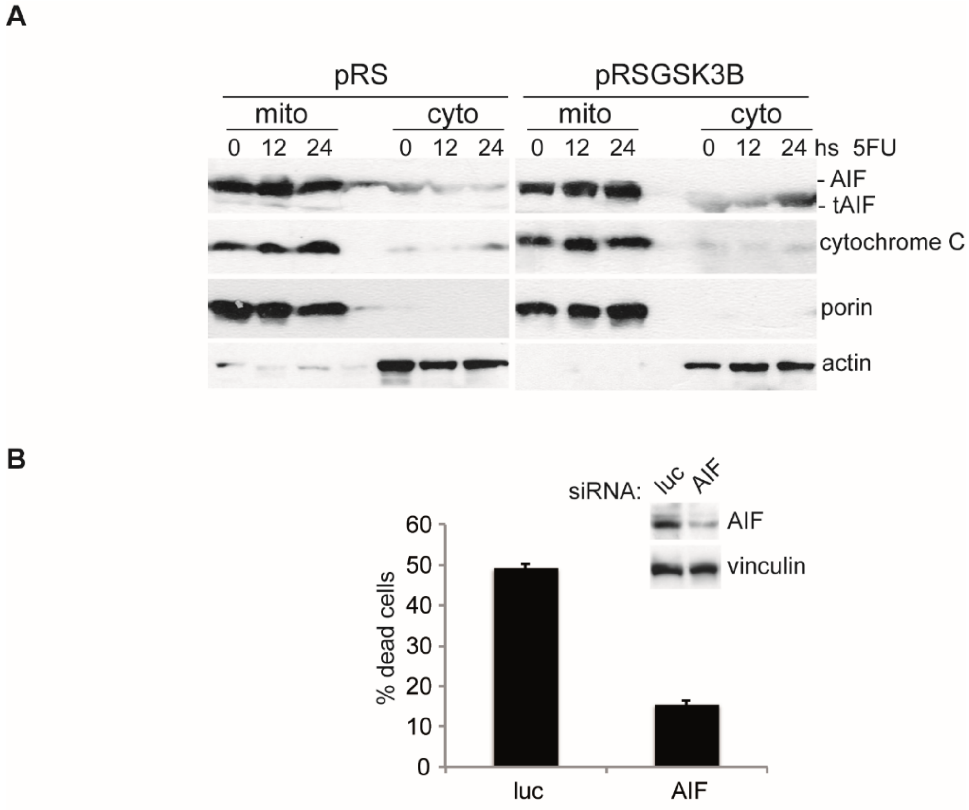

Supplementary Figure 5*. tAIF is released from mitochondria upon 5FU treatment in GSK3B-silenced HCT116p53KO cells. (**A**) mitochondrial and cytoplasmic fractions from untreated and 5FU-treated HCT116p53KO-pRS and –pRSGSK3B cells were probed with anti-AIF and anti-cytochrome C antibodies to assess the release of mitochondrial proteins in the cytoplasm; uncleaved (AIF) and truncated (tAIF) derived from proteolytic processing are indicated; anti-porin and anti-actin were used to assess the loading and purity of the mitochondrial and cytoplasmic fractions, respectively. (**B**) siRNA transfection in HCT116p53KO-pRSGSK3B was performed using custom-made oligos for AIF. 24hs after transfection medium was replaced with complete medium containing 200μM 5FU and cells were harvested 72hs later for analyzing AIF levels by western blot and counting dead cells after Trypan blue staining.*

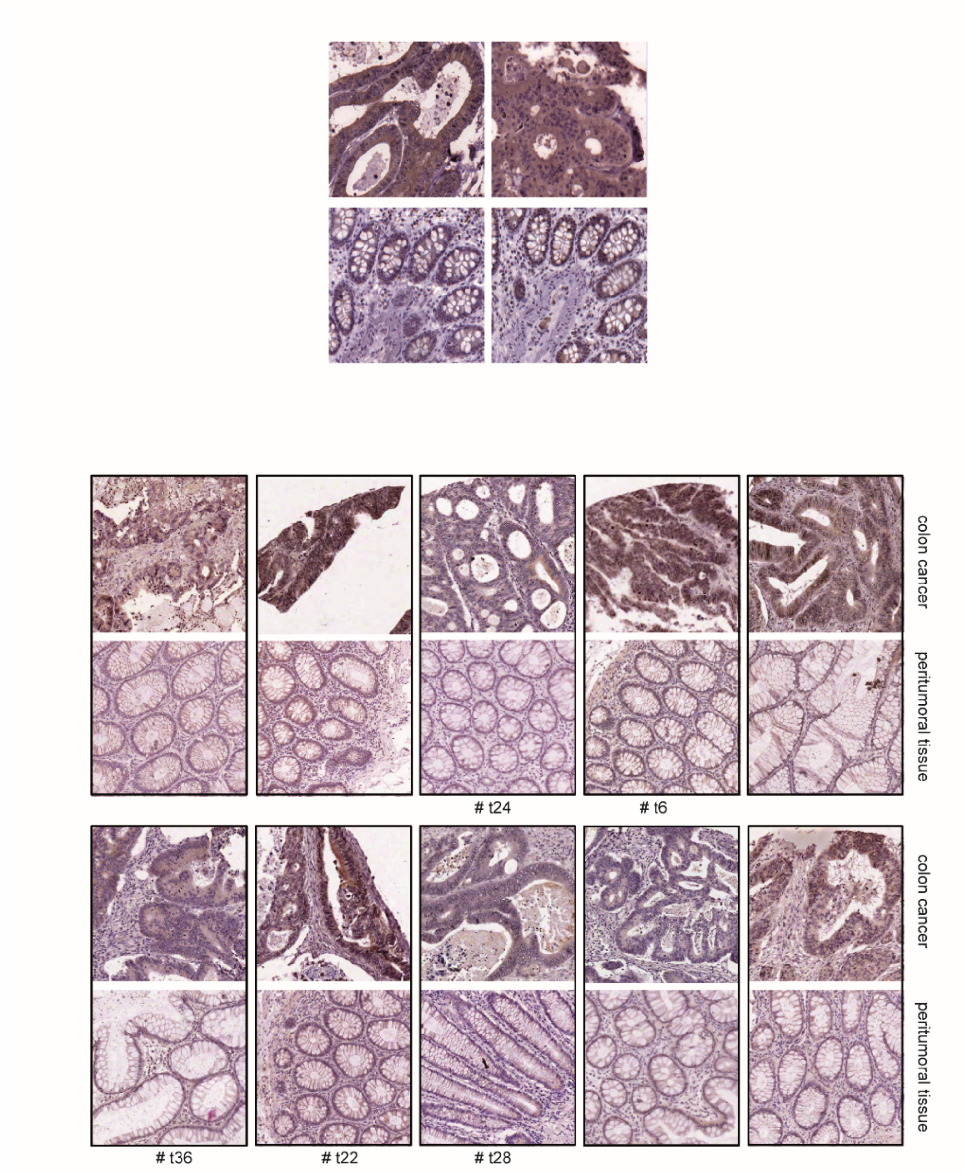

Supplementary Figure 6. *GSK3B is activated in colon carcinoma samples. (**A**) Representative sections of colon carcinoma (upper) and non-neoplastic pathology i.e. diverticulosis (lower) stained with anti-pTyr216-GSK3B antibodies. (**B**) Representative sections of 10 sample pairs from colon carcinoma patients (upper: colon cancer; lower: peri-tumoral colon) stained with anti-pTyr216-GSK3B antibodies.*

Chapter 5

The TGF-β pathway is activated by 5-fluorouracil treatment in drug resistant colorectal carcinoma cells

Gabriele Romano[1], Ludovica Santi[1], Maria Rosaria Bianco[2], Maria Rita Giuffrè[1], Mariateresa Pettinato[1], Cristina Bugarin[3], Cristina Garanzini[1], Leonilde Savarese[4], Silvia Leoni[1], Maria Grazia Cerrito[1], Biagio Eugenio Leone[1], Giuseppe Gaipa[3], Emanuela Grassilli[1], Michele Papa[4], Marialuisa Lavitrano[1], Roberto Giovannoni[1]

Author's Affiliations: [1] Department of Surgery and Translational Medicine, University of Milano-Bicocca, via Cadore, 48, 20900, Monza, Italy. [2] Department of Surgery and Translational Medicine, University of Milano-Bicocca, c/o Department of Mental and Physical Health and Preventive Medicine, Second University of Naples, Via L. Armanni, 5, 80138, Naples, Italy. [3] M. Tettamanti Research Center, Pediatric Clinic, University of Milano Bicocca, Via Pergolesi, 33, 20900 Monza, Italy. [4] Laboratory of Neuronal Networks, Department of Mental and Physical Health and Preventive Medicine, Second University of Naples, Via L. Armanni, 5, 80138, Naples, Italy.

(Submitted to: **Oncotarget)**

Keywords

TGF-β; chemoresistance; 5-fluorouracil; colorectal cancer; SMAD3

Abstract

TGF-β pathway is generally associated with the processes of metastasis, angiogenesis and EMT in cancer. Very little is known, however, about the role of TGF-β in cancer drug resistance. In this work, we show a specific activation of the TGF-β pathway in consequence of chemotherapeutic treatment in *in vivo* and *in vitro* models of colorectal carcinoma. 5-Fluorouracil (5FU) was able to stimulate nuclear translocation of SMAD3 and the transcription of specific genes such as *ACVRL1*, *FN1* and *TGFB1*. On the other hand, the specific inhibition of TGF-βRI was able not only to repress the 5FU-induced genes transcription, but also to restore the sensitivity of chemoresistant cells to the toxic action of the drug, by modulating the expression of *BCL2L1* and *ID1* genes. The role of the TGF-β molecule in the chemoresistant colon carcinoma cells' response to 5FU was further demonstrated by conditioned medium (CM) experiments: CM from 5FU-treated chemoresistant cells, was able to protect chemosensitive cells against the toxic action of 5FU. In conclusion, these findings showed the pivotal role of TGF-β pathway in colon cancer mechanisms of drug resistance suggesting new possible approaches in diagnosis and treatment of colon cancer patients.

Introduction

TGF-β is known to have paradoxical roles in carcinogenesis and cancer development: in the early stages of oncogenesis TGF-β pathway activation is generally associated with oncosuppression [1], whereas in the more advanced

stages of tumor development TGF-β promotes metastasis, angiogenesis, immunosuppression and Epithelial to Mesenchymal transition (EMT) [2,3].

TGF-β ligands bind type 2 TGF-β receptors, which dimerize with the type 1 TGF-β receptor (TGF-βR1) and causes its phosphorylation. TGF-βRI activates downstream pathways via the canonical SMAD pathway, in which receptor SMADs (SMAD2/3) form a complex with co-smads (such as SMAD4) and translocate to the nucleus to regulate transcription of target genes [4,5]. In the non-canonical SMAD-independent pathways, TGF-β can activate or in-activate a plethora of alternative signaling pathways, such as p38 mitogen-activated protein kinases (MAPK), phosphoinositide 3-kinase (PI3K)-AKT, Glycogen Synthase Kinase 3 (GSK3) and Rho GTPases. SMAD and non-SMAD pathways activation is strongly dependent on physiological or pathological cellular subset in which TGF-β exerts its action [6–8].

In epithelial tumors, TGF-β paradoxical role is due to the loss of the anti-proliferative effects of the TGF-β pathway in the first stages of tumor development and the consequent exacerbation of tumor-promoting effects [9]. For example, ATF3-mediated ID1 repression is one of the tumor suppressor arms of TGF-β signaling [10], but in patient-derived metastatic breast cancer cells TGF-β causes an aberrant increase of ID1 expression promoting lung metastasis [11].

In colon cancer models, TGF-β pathway hyper activation can eventually lead to the expression of PAI-1, and α-smooth muscle actin (α-SMA) in cancer associated fibroblasts (CAFs) [12] by creating a positive loop of TGF-β production and a tumor promoting microenvironment. TGF-β is also associated with tumor progression, neo-angiogenesis and lymph-node metastases in colorectal cancer, and it has been suggested as a possible biomarker for cancer progression and aggressiveness [13].

In addition, TGF-β is able to recruit macrophages to the tumor site and direct their response to a M2 phenotype, which is immunosuppressive and pro-angiogenetic [14,15]. In spite of plenty of literature about the pivotal role of TGF-β in colon

cancer, very little is known about the molecular mechanisms activated by TGF-β in colon cancer drug resistance. Recent findings showed that MED12 (Mediator Complex Subunit 12) expression was able to modulate TGF-β signaling and to influence chemotherapeutic response in colorectal cancer cells [16,17]. However, this kind of induced resistance is generically associated to the acquisition of a mesenchymal phenotype by cancer cells and patient tumors, and not to a TGF-β-specific response to chemotherapeutic administration.

On the basis of all previous observations, the aim of this work was to deepen the molecular aspects of TGF-β signaling in a colorectal cancer model of reversion of chemoresistance [18]. The translational relevance of this study is highlighted by the finding that TGF-β pathway was up-regulated in consequence of chemotherapeutic administration, and that specific inhibition of TGF-β signaling was able to restore drug sensitivity in colorectal cancer cells, *in vivo* and *in vitro* models.

Results

5-fluorouracil treatment causes an activation of TGF-β pathway in vivo.

We previously set up a xenograft model of colon cancer chemoresistance reversion and in this model we reported that Lithium (LiCl), which inhibits glycogen synthase kinase 3 (GSK3), administration was able to re-sensitize chemoresistant colon cancer cells to 5-Fluorouracil (5FU) chemotherapeutic action [18]. Since it has been reported a relationship between GSK3 and TGF-β pathways in tumor progression of different carcinomas [19,20] and it has been demonstrated the relationship between chemoresistance and TGF-β in colon cancer [16], we investigated how the TGF-β pathway could contribute to the chemoresistance/chemoreversion phenomenon in our model. Immunohistochemistry analysis of TGF-βRI on

xenografted tumor masses indicated that LiCl administration caused a significant downregulation of this receptor kinase expression, independently from 5FU administration in chemoresistant xenograft tumors (Fig. 1A and 1B, upper panels).

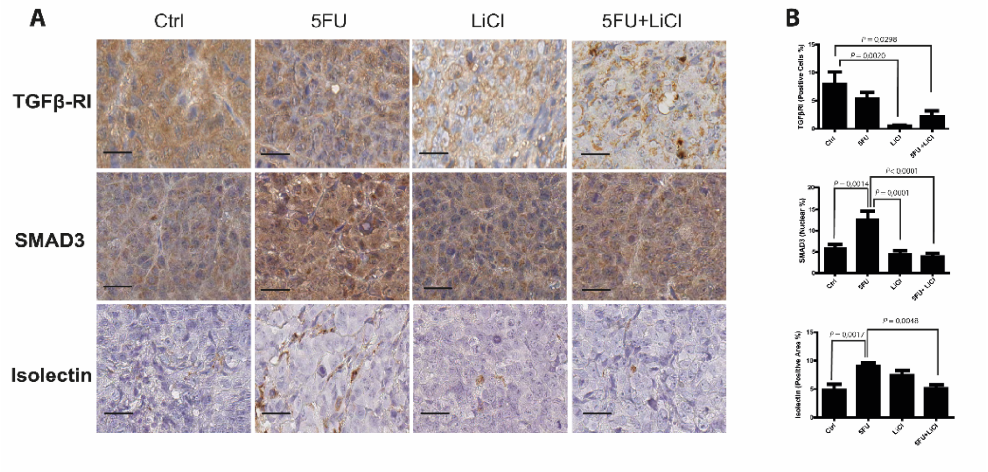

Figure 1. 5-fluorouracil treatment causes an activation of TGF-β pathway in xenografted chemoresistant cells. *(A) Representative images of IHC on HCT116p53KO tumor sections for each group of treatment. Bars represent 20 µm. 5FU increased SMAD3 nuclear translocation and tumor neo-angiogenesis . LiCl administration was able to downregulate TGF-βRI expression, to inhibit SMAD3 nuclear translocation and to restore basal levels of tumor vascularization. (B) Quantification was performed on whole tumor sections excluding necrotic areas (8 sections per group of treatment). One-way ANOVA followed by Tukey's test for multiple comparisons was performed to detect differences between groups of treatment. Significant P-values among groups after multiple comparisons are indicated above columns. Error Bars represent SEM.*

On the other hand, 5FU treatment increased nuclear translocation of SMAD3 as compared to control group, whereas LiCl was able to restore basal levels of nuclear SMAD3 (Fig. 1A and 1B, middle panels). As a result, LiCl-mediated TGF-βRI downregulation was able to contrast the 5FU-induced SMAD3 increased activation. Since the TGF-β pathway has a pro-angiogenic effect [21–23], we analyzed the microvasculature of the xenografted tumors in our model and we found a dramatic increase of tumor vascularization in consequence of 5FU administration (75mg/kg/d twice a week), whereas the combination of LiCl (160 mg/kg/d) and 5FU was able to significantly decrease the vasculature density, restoring the basal value

(Fig. 1A and 1B, bottom panels). Noteworthy, no significant changes in TGF-βRI expression, in SMAD3 localization nor in vascularization, were observed in chemosensitive HCT116 xenograft tumor sections (Supplementary Fig. S1), suggesting that the observed molecular events are selective for chemoresistant tumors. Taken together, these findings indicated that LiCl and 5FU exert opposite effects on TGF-β signaling pathway and that such regulations are exclusive for chemoresistant cells.

TGF-βRI inhibition reduces proliferation and increases cell death of chemoresistant cancer cells.

In order to better characterize the molecular aspects of TGF-β pathway regulation by 5FU and LiCl, we established an *in vitro* 3D model of colon carcinoma cells. Consistently to our findings in the *in vivo* model, immunofluorescence analysis of 3D cultured chemoresistant cells treated with 5FU, LiCl or a combination thereof revealed a downregulation of TGF-βRI exerted by LiCl (Fig. 2A and 2C) as well as a strong SMAD3 nuclear translocation in consequence of 5FU treatment (Fig. 2B and 2D). No significant changes in SMAD3 nuclear translocation or TGF-βRI expression were detected in chemosensitive HCT116 cells (Supplementary Fig. S2). On the basis of these results, we hypothesized an involvement of the TGF-βRI in the chemoresistant cells response to 5FU. In order to verify if the LiCl-mediated TGF-βRI downregulation was an off-target effect or a specific molecular regulation involved in chemoresistance, we inhibited the TGF-βRI by using SB431542, a well-known inhibitor of this serine/threonine kinase receptor [11,24,25]. Proliferation analysis showed that SB431542 treatment was able to dramatically decrease Ki67 expression in combination with 5FU, in HCT116p53KO cells (Fig. 3). Furthermore, cell death analysis by the Propidium Iodide (PI) incorporation assay revealed that the co-treatment with 5FU and SB431542 was able to significantly increase the number of cells in sub G0/G1cell cycle phase (apoptotic or dead cells) not only in

HCT116p53KO but also in HT-29 cells, another chemoresistant colon cancer cell line (Fig. 4). Taken together these data suggested that the TGF-βRI modulation is involved in the chemoresistance/chemoreversion phenomenon.

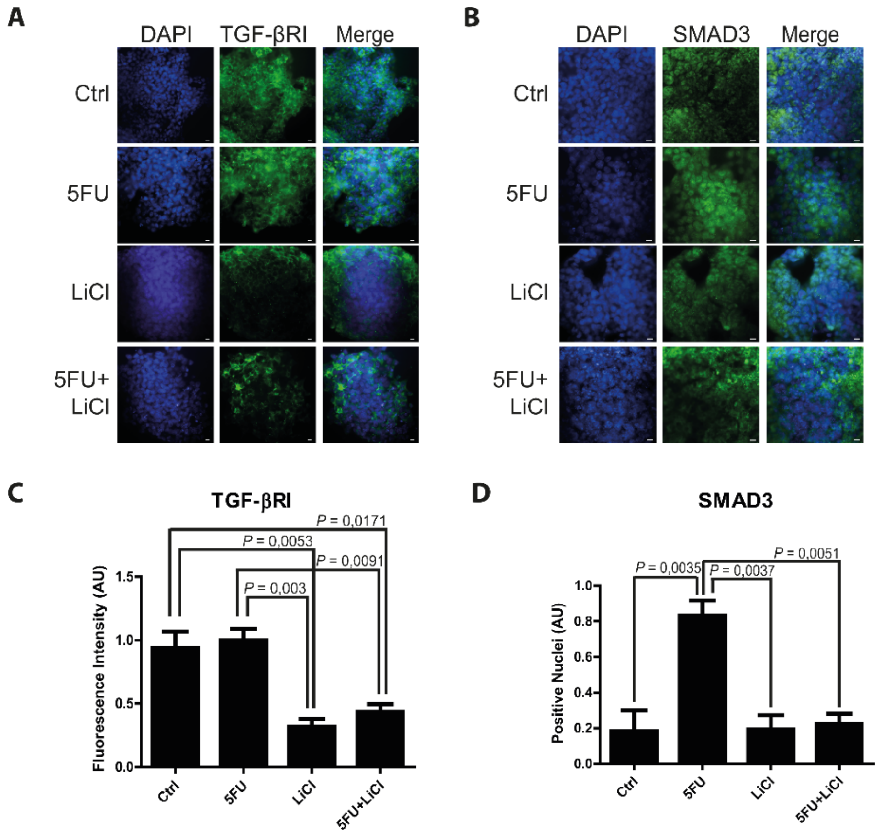

Figure 2. The in vitro 3D model recapitulates the molecular features of xenografted chemoresistant cells . *Representative pictures of immunofluorescence analysis for TGF-βRI (A) and SMAD3 (B) of 3D-cultured HCT116p53KO chemoresistant cell line. Antigens are stained in green. Bars represent 20 µm. Cellular nuclei were stained with DAPI (blue). (C). Lithium administration caused a reduction of TGF-βRI expression as compared to control group in immunofluorescence analysis. (D) 5FU treatment increased SMAD3 (green) nuclear translocation, whereas Lithium co-treatment with 5FU was able to restore the basal condition. One-way ANOVA followed by Tukey's test for multiple comparisons was performed to detect differences between groups of treatment. Significant P-values among groups after multiple comparisons are indicated above columns. Error Bars represent SEM.*

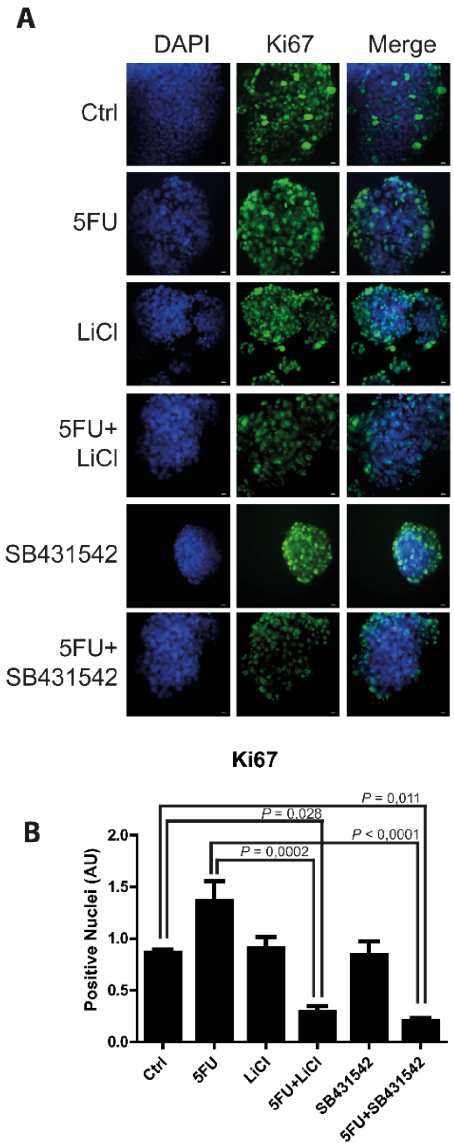

Figure 3. TGF-βRI inhibition reduced proliferation of 3D-cultured chemoresistant cancer cells. (A) Representative pictures of immunofluorescence analysis for Ki67 (marker of cell proliferation, green) on 3D-cultured HCT116p53KO chemoresistant cell lines. Bars represent 20 µm. Cellular nuclei were stained with DAPI (blue). (B) Lithium or SB431542 treatments in combination with 5FU strongly downregulated Ki67 expression.

5FU modulates TGF-β target genes expression in chemoresistant colon carcinoma cells

In order to better elucidate which TGF-β signaling pathway molecules are possibly involved in the colon cancer chemoresistance, we analyzed the expression levels of 84 different genes known to be fundamental players in TGF-β signaling. To this extent, HCT116p53KO 3D-cultured cells were treated with vehicle, 5FU, LiCl, SB431542 or a combination of 5FU and LiCl or 5FU and SB431542 and the corresponding RNA samples were analyzed by quantitative RT^2-PCR Profiler Array (Qiagen). Expression array analysis revealed a strong up-regulation of TGF-β target genes in consequence of 5FU treatment: 52 genes were found to be up-regulated, 10 didn't reveal any change and 12 genes were downregulated (Supplementary Fig. S3). Among the analyzed genes, 4 were selected for

their significant modulation and biological function and further validated (Table 1): *ACVRL1* (Activin A receptor type II-like 1), known to be involved in angiogenesis and tumor growth; *FN1* (Fibronectin-1), a master regulator of ECM remodeling and cell-matrix adhesion; *ID1* (Inhibitor of DNA binding 1), which promotes cells proliferation and migration; *BCL2L1* (BCL-2 like 1), encoding for a well known anti-apoptotic protein. *ACRVL1* and *FN1* were found to be significantly upregulated by 5FU administration, whereas LiCl or SB431542 treatments inhibited such increased gene transcription (Fig. 5). On the other hands, *ID1* and *BCL2L1* did not show any significant change in cells treated with 5FU alone, whereas LiCl or SB431542 co-treatments with 5FU strongly downregulated the expression of these two genes (Fig. 5). Consistently with all previous data, LiCl and SB431542 had similar effects on gene expression profiling in chemoresistant cells. Taken

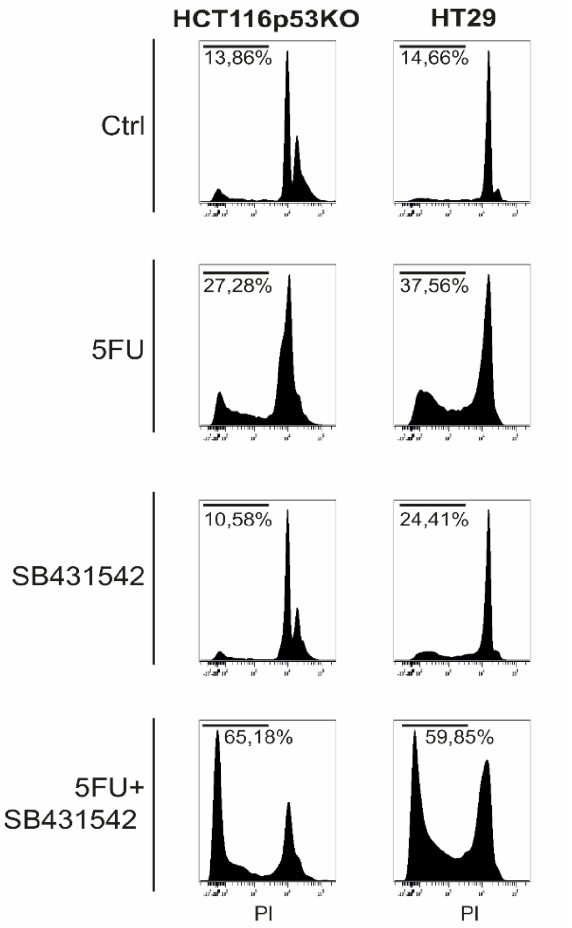

Figure 4. TGF-βRI inhibition increased cell death of 3D-cultured chemoresistant cancer cells. *Propidium iodide incorporation assay analysis on chemoresistant HT-29 and HCT116p53KO cells: TGF-βRI inhibition caused a re-sensitization to 5FU toxicity, dramatically increasing chemoresistant cell death (sub-G0/G1 cell populations indicated as percentage). All images are representative of at least 3 independent experiments.*

together, these results suggested that, in chemoresistant colon carcinoma cells exposed to 5FU, the chemotherapeutic agent stimulates proliferative and pro-migratory signaling, whereas 5FU and LiCl or SB431542 co-treatments were able to abolish the 5FU-activated pathway. Furthermore, the 5FU and LiCl or SB431542 co-treatments were also able to inhibit the pro-survival signals in chemoresistant cells, thus re-sensitizing HCT116p53KO cells to the chemotherapeutic action.

Gene	5FU vs Ctrl	5FU+LiCl vs 5FU	5FU+SB431542 vs 5FU
ACVRL1	7,99	-2,82	-2,01
BCL2L1	-2,00	-2,81	-3,99
FN1	5,67	1,00	-2,83
ID1	-2,00	-2,81	-4,01

Table 1. *Expression of relevant TGFβ target genes in HCT116p53KO cells treated with 5FU alone and in combination with LiCl or SB431542. Data are expressed as fold change as compared to the indicated controls.*

TGF-β1 exerts a protective action against 5-fluorouracil treatment.

The observed increase in nuclear localization of SMAD3 *in vivo* and *in vitro* in our models of chemoresistance together with the observation that the TGF-β target genes were strongly modulated in consequence of 5FU treatment only in chemoresistant colon carcinoma cells, led us to hypothesize a possible role of the TGF-β molecule in the cell response to 5FU. To verify this hypothesis, we investigated the expression levels of TGF-β1 in HCT116p53KO cells. Interestingly, we found that TGF-β1 expression was significantly increased by 5FU treatment and, oppositely, LiCl or SB431542 co-treatments with 5FU were able to restore basal levels of TGF-β1 (Fig. 6A). This finding led us to speculate a kind of autocrine signal operated by chemoresistant cells in presence of 5FU. We then investigated if TGF-β1 could be a protective

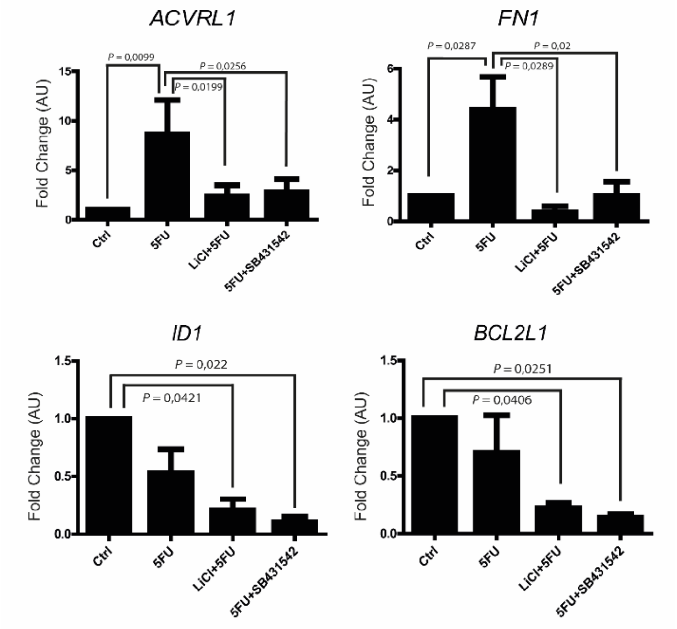

Figure 5. 5FU modulates the mRNA expression of selected TGF-β target genes in chemoresistant colon carcinoma cells. ACVRL1 and FN1 expression was upregulated by 5FU administration to chemoresistant cells. TGF-βRI inhibition (LiCl- or SB431542-mediated) in combination with 5FU treatment, not only reduced ACVRL1 and FN1 up-regulation, but also strongly repressed ID1 and BCL2L1 genes transcription. Columns represent the fold change values as compared to the control group, expressed by the 2-ΔΔCt algorithm as detailed in Materials and Methods section. Significant P-values among groups after multiple comparisons are indicated above columns. Bars represent SEM. Data shown are representative of at least three independent experiments.

factor against 5FU toxicity. To this extent, we treated chemosensitive colon carcinoma HCT116 cells with TGF-β1 in combination with standard 5FU treatment and cell proliferation and death were measured. HCT116 cells treated with both TGF-β1 and 5FU, did not show any decrease in Ki67 expression as compared to the 5FU-treated cells without TGF-β1 treatment (Fig. 6B-C). These findings, consistently with previous observations, suggested that TGF-β1 treatment was able to protect

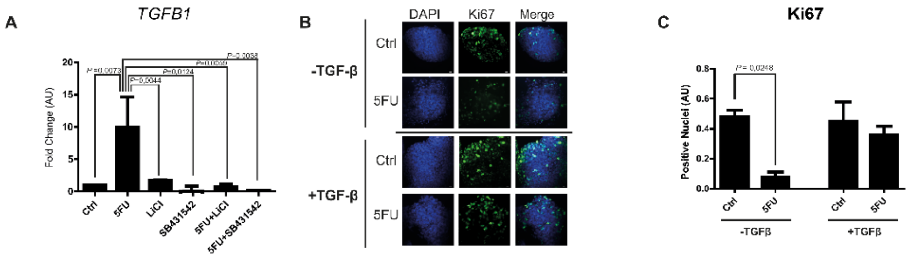

Figure 6. TGF-β1 exerts a protective role action against 5FU treatment in chemosensitive colon carcinoma cells. *(A) Real time PCR analyses on mRNA extracted from chemoresistant HCT116p53KO cells treated with 5FU alone or in combination with LiCl or SB431542. The treatment with 5FU significantly up-regulated TGF-β1 expression, but this increase was abolished by the co-treatment with LiCl or SB431542. Columns represent the fold change values as compared to the control group, expressed by the $2^{-\Delta\Delta Ct}$ algorithm as detailed in Materials and Methods section. Significant P-values among groups after multiple comparisons are indicated above columns. Bars represent SEM. Data shown are representative of at least three independent experiments. (B) Representative pictures of immunofluorescence analysis of Ki67 (green) on chemosensitive HCT116 carcinoma cells treated with 5FU with or without exogenous TGF-β1. Bars represent 20 μm. Cellular nuclei were stained with DAPI (blue). (C) TGF-β1 treatment protected HCT116 cells against 5FU toxicity, in terms of Ki67 expression (proliferation index).*

chemosensitive cells against the action of 5FU. To further support the hypothesis of an autocrine protective loop of TGF-β1, we administered 5FU to HT-29 and HCT116p53KO cells, and then we added such conditioned medium to 5FU-treated chemosensitive cells. As shown in Fig. 7, the medium conditioned from chemoresistant HT-29 and HCT116p53KO cells was able to protect chemosensitive cells from the chemotherapeutic toxicity.

Discussion

The results presented in this work showed that the TGF-β pathway has a pivotal role in colon cancer models of chemoresistance. TGF-β is known to be a main player in the processes of tumor development, metastasis and angiogenesis [1–3,13,26]; the TGF-β pathway has been recently associated to drug resistance [16], but very little is known about TGF-β pathway specific activation in the contest of chemotherapeutic administration in colon carcinoma. In a recent work from our lab, we reported that LiCl, which inhibits glycogen synthase kinase 3 (GSK3), administration was able to re-sensitize chemoresistant colon cancer cells to 5FU chemotherapeutic action, *in vitro* and *in vivo* [18] and we used this model of chemoresistance to investigate a possible involvement of TGF-β pathway in this phenomenon. We observed that LiCl administration to xenografted tumors-bearing mice significantly downregulated TGF-βRI expression in chemoresistant tumors (Fig. 1). SMAD3 is one of the main effectors downstream the TGF-βRI activation and the immunohistochemistry analysis of this marker surprisingly revealed that 5FU dramatically increased SMAD3 nuclear translocation, suggesting an activation of the TGF-β pathway (Fig. 1). The treatment with LiCl

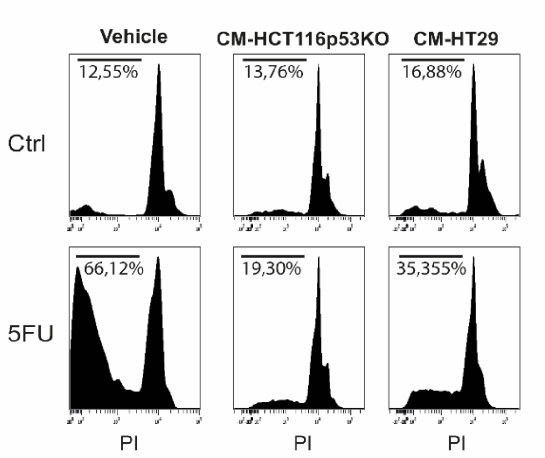

Figure 7. Culture medium conditioned by chemoresistant cells is able to protect HCT116 against 5FU toxicity. Propidium iodide incorporation assay analysis of conditioned medium (CM) experiments. CM from HCT116p53KO or HT-29 cells that received 5FU administration was able to induce chemoresistance in HCT116 cells (sub-G0/G1 cell populations indicated as percentage). All images are representative of at least 3 independent experiments.

abolished this induction, preventing SMAD3 to enter the nucleus even if the 5FU had been administered together with LiCl (Fig. 1), suggesting that the inhibition of GSK3 pathway could switch off the TGF-β pathway activation induced by 5FU. Moreover, the LiCl-induced impairment of SMAD3 nuclear translocation was consistent with TGF-βRI downregulation observed in tumors from LiCl-treated mice. As TGF-β is known to be a main player in the neo-angiogenesis and vascular sprouting processes [21–23], we investigated if the observed modulation of TGF-βRI and SMAD3 molecules correlated with modifications in the microvasculature of the xenografted tumors. Again, consistently with a hypothesis of a specific modulation of TGF-β pathway induced by 5FU and LiCl treatments, we observed that the group of tumors that received chemotherapeutic administration showed increased vascularization as compared to control group (Fig. 1). Furthermore, the number of microvessels was restored to basal levels by LiCl administration. Noteworthy, no significant changes were observed in chemosensitive tumors in SMAD3, TGF-βRI or vasculature modulation (Supplementary Fig. S1).

In order to deepen the aspects of the involvement of TGF-β pathway in the chemoresistance and in the reversion of this phenotype, we investigated, in an *in vitro* model, the molecular events occurring in colon carcinoma cells exposed to 5FU. To better recapitulate the tumor tissue architecture and some microenvironment features *in vitro*, we used an established 3D-model [27,28] in which cancer cells are seeded on a gelled bed of Extracellular Matrix (ECM) and immersed in a gradient of ECM, thus mimicking a three-dimensional structure of a tissue. In this model, the 5FU-induced SMAD3 nuclear translocation and its inhibition by LiCl administration as well as the down-regulation of TGF-βRI in LiCl-treated cells were confirmed (Fig. 2). A previous work in rat neuron-enriched cerebral cortical cultures, showed that LiCl administration was able to inhibit SMAD3/SMAD4 transactivation, but this kind of inhibition was reported as a result

of a regulation of cAMP– protein kinase A (PKA), AKT–glycogen synthase kinase-3β (GSK3β), and CRE-dependent signaling pathways [29]. No previous literature reports LiCl-mediated TGF-βRI downregulation. In order to exclude a LiCl off-target effect on TGF-βRI, we specifically inhibited TGF-βRI by using SB431542, a well-known TGF-βRI inhibitor [11,24,25]. We observed that TGF-βRI specific inhibition in combination with 5FU was able to re-sensitize chemoresistant cells to chemotherapeutic action, in terms of inhibition of proliferation and induction of cell death (Fig. 3-4). These findings excluded the possibility of an off-target effect of LiCl on TGF-βRI, and confirmed the active involvement of the TGF-β pathway in the phenomenon of chemoresistance.

Trying to unravel which molecules could be involved in the TGF-β pathway modulation in colon cancer chemoresistance, we performed a gene profiling by analyzing 84 TGF-β target genes: chemoresistant colon carcinoma cells that received 5FU showed an up-regulation of 52 out of 84 genes analyzed (Supplementary Fig. S3). More interestingly, SB431542 and LiCl treatments were both able to inhibit 5FU-induced modification of TGF-β target genes expression. Among the analyzed genes, four were selected on the basis of significance and biological function and were further validated. *ACRVL1*, a receptor known to have role in neo-angiogenesis [30,31] and tumor cell proliferation [32,33] was found to be up-regulated by 5FU administration, while its expression was reduced in cells co-treated with 5FU with LiCl or SB431542 (Fig. 3). 5FU alone also strongly induced *FN1*, a protein involved in ECM reorganization and cell to matrix adhesion processes [34,35], but *FN1* up-regulation was abolished by the co-treatment of 5FU and LiCl or 5FU and SB431542 (Fig. 3). The expression levels of *BCL2L1* (a gene encoding for anti-apoptotic proteins [36,37]) were found to be consistent with cell death evaluated by PI incorporation assay (Fig. 4): as expected, in chemoresistant cells, 5FU treatment did not induce any significant change in expression of an anti-

apoptotic gene (Fig. 5). On the other hand, the expression of *BCL2L1* was significantly reduced in cells co-treated with 5FU and LiCl or SB432541 (Fig. 3). Interestingly, the inhibition of TGF-βRI (LiCl- or SB431532-mediated) in combination with 5FU, was able to significantly repress the expression of *ID1* (Fig. 5), which is a strong promoter of TGF-β-mediated cell proliferation and migration [38–40].

Taken together, these findings suggested that the activation of TGF-β pathway was specifically induced by 5FU treatment in chemoresistant colon carcinoma cells, and that the target genes modulated during this phenomenon are involved in the regulation of surrounding microenvironment as well as in cell mechanisms of death and proliferation. In addition, the inhibition of TGF-β pathway not only was able to counteract 5FU-induced genes modulation, but it restored some of the mechanisms generally lost in chemoresistant cells (BCL2L1 and ID1).

The increase in nuclear localization of SMAD3 in our *in vivo* and *in vitro* models of chemoresistance together with the modulation of TGF-β target genes only in chemoresistant, 5FU-treated, colon carcinoma cells led us to hypothesize a possible role of the TGF-β molecule in the response to 5FU. TGF-β1 was found to be upregulated by chemotherapeutic treatment and restored to basal levels by co-treatment of 5FU with LiCl or SB431542 in HCT116p53KO cells (Fig. 6A). This finding suggested a sort of autocrine loop: the chemoresistant cells increase SMAD3 signaling, which increases TGF-β1 expression, which in turn increases SMAD3 signaling again. In fact, TGF-β1 is known to be the main inducer of TGF-β1 itself [41,42]. In our model, the loop would be interrupted by TGF-βRI inhibition, as it is the receptor which is up-stream of the whole signaling pathway.

To support this hypothesis, we then investigated if TGF-β1 could be a protective factor against 5FU toxicity in chemosensitive colon carcinoma cells, HCT116. As expected, we observed that TGF-β1 treatment was able to protect HCT116 (chemosensitive) cells to the action of 5FU (Fig. 6C-D); in order to further

demonstrate that the protection against 5FU is induced in chemoresistant cells exposed to 5FU, we treated chemoresistant colon carcinoma cell lines (HT-29 and HCT116p53KO) with 5FU and used such conditioned medium to protect HCT116 chemosensitive cells from 5FU-induced toxicity. Consistently, HCT116 showed an increased protection against 5FU action when treated with chemoresistant-cells-conditioned medium (Fig. 7).

In conclusion, this study demonstrated for the first time that the 5-fluorouracil treatment activated the TGF-β pathway in drug resistant colorectal carcinoma cells in *in vivo* and *in vitro* models. The specific abrogation of TGF-β pathway was able to restore sensitivity to chemotherapeutic action by specifically modulating the gene expression profile. The TGF-β pathway activation of 5FU-stimulated chemoresistant cancer cells conferred protection, by modulating surrounding microenvironment as well as cell mechanisms of death and proliferation genes, against 5FU toxicity.

Materials and Methods

Reagents and antibodies.

Lithium Chloride (LiCl), TGF-β1, Propidium Iodide and DNAse-free RNAse were purchased from Sigma Aldrich, SB431542 was purchased from Selleck Chemicals. Anti-TGF-βR1 (Rabbit polyclonal, Abcam), anti-SMAD3 (Rabbit monoclonal [EP568Y], Abcam) primary antibodies were used for immunohistochemistry (1:50 and 1:75, respectively) and immunofluorescence (1:50 and 1:300, respectively) analyses. Anti-Ki67 (1:100, Rabbit monoclonal [SP6], Abcam) primary antibody was used for immunofluorescence analysis. HRP-conjugated anti-rabbit (ImmPRESS Reagent Kit, Vector Laboratories) or Alexa Fuor 488-conjugated donkey anti-rabbit (Life Technologies) secondary antibodies were used.

Xenograft model, Immunohistochemistry and Microvasculature Density quantification.

Xenograft model and treatments were performed as previously reported [18]. Resected tumors were put in formalin. Sections were then dehydrated, diafanized with xylene, put in paraffin, sectioned with microtome and put on slides. After deparaffinization, citrate based antigen retrieval was performed. Blocking was performed using Normal Horse Serum (ImmPRESS™ Reagent Kit, Vector Labs). Slides were then incubated with specific primary antibody diluted in PBS-Tween 0.1% for 1 hour in a humid chamber, avoiding drying of specimens. Slides were then incubated with HRP-conjugated anti-rabbit secondary antibody. For the detection of mouse microvasculature, after deparaffinization, slides were blocked with Carbo-Free™ Blocking Solution (Vector Laboratories) and incubated with Biotinylated GSL I –isolectin B4 (10 ug/ml, Vector Laboratories). VECTASTAIN® ABC peroxidase was then applied to the specimens.

Processed slides were finally added with 3,3'-diaminobenzidine (DAB, Vector Laboratories) to develop the chromogenic reaction, and counter-stained with Hematoxylin (Vector Laboratories). Coverslips were mounted after de-hydration of the sections, using Permanent Mounting Medium (Vector Laboratories). Images were digitally acquired with ScanScope (Aperio) and quantified using ImageScope software (Aperio). The quantification was performed on the whole tumor section excluding necrotic areas and using Positive Pixels Count or Nuclear algorithm (Aperio), on the basis of the antigen localization.

Cell lines, 3D cell culture and treatments.

HCT116 and HCT116p53KO colon carcinoma cell lines were a kind gift of Dr. Bert Vogelstein (Johns Hopkins University, Baltimore, MD), HT-29 cells were from American Type Culture Collection (LGC Standards, Sesto San Giovanni, Italy). All cell

lines were authenticated by STR analysis at Promega. Upon arrival, cells were expanded and frozen as a seed stocks of first or second passage. All cells were passaged for a maximum of 4 weeks, after which new seed stocks were thawed for experimental use. HCT116, HCT116p53KO and HT-29 cells were grown in McCoy's 5A-Glutamax medium with 10% FBS (Gibco, not Heat Inactivated), 100 U/ml Penicillin and 100 µg/ml Streptomycin. All cells were maintained in a 37°C incubator at 5% CO2.

For 3D culture, cells were seeded at a density of $1*10^5$/ml on a gelled bed of Extracellular Matrix (Cultrex®, Trevigen) in McCoy's 5A-Glutamax medium supplemented with 4% FBS (Gibco), 100 U/ml Penicillin and 100 µg/ml Streptomycin and 2% of Cultrex®, in order to create an Extracellular Matrix (ECM) gradient, modified from Debnath *et al* [43]. Three days after seeding, cells were pre-treated with LiCl (10mM) or with SB431542 (10µM) or TGF-β1 (10 ng/ml). After 24 hours of pre-treatment, old medium was discarded and fresh medium containing 5-Fluorouracil (5FU, 200 µM) and Lithium, SB431542 or TGF-β1 was added and maintained for 72 hours. For conditioned medium experiments, 3D-cultured HT-29 and HCT116p53KO cells were treated with vehicle or 5FU, and after 48h of conditioning, chemoresistant cells conditioned medium was used to treat 3D-coltured HCT116 cells for 72h.

Immunofluorescence.

For immunofluorescence analysis, cells were seeded in 8-well chamber slides (LabTek Chamber slides, Thermo Fisher Scientific), cultured and treated as described in the previous section. At the end of treatments cells were fixed with 4% Formaldehyde and, for intracellular antigens detection, permeabilized with Triton X-100 0.5% in PBS. Blocking with BSA 3% was performed to prevent non-specific binding of the antibodies. Cells were then incubated with primary antibody diluted in BSA 3% for 1 hour and for 30 minutes with appropriate secondary antibodies.

Coverslips were mounted on slides using ProLong Gold mounting medium with DAPI (Life Technologies). Slides were imaged with a Zeiss Axioskope 2 microscope (Zeiss) equipped with fluorescence lamp and filters and a high-resolution digital camera (C4742–95, Hamamatsu Photonics). Single channel grey-scale images were quantified using ImageJ Software (Rasband, W.S., ImageJ, U. S. National Institutes of Health, Bethesda, Maryland, USA, http://imagej.nih.gov/ij/, 1997-2014). Threshold was fixed and applied to all images stained with the same antibody. For nuclear antigens, images were processed and threshold was fixed in order to measure only nuclear staining signal. Obtained fluorescence intensity measurements were normalized to DAPI fluorescence signal. The images were then processed with Adobe Photoshop CS6 software for color assignation to the corresponding fluorescence signal.

Cell death analysis by Propidium Iodide incorporation assay.

The cell death evaluation by propidium iodide incorporation of 3D-cultured cells was performed according to a modified version of the protocol from Riccardi *et al* [44]. Briefly, at the end of the treatments cells were detached from gelled ECM using CellSperse™ (Trevigen) solution. Cells were then fixed in 70% v/v ethanol at -20°C. DNA was extracted using a solution of Na_2HPO_4 and Triton X-100. Staining solution (Propidium Iodide 20ug/ml, DNAse free RNAse 200ug/ml) was then added to cell suspension and incubated on dark for 1h. Fluorescence was assessed using FACS Aria flow cytometer (Becton Dickinson). Data were analyzed using Cytobank software [45].

RNA extraction, RT^2 array and single gene validation.

CellSperse™ solution was used to recover cells grown on Cultrex®, following manufacturer instructions. RNeasy® Mini Kit (Qiagen) was used to extract RNA from cells grown on a thin layer of Cultrex®. RNA samples were treated with DNase to ensure elimination of genomic DNA. At the end of the procedure, the RNA

concentration was measured with Nanodrop 2000 (Thermo Scientific) and samples were checked for RNA quality and integrity by 1.5% agarose gel electrophoresis in denaturing conditions. One microgram of extracted RNA was then converted to cDNA by using the RT^2 First Strand Kit (Qiagen) according to manufacturer's instructions.

The expression of 84 Human TGF-β Signaling Targets genes was analyzed by RT^2 profiler PCR array (PAHS-235ZA, Qiagen) using the StepOne Plus instrument (Applied Biosystems) following the manufacturer's protocol. Two independent experiments were performed for each group of treatment. Untreated cells were used as reference control sample. The mRNA expression levels of each gene in each cell treatment were normalized using the expression of the housekeeping genes *B2M*, *GAPDH*, *RPLP0*, *HPRT1* and *ACTB.* The results were confirmed by qRT-PCR experiments on selected genes by using StepOne Plus instrument (Applied Biosystems). At least three independent experiments were performed for each single gene validation. The primers used for qRT-PCR were selected from PrimerBank [46–48] and are listed in Supplementary Table S1. Data, normalized for *B2M* gene, are expressed as fold change value respect to the untreated cells according to the $2^{-\Delta\Delta Ct}$ algorithm.

Statistical Analysis.

Data are presented as means ± SEM. Statistical analysis were performed with ANOVA test followed by Tukey's Test for multiple comparisons. Exact P values are indicated in figures or in legends and a P value <0.05 was considered as statistically significant. Statistical analysis was performed using GraphPad Prism (GraphPad Software).

Conflict of Interests disclosure

The authors declare that no potential conflicts of interests exist.

Grant Support

This work was supported by grants from MIUR [PON01_02782 to M.L.], Ministry of Health [RF-2010-2305526 to M.L.] and University of Milano-Bicocca [F.A.R. to M.L. and R.G.].

References

1. Ikushima H, Miyazono K. TGFbeta signalling: a complex web in cancer progression. Nat Rev Cancer. 2010;10:415–24.
2. Pickup M, Novitskiy S, Moses HL. The roles of TGFβ in the tumour microenvironment. Nat Rev Cancer. 2013;13:788–99.
3. Drabsch Y, Dijke P. TGF-β signalling and its role in cancer progression and metastasis. Cancer Metastasis Rev. 2012;31:553–68.
4. Attisano L, Wrana JL. Signal transduction by the TGF-beta superfamily. Science. 2002;296:1646–7.
5. Massagué J, Seoane J, Wotton D. Smad transcription factors Smad transcription factors. 2005;2783–810.
6. Zhang YE. Non-Smad pathways in TGF-β signaling. Cell Res. 2009;19:128–39.
7. Zhang Q, Yu N, Lee C. Mysteries of TGF-β Paradox in Benign and Malignant Cells. Front Oncol. 2014;4:94.
8. Akhurst RJ, Hata A. Targeting the TGFβ signalling pathway in disease. Nat Rev Drug Discov. 2012;11:790–811.
9. Massagué J. TGFbeta in Cancer. Cell. 2008;134:215–30.

10. Kang Y, Chen CR, Massagué J. A self-enabling TGFβ response coupled to stress signaling: Smad engages stress response factor ATF3 for Id1 repression in epithelial cells. Mol Cell. 2003;11:915–26.
11. Padua D, Zhang XHF, Wang Q, Nadal C, Gerald WL, Gomis RR, Massagué J. TGFβ Primes Breast Tumors for Lung Metastasis Seeding through Angiopoietin-like 4. Cell. 2008;133:66–77.
12. Hawinkels LJ a C, Paauwe M, Verspaget HW, Wiercinska E, van der Zon JM, van der Ploeg K, Koelink PJ, Lindeman JHN, Mesker W, ten Dijke P, Sier CFM. Interaction with colon cancer cells hyperactivates TGF-β signaling in cancer-associated fibroblasts. Oncogene. 2014;33:97–107.
13. Xiong B, Gong L-L, Zhang F, Hu M-B, Yuan H-Y. TGF beta1 expression and angiogenesis in colorectal cancer tissue. World J Gastroenterol. 2002;8:496–8.
14. Erreni M, Mantovani A, Allavena P. Tumor-associated macrophages (TAM) and inflammation in colorectal cancer. Cancer Microenviron. 2011;4:141–54.
15. Mantovani A, Sica A. Macrophages, innate immunity and cancer: balance, tolerance, and diversity. Curr Opin Immunol. 2010;22:231–7.
16. Brunen D, Willems SM, Kellner U, Midgley R, Simon I, Bernards R. TGF-β: An emerging player in drug resistance. Cell Cycle. 2013;12:2960–8.
17. Huang S, Hölzel M, Knijnenburg T, Schlicker A, Roepman P, McDermott U, Garnett M, Grernrum W, Sun C, Prahallad A, Groenendijk FH, Mittempergher L, Nijkamp W, et al. MED12 controls the response to multiple cancer drugs through regulation of TGF-β receptor signaling. Cell. 2012;151:937–50.
18. Grassilli E, Narloch R, Federzoni E, Ianzano L, Pisano F, Giovannoni R, Romano G, Masiero L, Leone BE, Bonin S, Donada M, Stanta G, Helin K, et al.

Inhibition of GSK3B bypass drug resistance of p53-null colon carcinomas by enabling necroptosis in response to chemotherapy. Clin Cancer Res. 2013;19:3820–31.

19. Cozzolino AM, Alonzi T, Santangelo L, Mancone C, Conti B, Steindler C, Musone M, Cicchini C, Tripodi M, Marchetti A. TGFβ overrides HNF4α tumor suppressing activity through GSK3β inactivation: implication for hepatocellular carcinoma gene therapy. J Hepatol. 2013;58:65–72.
20. Basu D, Lettan R, Damodaran K, Strellec S, Reyes-Mugica M, Rebbaa A. Identification, mechanism of action, and antitumor activity of a small molecule inhibitor of hippo, TGF-β, and Wnt signaling pathways. Mol Cancer Ther. 2014;13:1457–67.
21. Lebrin F, Deckers M, Bertolino P, Ten Dijke P. TGF-beta receptor function in the endothelium. Cardiovasc Res. 2005;65:599–608.
22. Pepper MS. Transforming growth factor-beta: vasculogenesis, angiogenesis, and vessel wall integrity. Cytokine Growth Factor Rev. 1997;8:21–43.
23. Pepper MS, Vassalli JD, Orci L, Montesano R. Biphasic effect of transforming growth factor-beta 1 on in vitro angiogenesis. Exp Cell Res. 1993;204:356–63.
24. Burch ML, Osman N, Getachew R, Al-Aryahi S, Poronnik P, Zheng W, Hill M a, Little PJ. G protein coupled receptor transactivation: extending the paradigm to include serine/threonine kinase receptors. Int J Biochem Cell Biol. 2012;44:722–7.
25. Chaffer CL, Marjanovic ND, Lee T, Bell G, Kleer CG, Reinhardt F, D'Alessio AC, Young RA, Weinberg RA. Poised chromatin at the ZEB1 promoter enables breast cancer cell plasticity and enhances tumorigenicity. Cell. 2013;154:61–74.

26. Shen L, Qu X, Ma Y, Zheng J, Chu D, Liu B, Li X, Wang M, Xu C, Liu N, Yao L, Zhang J. Tumor suppressor NDRG2 tips the balance of oncogenic TGF-β via EMT inhibition in colorectal cancer. Oncogenesis. 2014;3:e86.

27. Young M, Ordonez L, Clarke AR. What are the best routes to effectively model human colorectal cancer ? Mol Oncol. 2013;7:178–89.

28. Tsunoda T, Takashima Y, Fujimoto T, Koyanagi M, Yoshida Y, Doi K, Tanaka Y, Kuroki M, Sasazuki T, Shirasawa S. Three-dimensionally specific inhibition of DNA repair-related genes by activated KRAS in colon crypt model. Neoplasia. 2010;12:397–404.

29. Liang M, Wendland JR, Chuang D. Lithium inhibits Smad3/4 transactivation via increased CREB activity induced by enhanced PKA and AKT signaling. Mol Cell Neurosci. 2008;37:440–53.

30. Vecchia L, Olivieri C, Scotti C. Activin Receptor-like kinase 1: a novel anti-angiogenesis target from TGF-β family. Mini Rev Med Chem. 2013;13:1398–406.

31. Bhatt RS, Atkins MB. Molecular pathways: Can activin-like kinase pathway inhibition enhance the limited efficacy of vegf inhibitors? Clin Cancer Res. 2014;20:2838–45.

32. Venkatesha VA, Joshi A, Venkataraman M, Sonawane V, Bhatia D, Tannu P, Bose J, Choudhari S, Srivastava A, Pandey PK, Lad VJ, Sangana R, Ahmed T, et al. P7170, a novel inhibitor of mTORC1/mTORC2 and Activin receptor-like Kinase 1 (ALK1) inhibits the growth of non small cell lung cancer. Mol Cancer. 2014;13:259.

33. Hsu JW, Dang NH. ALK1 as a Novel Therapeutic Target for CD30+ T-Anaplastic Large Cell Lymphoma. JNCI J Natl Cancer Inst. 2014;106:djt454–djt454.

34. Pankov R, Yamada KM. Fibronectin at a glance. J Cell Sci. 2002;115:3861–3.

35. Lu P, Weaver VM, Werb Z. The extracellular matrix: A dynamic niche in cancer progression. J Cell Biol. 2012;196:395–406.
36. Perego P, Righetti SC, Supino R, Delia D, Caserini C, Carenini N, Bedogné B, Broome E, Krajewski S, Reed JC, Zunino F. Role of apoptosis and apoptosis-related proteins in the cisplatin-resistant phenotype of human tumor cell lines. Apoptosis. 1997;2:540–8.
37. Boise LH, González-García M, Postema CE, Ding L, Lindsten T, Turka LA, Mao X, Nuñez G, Thompson CB. bcl-x, a bcl-2-related gene that functions as a dominant regulator of apoptotic cell death. Cell. 1993;74:597–608.
38. Wong YC, Wang X, Ling MT. Id-1 expression and cell survival. Apoptosis. 2004;9:279–89.
39. Lasorella A, Uo T, Iavarone A. Id proteins at the cross-road of development and cancer. Oncogene. 2001;20:8326–33.
40. Di K, Wong YC, Wang X. Id-1 promotes TGF-β1-induced cell motility through HSP27 activation and disassembly of adherens junction in prostate epithelial cells. Exp Cell Res. 2007;313:3983–99.
41. Kelley J, Shull S, Walsh JJ, Cutroneo KR, Absher M. Auto-induction of transforming growth factor-beta in human lung fibroblasts. Am J Respir Cell Mol Biol. 1993;8:417–24.
42. Yu N, Kozlowski JM, Park II, Chen L, Zhang Q, Xu D, Doll J a, Crawford SE, Brendler CB, Lee C. Overexpression of transforming growth factor β1 in malignant prostate cells is partly caused by a runaway of TGF-β1 auto-induction mediated through a defective recruitment of protein phosphatase 2A by TGF-β type I receptor. Urology. 2010;76:1519.e8–13.
43. Debnath J, Muthuswamy SK, Brugge JS. Morphogenesis and oncogenesis of MCF-10A mammary epithelial acini grown in three-dimensional basement membrane cultures. Methods. 2003;30:256–68.

44. Riccardi C, Nicoletti I. Analysis of apoptosis by propidium iodide staining and flow cytometry. Nat Protoc. 2006;1:1458–61.

45. Kotecha N, Krutzik PO, Irish JM. Web-based analysis and publication of flow cytometry experiments. Curr Protoc Cytom. 2010;81:8715–23.

46. Spandidos A, Wang X, Wang H, Seed B. PrimerBank: A resource of human and mouse PCR primer pairs for gene expression detection and quantification. Nucleic Acids Res. 2009;38.

47. Spandidos A, Wang X, Wang H, Dragnev S, Thurber T, Seed B. A comprehensive collection of experimentally validated primers for Polymerase Chain Reaction quantitation of murine transcript abundance. BMC Genomics. 2008;9:633.

48. Wang X, Seed B. A PCR primer bank for quantitative gene expression analysis. Nucleic Acids Res. 2003;31:e154.

Supplementary Data

Supplementary Table S1. List of the primers used in qRT-PCR experiments. qRT-PCR was carried out using 2X SYBR Green Master Mix (Applied Biosystem), primers with a final concentration of 0.1 µM and cDNA samples with a final concentration of 10 ng/µl in order to perform PCR reactions on 10 ng cDNA template. The PCR reactions were performed with the following thermal cycling conditions: 95°C for 10 min, followed by 40 cycles of 95°C for 15 sec and 60°C for 1 min. Melting curve analysis were performed to verify PCR specificity at the end of each PCR run.

Gene	Forward Primer	Reverse Primer	PrimerBank ID
ACVRL1	5'-CGAGGGATGAACAGTCCTGG-3'	5'-GTCATGTCTGAGGCGATGAAG-3'	116734711c1
B2M	5'-GAGGCTATCCAGCGTACTCCA-3'	5'-CGGCAGGCATACTCATCTTTT-3'	37704380c1
BCL2L1	5'-GAGCTGGTGGTTGACTTTCTC-3'	5'-TCCATCTCCGATTCAGTCCCT-3'	20336333c1
FN1	5'-AGGAAGCCGAGGTTTTAACTG-3'	5'-AGGACGCTCATAAGTGTCACC-3'	47132556c2
ID1	5'-CTGCTCTACGACATGAACGG-3'	5'-GAAGGTCCCTGATGTAGTCGAT-3'	341865545c1
TGFB1	5'-CAATTCCTGGCGATACCTCAG-3'	5'-GCACAACTCCGGTGACATCAA-3'	260655621c3

Supplementary Figure S1. 5-fluorouracil treatment did not cause any modulation of TGF-β pathway in xenografted chemosensitive cells. TGFβ pathway was not involved in HCT116 xenografted tumors drug response. Quantification was performed on whole tumor sections excluding necrotic areas (8 sections per group of treatment). One-way ANOVA followed by Tukey's test for multiple comparisons was performed to detect differences between groups of treatment. No significant differences were detected among groups in terms of TGFβ-RI expression (A), SMAD3 sub-cellular localization (B) nor vascularization (C). Error Bars represent SEM.

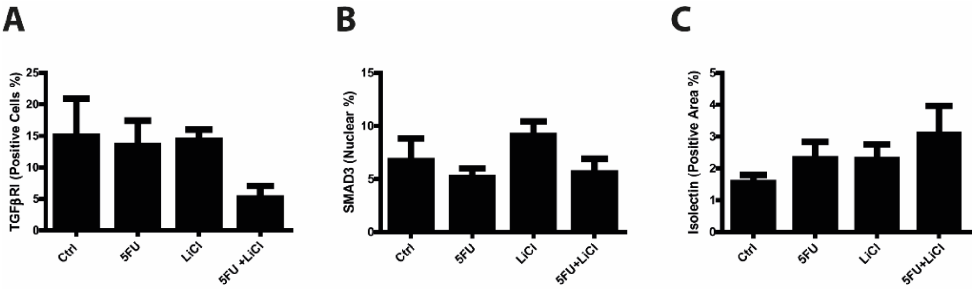

Supplementary Figure S2. 5-fluorouracil treatment did not cause any modulation of TGF-β pathway in 3D-cultured chemosensitive cells. Representative pictures of immunofluorescence analysis for TGF-βRI (A) and SMAD3 (B) of 3D-cultured HCT116 chemosensitive cell line. Antigens are stained in green. Bars represent 20 µm. Cellular nuclei were stained with DAPI (blue). Differently from that observed in chemoresistant cells, Lithium administration did not influence TGF-βRI expression (C) in HCT116 cells in any treatment analyzed (control, 5FU, LiCl or 5FU+LiCl). (D) SMAD3 (green) nuclear localization did not reveal any significant changes in consequence of the indicated treatments. One-way ANOVA followed by Tukey's test for multiple comparisons was performed to detect differences between groups of treatment. No significant differences among groups were detected. Error Bars represent SEM.

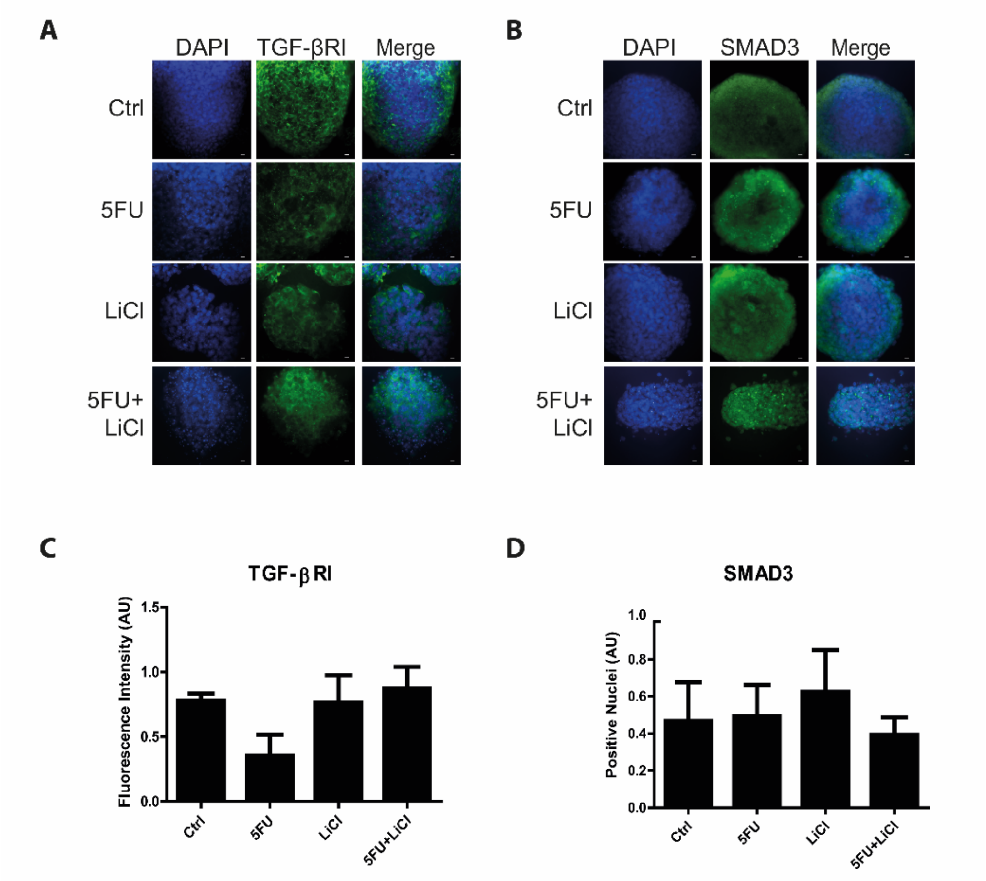

Supplementary Figure S3. 5FU modulates TGF-β target genes expression in chemoresistant colon carcinoma cells. Volcano plot of gene expression array (84 Human TGF-β Signaling Targets genes, RT^2 profiler PCR array PAHS-235ZA, Qiagen) on HCT116p53KO cells. The graph shows that 5FU treatment caused an increase of transcription of 52 out of 84 TGFβ target genes analyzed as compared to control cells, suggesting a specific response by chemoresistant cells to chemotherapeutic action. Genes are represented by points. In the X axis is plotted the Log_2 of fold change of genes in cells treated with 5FU normalized to control cells. In Y axis are plotted the P-values of the t-student test between the two groups of treatment. The horizontal line stands for the threshold p-value (P=0.05).

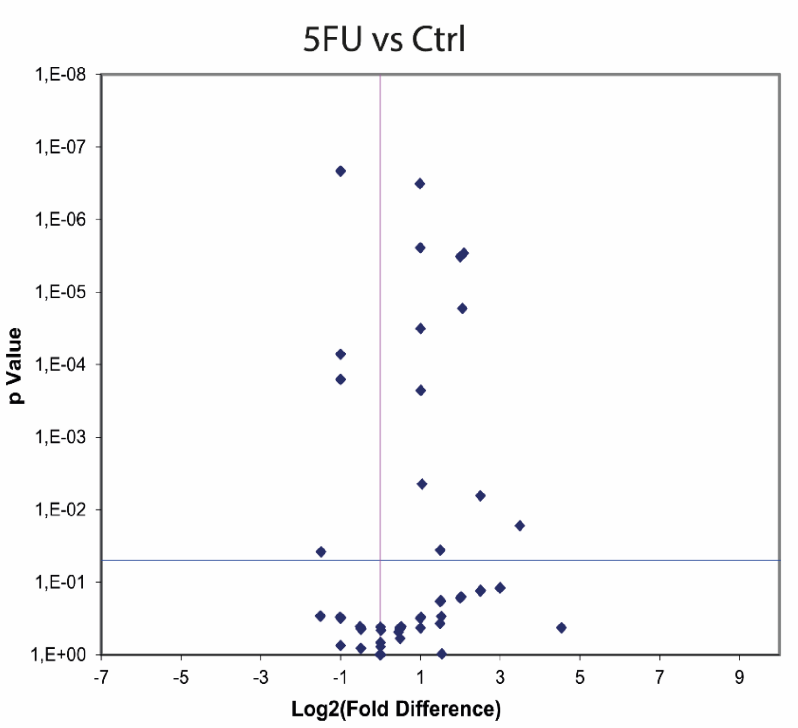

Chapter 6

Conclusions, translational relevance and future perspectives

During my PhD program I focused my attention on the molecular mechanisms involved in cancer drug resistance, in particular for glioblastoma multiforme (GBM) and colorectal cancer. The main aim of the four works presented in this thesis was to identify new therapeutic and diagnostic strategies using different approaches in dependence on the biological target under investigation.

Chapter 2 - Resveratrol and GBM: a possible strategy to circumvent chemotherapy failure

Despite the strong efforts to develop an efficacious therapy against GBM, very few patients are able to survive longer than 5 years [1]. Unluckily, chemotherapy, surgical resection and radiotherapy are generally palliative treatments for GBM. One of the main reasons of the failure of GBM therapeutic strategies has been attributed to the presence of CSCs (Cancer Stem Cells) within the tumor masses [2]. Intrinsic (detoxifying enzymes, genetic background) or extrinsic (chemotherapeutic concentrations in the brain parenchyma or dosing schemes, hypoxic microenvironments, niche factors, and the re-acquisition of stem cell properties by non- stem cells) mechanisms of resistance exerted by CSCs need to be overcome by innovative therapeutic strategies.

In our work, we presented a new potential drug for GBM treatment: resveratrol (RSV). RSV is a pleiotropic molecule, whose role in plant biology was broadly studied [3]. In our experiments we obtained unexpected results on 7 well characterized GBM cell lines [4]: RSV was able to inhibit metabolic activity, induce cell death and decrease motility of GBM cell lines analysed,

even if with heterogeneous responses. Moreover, RSV was able to actively modulate the expression of some genes involved in the Wnt pathway, one of the key players in the self-renewal phenomenon [5–7]. Such specific molecular modulations are an interesting starting point for the understanding of the therapeutic potential of RSV in GBM treatment.

Future studies will be directed to better comprehend the heterogeneity of GBM cells response, starting from GBM2 cell line, which was the most responsive to resveratrol treatment. As the studied GBM cell lines had been previously characterized, the next investigations will determine the link between genetic and epigenetic alterations and response to RSV therapy. Pre-clinical *in vivo* models will also be established, in order to verify if RSV could be a potential therapeutic molecule to administer in combination and/or in substitution of standard chemotherapeutic regimen.

Chapter 3 - Computational biology and clinical studies: the interesting example of XRCC3

Prediction of response to Colorectal Cancer (CRC) therapy could be a powerful tool to correctly address CRC patient treatments. At the moment, the only accepted marker of response to therapy in CRC is carcinoembryonic antigen (CEA) [8]. The integration between *in vitro*, *in vivo*, *ex-vivo*, clinical retrospective and computational studies could definitely lead to the identification of biomarkers of therapeutic response. In particular, recent advances in computational science allow the processing, management and use of large sets of genomic and proteomic information, which are powerful tools to set up individualized treatments.

Patients enrolled for the reported study had received pre-operative-chemoradiotherapy, and then monitored for response to therapeutic regimen. Patient specimens underwent microarray analysis of expression, and, among the analysed genes, XRCC3 (a protein involved in homologous recombination repair of DNA) was found to be associated with the prediction and monitoring of the response to therapy. XRCC3 potential involvement in drug resistance was then confirmed in *in vitro* models of cancer drug resistance. Moreover, Protein-Protein Interaction analysis was able to detect TRAF6 as a central node of XRCC3 network involved in therapy resistance. Thanks to integrated high-throughput approach, we were able to contextualize experimental data in a more complex scenario, where we identified potential "hidden players" involved in the investigated biological process.

Next studies will be directed to clarify the molecular mechanisms underlying the relationship between XRCC3 and response to treatment in CRC. To achieve this aim, a broader number of patient samples will be analysed, and XRCC3 expression will be studied in relation to patient genetic background, proteomic profile and secretome. Moreover, TRAF6-centered molecular network will be dissected in *in vitro* and *in vivo* models of CRC chemoresistance, through RNA interference and gene over-expression experiments.

Chapter 4 – GSK3β is a master regulator of CRC chemoresistance

Protein kinases are frequently activated by chemoresistant cancer cells as compensative effectors to overcome impaired mechanisms fundamental for

cell survival [9,10]. GSK3β is known to be involved in a wide range of biological processes [11,12] and is generally described as an oncosuppressor because of its active involvement in degradation of β -catenin, a transcription factor positively regulating Myc and cyclin D1 expression [13].
In our work, we showed that GSK3β is actively involved in chemoresistance of CRC, as its inhibition re-sensitized p53-null tumor cells to chemotherapeutic action, in *in vitro* and *in vivo* models. Moreover, GSK3β activation in patient tumor specimens was found to be correlated with poor prognosis and worse survival percentages. These findings are particularly relevant taking into account that the treatment for stage II primary colon cancer remains controversial. Although chemotherapy is often recommended for high-risk stage II disease, many tumors with similar histopathologic features will relapse, even after chemotherapy [14].
As a result, the addition of GSK3β inhibitors to standard chemotherapy might be beneficial to a large number of colon carcinomas, in which apoptotic mechanisms are frequently altered and such defects render treatment with traditional chemotherapeutic agents ineffective.
The successive studies, described in the next paragraph, have been oriented to understand the molecular mechanism underlying GSK3β activation and CRC chemoresistance. In particular, we started from the *in vivo* xenograft model of re-sensitisation to chemotherapeutic action to investigate how the inactivation of GSK3β could influence cellular and extra-cellular tumor processes.

Chapter 5 – TGFβ is an active player in CRC chemoresistance

Since it has been reported a relationship between GSK3β and TGF-β pathways in tumor progression of different carcinomas [15,16] and it has been demonstrated the relationship between chemoresistance and TGF-β in colon cancer [17], we investigated how the TGF-β pathway could contribute to the chemoresistance/chemoreversion phenomenon in our *in vivo* model of chemoresistance. Firstly, we observed that Lithium (a GSK3 inhibitor) was able to downregulate TGFBRI expression. More surprisingly, 5-fuorouracil (5FU) administration caused an activation of the TGF-β pathway, leading to an increase of tumor vascularisation. Lithium contrasted 5FU action, preventing TGF-β pathway activation and causing chemoresistant cells re-sensitization to chemotherapeutic action. Further experiments in 3D cultured colon carcinoma cells, showed that TGF-β pathway activation was specific of chemoresistant cells and that Lithium or TGFBRI-specific inhibitor treatment was able to contrast TGF-β pathway activation acted by 5FU. In addition, TGF-β administration (as recombinant protein or in chemoresistant cells conditioned medium) protected chemosensitive cells to chemotherapeutic action.

These data led us to hypothesize a sort of autocrine loop of TGF-β in chemoresistant cells, which seems to be fundamental for the drug resistance process. In fact, if this autocrine stimulation is interrupted, chemoresistant cells die in consequence of 5FU administration.

These findings can open new perspectives in the comprehension of the molecular mechanisms of resistance to 5FU, as, to our knowledge, a specific activation of TGF-β pathway in consequence of chemotherapeutic

administration was not previously reported in literature. Future studies will investigate not only how 5FU is able to induce TGF-β pathway activation, but how TGF-β and GSK3β are biologically related and their potential in the therapy of CRC patients. Moreover, further experiments will be conducted to verify if the described mechanisms are active also in other type of epithelial tumors.

References

1. Stupp R, Hegi ME, Mason WP, van den Bent MJ, Taphoorn MJ, Janzer RC, Ludwin SK, Allgeier A, Fisher B, Belanger K, Hau P, Brandes A a., Gijtenbeek J, et al. Effects of radiotherapy with concomitant and adjuvant temozolomide versus radiotherapy alone on survival in glioblastoma in a randomised phase III study: 5-year analysis of the EORTC-NCIC trial. Lancet Oncol. 2009;10:459–66.

2. Beier D, Schulz JB, Beier CP. Chemoresistance of glioblastoma cancer stem cells - much more complex than expected. Mol Cancer. 2011;10:128.

3. Gagliano N, Aldini G, Colombo G, Rossi R, Colombo R, Gioia M, Milzani A, Dalle-Donne I. The potential of resveratrol against human gliomas. Anticancer Drugs. 2010;21:140–50.

4. Baronchelli S, Bentivegna A, Redaelli S, Riva G, Butta V, Paoletta L, Isimbaldi G, Miozzo M, Tabano S, Daga A, Marubbi D, Cattaneo M, Biunno I, et al. Delineating the cytogenomic and epigenomic landscapes of glioma stem cell lines. PLoS One. 2013;8:e57462.

5. Wu JQ, Seay M, Schulz VP, Hariharan M, Tuck D, Lian J, Du J, Shi M, Ye Z, Gerstein M, Snyder MP, Weissman S. Tcf7 is an important regulator of the switch of self-renewal and differentiation in a multipotential hematopoietic cell line. PLoS Genet. 2012;8:e1002565.

6. Panicker SP, Raychaudhuri B, Sharma P, Tipps R, Mazumdar T, Mal AK, Palomo JM, Vogelbaum M a, Haque SJ. p300- and Myc-mediated regulation of glioblastoma multiforme cell differentiation. Oncotarget. 2010;1:289–303.

7. Teo JL, Kahn M. The Wnt signaling pathway in cellular proliferation and differentiation: A tale of two coactivators. Adv Drug Deliv Rev. 2010;62:1149–55.

8. Desch CE. Colorectal Cancer Surveillance: 2005 Update of an American Society of Clinical Oncology Practice Guideline. J Clin Oncol. 2005;23:8512–9.

9. Longley D, Johnston P. Molecular mechanisms of drug resistance. J Pathol. 2005;205:275–92.

10. Wilson TR, Longley DB, Johnston PG. Chemoresistance in solid tumours. Ann Oncol. 2006;17:x315–24.

11. Forde JE, Dale TC. Glycogen synthase kinase 3: a key regulator of cellular fate. Cell Mol Life Sci. 2007;64:1930–44.

12. Doble BW, Woodgett JR. GSK-3: tricks of the trade for a multi-tasking kinase. J Cell Sci. 2003;116:1175–86.

13. Beurel E, Jope RS. The paradoxical pro- and anti-apoptotic actions of GSK3 in the intrinsic and extrinsic apoptosis signaling pathways. Prog Neurobiol. 2006;79:173–89.

14. Benson 3rd AB, Schrag D, Somerfield MR, Cohen AM, Figueredo AT, Flynn PJ, Krzyzanowska MK, Maroun J, McAllister P, Van Cutsem E, Brouwers M, Charette M, Haller DG. American Society of Clinical Oncology recommendations on adjuvant chemotherapy for stage II colon cancer. J Clin Oncol. 2004;22:3408–19.

15. Cozzolino AM, Alonzi T, Santangelo L, Mancone C, Conti B, Steindler C, Musone M, Cicchini C, Tripodi M, Marchetti A. TGFβ overrides HNF4α tumor suppressing activity through GSK3β inactivation: implication for hepatocellular carcinoma gene therapy. J Hepatol. 2013;58:65–72.

16. Basu D, Lettan R, Damodaran K, Strellec S, Reyes-Mugica M, Rebbaa A. Identification, mechanism of action, and antitumor activity of a small molecule inhibitor of hippo, TGF-β, and Wnt signaling pathways. Mol Cancer Ther. 2014;13:1457–67.

17. Brunen D, Willems SM, Kellner U, Midgley R, Simon I, Bernards R. TGF-β: An emerging player in drug resistance. Cell Cycle. 2013;12:2960–8.